BRITISH ANTARCTIC SURVEY

SCIENTIFIC REPORTS

No. 54

THE JAMES ROSS ISLAND VOLCANIC GROUP OF NORTH-EAST GRAHAM LAND

By

P. H. H. NELSON, B.Sc., Ph.D.

British Antarctic Survey

and

Department of Geology, University of Birmingham

LONDON: PUBLISHED BY THE BRITISH ANTARCTIC SURVEY: 1975

BRITISH ANTARCTIC SURVEY SCIENTIFIC REPORTS: No. 54

THE JAMES ROSS ISLAND VOLCANIC GROUP OF NORTH-EAST GRAHAM LAND

By

P. H. H. NELSON, B.Sc., Ph.D.

British Antarctic Survey
and
Department of Geology, University of Birmingham

(Manuscript received 29th July, 1965)

ABSTRACT

THE Middle to Upper Miocene James Ross Island Volcanic Group is composed predominantly of alkalic olivine-basalt lavas, palagonite-breccias and subordinate palagonite-tuffs. These volcanic rocks, which form magnificent cliff exposures, have been systematically mapped and collected at James Ross and Vega Islands, Tabarin Peninsula, and at most of the smaller islands of the James Ross Island group. The sub-horizontal lavas and steeply dipping palagonite-breccias beneath them are genetically related, and are separated from each other by level contacts. Lavas and palagonite-breccias occur either as "deltaic" structures around the margins of James Ross Island, where they probably resulted from aqueous brecciation of large lava streams flowing from a major volcanic centre, or as individual lava/palagonite-breccia volcanoes, which were produced by the subaqueous initiation of central eruptions. Ash cones and the cores of lava/palagonite-breccia volcanoes are composed of massive or thinly bedded fine-grained palagonite-tuff. Although well-preserved sedimentary structures confirm the subaqueous origin of some other palagonite-tuffs, the distinction between those formed by the aqueous brecciation of molten basalt and those formed by true pyroclastic activity is not always clear. Overlap structures, some of which were caused by relative sea-level changes, occur in some palagonite-breccias and against the palagonite-tuffs which form ash cones. Dykes, rare sills, volcanic plugs and a laccolith comprise the associated intrusive rocks. Although it is absent from the dykes, primary interstitial analcite is ubiquitous in the olivine-dolerite plugs and the laccolith.

Large-scale faulting has not been observed displacing the rocks of this volcanic group, except in the Tabarin Peninsula area, where faults with throws of up to 1,000 ft. (305 m.) have been inferred. The termination of some rock units by overlap structures accounts for most of the stratigraphic discontinuities.

Four grades of secondary zeolitization (involving chabazite, phillipsite and analcite) have been recognized in the extrusive rocks and dykes. There is a correlation between the zeolite grade and the degree of palagonitization of the constituent hyalobasalt fragments in the palagonite-tuffs and breccias, and in these rocks zeolites are generally more abundant than in the olivine-basalt lavas. The zeolites which occur in the plugs and the laccolith (analcite, thomsonite, chabazite, natrolite and gismondite) have a pyrogenetic origin related to the final stages of olivine-dolerite crystallization.

This volcanic group has alkalic basalt geochemical characteristics, which are more closely related to alkalic basalts from orogenic environments than to those from oceanic ones. Little differentiation has been observed in the extrusive rocks, although peralkaline rocks may exist as plugs, or flows of limited extent, high on James Ross Island beneath the ice cap of Mount Haddington. However, crystallization differentiation has resulted in dolerite-pegmatite schlieren and late-stage peralkaline veins in the analcite-bearing olivine-dolerite laccolith of Palisade Nunatak. The course of differentiation in this intrusion is comparable with those of alkalic basalts generally but it is most characteristic of differentiation in a single intrusive mass. Although little differentiation has occurred in the dykes, they were evidently committed to a geochemical trend of initial absolute iron enrichment.

Five phases of eruption and lava/palagonite-breccia deposition have been recognized in the James Ross Island area. Although the first phase certainly post-dates the formation of a major volcanic centre situated near the middle of James Ross Island, the superposition of one lava/palagonite-breccia unit on another indicates that there was a gradual submergence of the area during the formation of the volcanic group. Because the upper 2,000 ft. (610 m.) of James Ross Island are obscured by ice, the total extent of this submergence is unknown. However, lava/palagonite-breccia horizons occur at intervals up to nearly 3,000 ft. (914 m.) above sea-level, suggesting that at least this amount of submergence took place. Since the close of vulcanicity, re-elevation of the landmass has returned this area to its present position. Raised beaches and benches around the margins of James Ross and Vega Islands testify to minor sea-level fluctuations in the recent past.

CONTENTS

		PAGE
I.	Introduction	4
	Physiography	5
	a. James Ross Island	5
	b. Vega Island	6
	c. Small Islands and Tabarin Peninsula	6
II.	Stratigraphy	6
	1. General Account	6
	2. James Ross Island Volcanic Group	7
	a. Methods of Mapping and Correlation	7
	b. Field Relations	8
III.	James Ross Island Volcanic Group	9
	A. Extrusive Rocks	9
	1. Tuffaceous Conglomerates	10
	2. Rocks of Phase I	11
	a. Palagonite-breccias	11
	b. Olivine-basalt Flow Lavas	14
	c. Subaerial Palagonite-tuffs	14
	d. Subaqueous Palagonite-tuffs	15
	3. Rocks of Phase II	16
	a. Palagonite-breccias	16
	b. Flow Lavas	18
	c. Palagonite-tuffs	20
	4. Rocks of Phase III	20
	a. Lavas and Palagonite-breccias	20
	b. Palagonite-tuffs	21
	5. Lavas and Palagonite-breccias of Phase IV	22
	6. Rocks of Phase V	23
	7. Cain and Abel Nunataks, Trinity Peninsula	23
	B. Intrusive Rocks	23
	1. Dykes	24
	2. Sills	25
	3. Volcanic Plugs	25
	4. Palisade Nunatak Laccolith	26
	a. Analcite-bearing Olivine-dolerites	27
	b. Dolerite-pegmatites and Alkali-rich Segregations	27
	c. Late-stage Veins	29
	d. Xenolithic Pods	29
	e. Contact Metamorphism	29
	f. Summary	30
	C. Palagonitization and Zeolites	30
	1. Hyalobasalt Fragments and Palagonite Rim Thicknesses	30
	2. Zeolites	31
	a. Paragenesis of Zeolites in the Extrusive Rocks	31
	b. Distribution and Origin of Zeolites in the Extrusive Rocks	33
	c. Zeolites in the Intrusive Rocks	34
IV.	Structural Geology	35
	A. Cone Structures	35
	B. Overlap Structures	38
	1. Cone Surface Overlap Structures	38
	2. Overlap Structures Probably due to Sea-level Changes	38
	3. "Terminal Slope" Overlap Structures	40
	C. Lava Tunnels	40
	D. Faults	40
	1. Minor Faulting	40
	2. Absence of Evidence for Major Faulting	42
V.	Geochemistry	42
	A. Variation Trends	42
	B. Discussion	47
	1. Chemical Classification	47
	2. Differentiation in the Extrusive Rocks	48
	3. Differentiation in the Intrusive Rocks	50
	a. Main Trend	50
	b. Dyke Rocks	54
	4. Crystallization and Sequence of Eruptions	54
	5. Palagonitization	54
	6. Comparison with Other Alkaline Rock Series	56
	a. Composition of Parental Magmas	56
	b. Differentiation Trends	56
VI.	Geological History and Conclusions	57
VII.	Acknowledgements	60
VIII.	References	60
	Maps 1 and 2	In end pocket

I. INTRODUCTION

THIS report is based on the results of field work carried out between 1960 and 1962 in the James Ross Island area from the British Antarctic Survey station at Hope Bay, north-east Graham Land.

The James Ross Island group is situated off the north-east coast of Graham Land between lat. 63°30′ and 64°35′S., and long. 56°30′ and 58°30′W. (Fig. 1). Dominating the group is James Ross Island itself, which is surrounded by many smaller islands. The largest of these are Vega, Seymour and Snow Hill Islands, while Humps, Cockburn, Lockyer, Persson and Carlson Islands are the smaller ones immediately surrounding James Ross Island. Red, Vortex, Egg, Tail, Eagle and Beak Islands form a distinct group farther north in Prince Gustav Channel, which separates the James Ross Island group from Graham Land. All the islands of the James Ross Island group consist predominantly of the Middle to Upper Miocene James Ross Island Volcanic Group. Snow Hill and Seymour Islands are composed entirely of Upper Cretaceous and Lower Miocene marine sediments, except for a few dykes. These dykes and others at Cape Longing, 40 miles (64 km.) south-west of James Ross Island, are probably associated with the James Ross Island Volcanic Group.

To the north-east of James Ross Island, rocks of the James Ross Island Volcanic Group occur at Tabarin Peninsula and Andersson, Jonassen, Rosamel and Paulet Islands, and the southern half of Dundee Island. Rocks which are believed to form part of the James Ross Island Volcanic Group also occur at the Seal Nunataks, 90 miles (145 km.) south-west of James Ross Island in the Larsen Ice Shelf (Fig. 1).

Most of the areas mentioned above are south-east of a semi-circular line coincident with the trend of Prince Gustav Channel, which divides the rocks of the James Ross Island area from the older rocks of Trinity Peninsula. However, the volcanic rocks at Cain and Abel Nunataks (Aitkenhead, 1965), situated on Trinity Peninsula 8 miles (12·9 km.) north of Egg Island, are outliers of the James Ross Island Volcanic Group.

Geological exploration in the James Ross Island area up to 1958 has been summarized by Adie (1957, 1958). However, the important results of some previous investigators should be mentioned here, because they provide an essential background to the present work. Perhaps the most notable contribution to the study of the James Ross Island Volcanic Group was made by J. G. Andersson, geologist to the Swedish South Polar Expedition (1901–03) led by Dr. Otto Nordenskjöld. Andersson (1906) assigned the James Ross Island Volcanic Group (named by him the "Ross Island Formation") to a Middle to Upper Miocene age, because he found that the volcanic rocks were interposed between Lower Miocene marine sediments and a Pliocene Pecten Conglomerate at Cockburn Island (Fig. 1). Although Andersson made no attempt to establish a stratigraphical sequence for this volcanic group, he indicated that the rocks were basically undisturbed. With particular reference to the north coastal cliffs of Vega Island, Andersson (1906, p. 46–47, fig. 6) described steeply dipping "agglomerates" underlying sub-horizontal flow lavas. He concluded that the dip of the "agglomerates" is primary and that the "agglomerates" were deposited in a subaerial environment; a period of erosion intervening between their deposition and the subsequent outpouring of lavas.

It was not until 1947 that R. J. Adie resumed the systematic study of these volcanic rocks and re-named them the James Ross Island Volcanic Group. Adie (1953) concluded that there were at least two main lava and three main explosive phases in the James Ross Island area, but only one lava and two explosive phases at the Seal Nunataks. He deduced that the second lava phase in the James Ross Island area was the most important, and he recognized volcanic centres on the west coasts of Andersson and Jonassen Islands and at Paulet Island. Adie suggested that Mount Haddington, the summit of James Ross Island (Fig. 1), marks the most important centre of eruption and that most of the extrusive rocks were derived "from one major and several parasitic centres in the James Ross Island Group" (Adie, 1953, p. 214). He subdivided the flow lavas into vesicular olivine-basalts, vesicular trachytic olivine-basalts and vesicular olivine-hyalobasalts. He also subdivided the tuffs on the basis of colour into yellow-brown, green and red groups, of which the yellow-brown palagonitic tuffs were recognized as the commonest. Adie also identified two distinct types of dykes: porphyritic trachytic basalts and ophitic to subophitic olivine-dolerites.

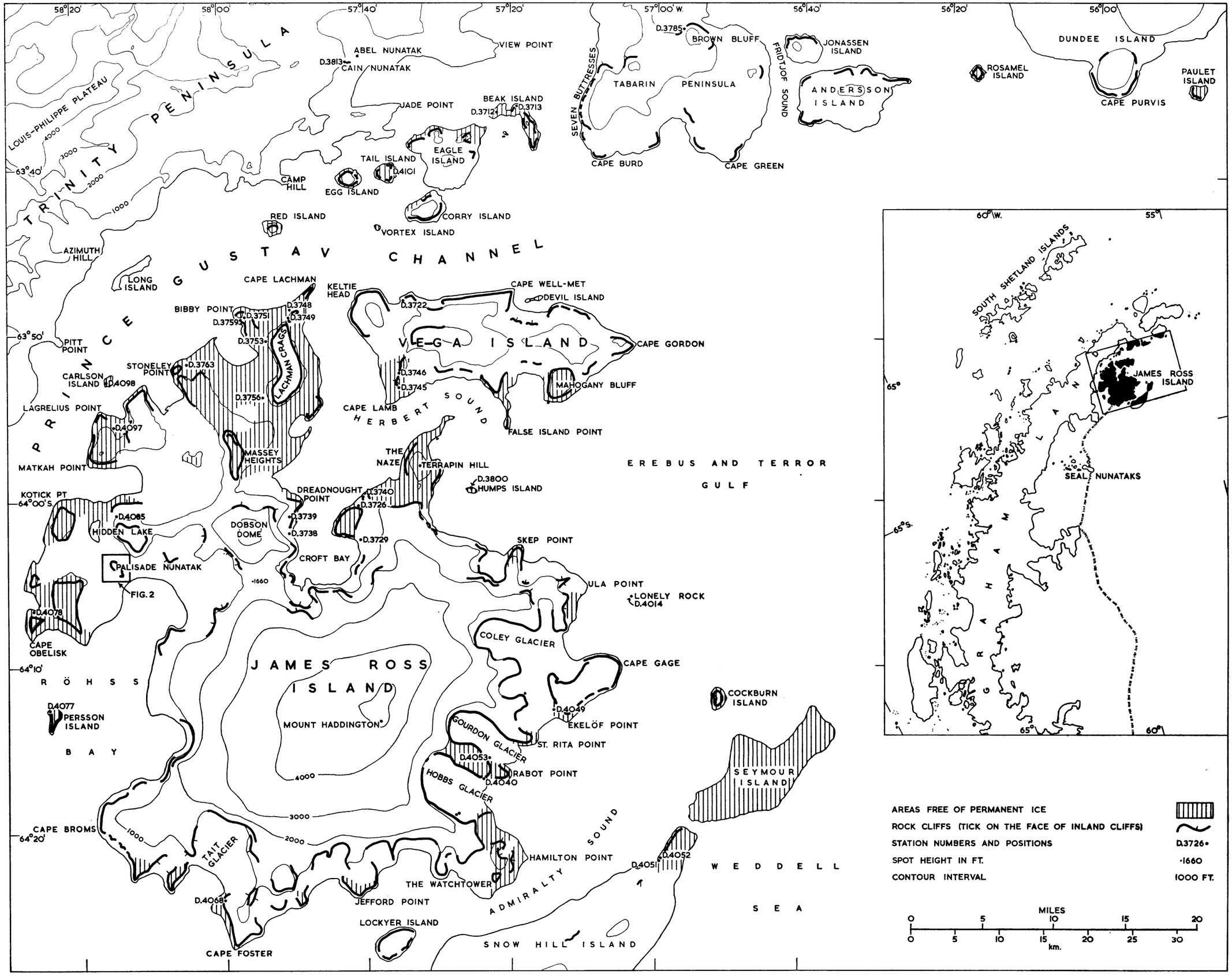

FIGURE 1

Map of the James Ross Island area showing major physiographic features, place-names and station numbers. The inset shows the position of the James Ross Island area in relation to Graham Land.

In 1958–59 J. S. Bibby studied the angular unconformity between the James Ross Island Volcanic Group and the underlying Upper Cretaceous sediments, which form a buried hill-and-valley topography on which the volcanic rocks have been deposited. Bibby (1966, p. 27) collected several ophiuroids from the tuffs near Hidden Lake, and the presence of these fossils in rocks of the James Ross Island Volcanic Group led him to believe that the bulk of the lower part of the group is marine in origin. Bibby (1966, p. 28) also reported pillow lavas at Cape Lachman, near Hidden Lake and Lagrelius Point (Fig. 1), thus providing additional evidence in support of a marine origin for the volcanic group. Bibby believed that the steeply dipping "agglomerates" are current-bedded, but he also reported two anticlines and a syncline in the volcanic rocks at Vega Island.

This report describes the stratigraphy, petrography and geochemistry of the James Ross Island Volcanic Group. The nature of deposition of the "agglomerates", now known to be palagonite-breccias, is discussed in the light of geological studies in British Columbia, Iceland and particularly at Surtsey, the marine volcano which erupted off south-west Iceland in November 1963.

Physiography

a. *James Ross Island.* With maximum dimensions of 47 miles (76 km.) in a north—south direction and 42 miles (68 km.) in an east—west direction, James Ross Island can be described in two parts. North-western James Ross Island (between Cape Obelisk and Cape Lachman (32 miles; 51·5 km.)) is dominated by ice-capped Dobson Dome (3,110 ft.; 948 m.), and this is separated by an ice col 1,660 ft. (506 m.) high from south-eastern James Ross Island, which is a larger area dominated by Mount Haddington (5,340 ft.; 1,628 m.) (Fig. 1).

North-western James Ross Island, which is characterized by mesas such as Lachman Crags and Massey Heights, has a well-dissected topography. The ice-drainage and valley directions are approximately radial to Dobson Dome, which is situated near the south-east corner of this triangular area. Apart from glacier snouts, the coast is composed of rock or scree-covered talus slopes. However, the position of the coastline at the north of Röhss Bay is generally obscured by the mergence of land ice and ice shelf.

Much of north-western James Ross Island is free of permanent ice. To the north of Dobson Dome, the area between Cape Lachman, Stoneley Point and Dreadnought Point contains only the Lachman Crags ice cap and a small dead glacier near Massey Heights (Fig. 1). Along the western margin of James Ross Island, ice-free ground occurs intermittently between Lagrelius Point and Cape Obelisk. In all these areas the ice-free terrain is due to local glacial retreat. Although it was initiated by climatic amelioration, this retreat has severed the highland ice supply to some of the pre-existing valley glaciers, thus hastening the ice recession.

The valley containing Hidden Lake, which isolates the mesas in the area between Kotick Point and Cape Obelisk from the remainder of the island, is an interesting feature. Much of the erosion of this valley was probably effected by overspill ice from northern Röhss Bay at a time when glacierization was more extensive than at present. A subsequent ice stream, responsible for the formation of the Hidden Lake rock basin, may have initiated the more extensive erosion in this area.

In contrast, the larger south-eastern part of James Ross Island is composed of one large dome (Mount Haddington) which is dissected peripherally (Fig. 1). Unlike the gently convex summit of Dobson Dome, the distinctive ice peak of Mount Haddington rises about 300 ft. (91 m.) above the surrounding ice cap, indicating the presence of rock to a height of approximately 5,000 ft. (1,525 m.) (Plate Ia).

Ice cliffs composed of glacier snouts, and the terminations of more ill-defined drainage channels between the main glaciers, form longer stretches of the coast of south-eastern James Ross Island. Here, the section of coast adjacent to the ice shelf in Röhss Bay consists partly of rock cliffs 500–600 ft. (152–183 m.) high and partly of steep ice falls. Most of this coastline is well defined. In south-eastern James Ross Island, the radial ice-drainage pattern centred on Mount Haddington is evidence of the original cone shape of the island (Plate Ib). The drainage may have originally been established as a river system well before glaciation. Ice-free areas are less common in south-eastern James Ross Island but they include Terrapin Hill and The Naze in the north, and the area between Hamilton Point and the Hobbs Glacier snout in the south (Fig. 1).

The topography of James Ross Island is characterized by mesas and steps (Plate Ic). Although the evidence is sparse, the following erosion surfaces, represented by the tops of mesas and steps, have been recorded from an analysis of cliff heights on the topographic maps and photographs: 350, 650, 900, 1,000

and 1,200 ft. (107, 198, 274, 305 and 366 m.) above sea-level. There are indications of other erosion levels at 1,500, 2,000 and 3,000 ft. (457, 610 and 914 m.) above sea-level but they are not so clearly defined. With the exception of the 350 ft. (107 m.) level, these surfaces commonly coincide with exposures of flow lavas just above their sub-horizontal contact with steeply dipping palagonite-breccias (Plate VIIc). Because the horizontal cliff tops are often underlain by slightly dipping lava/palagonite-breccia contacts, these levels are probably not structurally controlled. In most localities, nevertheless, the presence of sub-horizontal flow lavas has contributed largely towards the preservation of these levels. The lower levels, which may represent a series of strandflats formed in the manner described by Holtedahl (1929, p. 17, fig. 6), are believed to approximate closely to the position of sea-level during their formation. Although these levels can perhaps be correlated with some of the coastal platforms recorded by Feruglio (1949) in Patagonia, the greater depth of the continental shelf around Antarctica than elsewhere in the world (Nichols, 1960) may invalidate any such correlation.

The presence of large and small bench features at heights of up to 600 ft. (183 m.) above sea-level on Trinity Peninsula (Aitkenhead, 1965) provides some evidence to suggest that the whole north-eastern Graham Land area has risen relative to the Pliocene sea-level. The Pliocene Pecten Conglomerate of Cockburn Island is now at an elevation of approximately 722–820 ft. (220–250 m.) above sea-level. Therefore, the 1,200 and 1,000 ft. (366 and 305 m.) levels may be just pre-Pliocene, while the 900, 650 and 350 ft. (274, 198 and 107 m.) levels were formed during the Pliocene and Pleistocene. More recent raised beaches and gravel terraces between 10 and 80 ft. (3 and 24·4 m.) above sea-level have been described by Bibby (1965) from several parts of the James Ross Island coast.

b. *Vega Island.* Rising to only 2,000 ft. (610 m.) above sea-level, Vega Island may be regarded as a physiographic outlier of James Ross Island, from which it is separated by Herbert Sound (Fig. 1). The 5 mile (8 km.) long cliff section trending west from Cape Well-met, the top of which is a remnant of the 650 ft. (198 m.) erosion surface, is the most striking feature of this island. The south coast of Vega Island is comparatively well indented and is sub-parallel to the adjacent coast of James Ross Island. At False Island Point and in the area north of Cape Lamb the terrain is free of permanent ice.

c. *Small islands and Tabarin Peninsula.* The islands described here are those which are close to James Ross Island, those in Prince Gustav Channel, and Andersson, Jonassen and Rosamel Islands (Fig. 1). Six of these islands (Lockyer, Egg, Corry, Eagle, Andersson and Jonassen Islands) carry ice caps and nine (Cockburn, Persson, Carlson, Red, Vortex, Tail, Beak, Rosamel and Humps Islands) are free of permanent ice. All the islands are characterized by steep coastal scree slopes and coastal rock or ice cliffs, and many of them have a flat top (Plate Id). Whether they are glaciated or not, these islands have physiographic features similar to those of James Ross and Vega Islands. Similarly, southern Tabarin Peninsula, which is composed of James Ross Island Volcanic Group rocks, has physiographic features more typical of the James Ross Island area than of Trinity Peninsula, to which it is connected by ice and possibly rock.

II. STRATIGRAPHY

1. *General account*

Rocks from four major formations are represented in the James Ross Island area (Table I). A landscape formed on Upper Cretaceous rocks provides the base upon which the greater part of the James Ross Island Volcanic Group was deposited, but there are two notable exceptions to this. First, some of the volcanic rocks on Cockburn Island rest directly on a local development of the Seymour Island Series (Andersson, 1906; Croft, 1947) and secondly, although their bases cannot be seen, Cain and Abel Nunataks probably rest on, or cut, rocks of the Trinity Peninsula Series (Aitkenhead, 1965). The upper limit of the James Ross Island Volcanic Group is marked by the Pliocene Pecten Conglomerate of Cockburn Island.

Over most of the area there is a marked angular unconformity at the base of the James Ross Island Volcanic Group. However, where the volcanic rocks rest on Tertiary sediments at Cockburn Island, the presence of an unconformity is not so clear. Tuffaceous material has been recorded from the uppermost sediments of the Seymour Island Series (Andersson, 1906; Standring, 1956), indicating that the vulcanicity responsible for the formation of the James Ross Island Volcanic Group was initiated before the close of Lower Miocene sedimentation. There was evidently a transition at this stage (Lower to Middle Miocene)

TABLE I

STRATIGRAPHICAL SUCCESSION IN THE JAMES ROSS ISLAND AREA

Recent	Raised beaches and elevated erosion levels
Pleistocene	
Pliocene	Pecten Conglomerate
Middle and Upper Miocene	James Ross Island Volcanic Group
Lower Miocene	Seymour Island Series
Upper Cretaceous (Lower to Middle Campanian)	Snow Hill Island Series

with subaerial erosion and deposition dominant in the west and continued sedimentation in the east of the James Ross Island area.

This is, however, a simplification which disregards the presence of a fault bringing Upper Cretaceous and Lower Miocene sediments into juxtaposition on Cockburn Island. This fault, which does not affect the overlying volcanic rocks transgressing both groups of sediments, suggests that there was some diastrophic movement at the close of the Lower Miocene (Croft, 1947).

2. *James Ross Island Volcanic Group*

a. *Methods of mapping and correlation.* The rocks of the James Ross Island Volcanic Group are commonly exposed in vertical or near-vertical cliffs, which are frequently capped by ice and attain heights of 1,000 ft. (305 m.) and more (Plate Ia). Since it was not possible to examine closely more than the lowermost 10 ft. (3 m.) of any section and, since one section may contain as many as three complete stratigraphical units, binoculars were used extensively to examine the units and locate their contacts. Fortunately, the three main rock types (the palagonite-breccias, flow lavas and palagonite-tuffs) have such characteristic appearances in cliff sections that it is difficult to confuse one with another. This aid to mapping proved successful, as many of the structural relationships are only apparent when observed from a distance. This is particularly true of the coarsely bedded palagonite-breccias, which frequently occur at the base of coastal cliffs that are capped by flow lavas (Plate VIIc).

Field mapping was on 1 : 50,000 enlargement sheets of the 1 : 200,000 published topographic maps.* Vertical aerial photographs of outcrops of the James Ross Island Volcanic Group cover only Cape Obelisk on James Ross Island, Tabarin Peninsula, Andersson, Jonassen, Rosamel, southern Dundee and Paulet Islands, and some of the islands in Prince Gustav Channel. Because of the cliff nature of most exposures of the volcanic group, the geological value of vertical air photographs is limited.

Since nearly all lithological and structural changes take place in the vertical sense, topographic heights above sea-level were found to be important. In certain parts of James Ross Island the published spot heights were used extensively as an aid to correlation and thickness determination. The spot heights, which are reliable, were checked whenever possible with an aneroid barometer. The accuracy to which altitudes higher than 1,000 ft. (305 m.) above sea-level were determined was only ± 100 ft. (30·5 m.), whereas up to 1,000 ft. (305 m.) above sea-level the accuracy was greater. Towards the end of the period of field work, Andersson, Jonassen and Rosamel Islands were examined in one afternoon from a helicopter of H.M.S. *Protector*. Altimeter readings taken during this flight provided confirmation of the heights above sea-level of several contacts.

Correlations have been based largely on the relative heights above sea-level of successive lava/palagonite-breccia horizons. In some areas, particularly the east coast of James Ross Island, correlation

* Sheets W 63 56, W 63 58, W 64 56 and W 64 58.

from one place to another is facilitated by the almost continuous cliff exposures, which form amphitheatres surrounding the larger glaciers. Because of the close similarity of one palagonite-breccia unit to the next, correlations over greater distances are difficult. However, several exposures of an overlap structure in the palagonite-breccias of phase II (p. 38), which may be directly correlated with each other in the east coast of James Ross Island, also occur on Jonassen Island and in a cliff on the west side of James Ross Island (Map 2B). This overlap structure, probably due to a change in relative sea-level at the time of deposition, may be used to correlate several phases of rocks by extrapolation. Provided that one phase (although not necessarily the same phase) can be traced from one outcrop to another, it is possible to correlate others simply by observing the orders of superposition of the rocks.

More recently, laboratory investigation of the average olivine compositions of extrusive rocks believed to belong to phases I, II and III has tended to support the stratigraphic sequence originally derived by considering relative superposition only. However, it has also supported the conclusion that correlations between James Ross Island, the offlying islands and southern Tabarin Peninsula may be difficult because of complicated structures. The average composition of the olivines in the palagonite-tuff forming the core of Brown Bluff (Table IX, D.3785.2) suggests that the lava/palagonite-breccia horizon, which is over 1,000 ft. (305 m.) above sea-level at this locality (Plate IIIa), correlates with phase I. Rocks from Seven Buttresses, where the lava/palagonite-breccia horizon is about 500 ft. (153 m.) above sea-level, also appear to belong to phase I as originally deduced. If the average olivine composition can be used as a stratigraphic indicator in this volcanic group, extensive examination of the olivines from localities in Tabarin Peninsula and the offlying islands could yield useful information regarding possible faults (p. 40).

b. *Field relations.* The James Ross Island Volcanic Group is composed predominantly of intercalated olivine-basalt flow lavas and palagonite-breccias. In the cliff sections bordering the large glaciers on the east of James Ross Island (Fig. 1) up to three alternations between lavas and palagonite-breccias can be observed; for instance, in the north wall of the Coley Glacier valley between 800 and 2,000 ft. (244 and 610 m.) above sea-level. It is apparent that the flow lavas cooled and solidified in a subaerial environment, whereas the palagonite-breccias were probably deposited subaqueously. Furthermore, it is suggested that the lavas and the palagonite-breccias are genetically connected and in some places they form unusual discoidal volcanoes.

In addition to the lava/palagonite-breccia volcanoes, there are one or two volcanoes which may have been formed under subaerial conditions. These are composed of a mixture of coarse- and fine-grained palagonitized vesicular fragments and shards, and they are distinct from the finer-grained palagonite-tuffs, which form "ash cones". The ash cones have been partially preserved in some sections and bear interesting relationships to the rocks which buried them (p. 38). The basalt glass in these rocks has also been converted into palagonite. Very fine-grained subaqueous tuffs occur even more locally than the tuffs which may have been deposited subaerially. The better laminated and sorted rocks of this group may be aquagene tuffs (Carlisle, 1963) formed entirely in a subaqueous environment between the lava and palagonite-breccia volcanoes. Pillow lavas occur in association with tuffs of a subaqueous character in several localities.

The largest intrusion associated with this volcanic group occurs at Palisade Nunatak, near the west coast of James Ross Island (Fig. 1). Palisade Nunatak (Plate VIa) is composed of a single laccolithic intrusion of columnar-jointed analcite-bearing olivine-dolerite capped by Upper Cretaceous sandstones, which formed the roof of the intrusion. Crystallization differentiation has led to the production of coarse-grained dolerite-pegmatite schlieren and cross-cutting felsitic veins during the final stages of consolidation. Four volcanic plugs, which probably represent the conduits of lava/palagonite-breccia volcanoes, have been located but dykes are uncommon, especially in James Ross and Vega Islands. However, unimpressive vesicular dykes, which commonly pinch out upwards, occur as minor swarms injected into the palagonite-tuffs of the islands in Prince Gustav Channel. In two localities there are more massive doleritic dykes, which are believed to be the feeders of fissure eruptions.

A generalized stratigraphic column of the James Ross Island Volcanic Group is given in Table II. In compiling this, correlations in the James Ross and Vega Islands area have been based on the inference that no major faulting has affected the volcanic rocks since they began to be deposited (p. 42). However, since faults probably occur in Tabarin Peninsula and some of the islands in Prince Gustav Channel (p. 40), correlations between them and James Ross and Vega Islands are difficult. In the lower levels, at least to the top of phase IV (Table II), the stratigraphical sequence should be considered essentially

TABLE II

GENERAL STRATIGRAPHY OF THE JAMES ROSS ISLAND VOLCANIC GROUP

Phase	*Entire Compiled Succession**	*East and West James Ross Island*	*South of Hobbs Glacier*
V	Olivine-basalt lavas Palagonite-breccias	Olivine-basalt lavas Palagonite-breccias	
IV	Olivine-basalt lavas Palagonite-breccias	Olivine-basalt lavas Palagonite-breccias	Olivine-basalt lavas Palagonite-breccias
III	Olivine-basalt lavas Palagonite-breccias	Olivine-basalt lavas Palagonite-breccias	Olivine-basalt lavas Palagonite-breccias
II	Olivine-basalt lavas Palagonite-breccias	Olivine-basalt lavas Palagonite-breccias	Olivine-basalt lavas
I	Olivine-basalt lavas Palagonite-breccias	UPPER CRETACEOUS	UPPER CRETACEOUS
	UPPER CRETACEOUS		

* Phases I to V comprise approximately 3,000 ft. (914 m.) of strata, the base of which coincides approximately with sea-level.

marginal to James Ross Island, because there are several indications that there was an island near the position of the present Mount Haddington during the greater part of the formation of the volcanic group (p. 58). It should be noted that the upper 2,000 ft. (610 m.) of James Ross Island are obscured by ice so that, although there are physiographic indications of further phases of similar volcanic rocks, there is no simple means of confirming this.

III. JAMES ROSS ISLAND VOLCANIC GROUP

A. EXTRUSIVE ROCKS

The main bulk of the James Ross Island Volcanic Group consists of extrusive rocks, comprising lavas, palagonite-breccias and palagonite-tuffs. Volcanic activity appears to have been centred at James Ross Island itself, where the total thickness of the volcanic pile is probably 5,000 ft. (1,524 m.). Of the five phases of activity which have been recognized at James Ross Island, only the first two are represented in the smaller offlying islands and Tabarin Peninsula. The top of the succession at Vega Island is marked by the palagonite-breccias of phase IV (Table II). It should be emphasized that the rocks attributed to phase I may not have been formed when vulcanism first broke out in this area.

Palagonite-breccias of phase I overlap against earlier volcanic rocks at the base of the cliff 6 miles (9·7 km.) north-east of Cape Broms and in the cliff 2 miles (3·2 km.) west of St. Rita Point, James Ross Island (Map 1; Fig. 4). The structural arrangement of the rocks is similar to a cone-surface overlap structure (p. 38) in that the sloping surface against which the phase I palagonite-breccias are banked is parallel to the bedding of the earlier fragmentary volcanic rocks, probably also palagonite-breccias.

Apart from the two exposed examples, there are often indications that rocks of phase I, and occasionally phase II, are cut out from below the nearer their outcrops are to the centre of James Ross Island. It is believed that at the two localities mentioned above the earlier rocks are part of perhaps a considerable volume of volcanic rocks, which were erupted prior to the activity of phase I but now are concealed beneath Mount Haddington. This earlier volcanic episode may have provided the tuffaceous material which was incorporated in the Lower Miocene Seymour Island Series (p. 6). The first of the five recognized phases of volcanic activity post-dates the formation of the volcanic nucleus, possibly a single large volcano. It is not known whether the depression of the James Ross Island area, which is indicated by the field relations of phases I–V (p. 59), had already started before phase I.

1. *Tuffaceous conglomerates*

Tuffaceous conglomerates have been found at Bibby Point (Bibby, 1966), near Hamilton Point (Andersson, 1906), on the north and south sides of the Hobbs Glacier snout and on the west coast of Croft Bay (Maps 1 and 2A). In all these localities the conglomerates are composed of an assortment of pebbles representative of rocks from Trinity Peninsula, fragments of sandstone and basalt cobbles set in a relatively fine-grained green or buff-coloured tuffaceous matrix, which is friable and quartzose.

The structure of the conglomerates varies from one locality to another. Bedding is well developed in the conglomerate on the west side of Croft Bay (Plate IIa), while those on the north and south sides of the Hobbs Glacier snout are more massive (Plate IIb). At the Croft Bay locality 17 specimens of plutonic rocks and greywacke pebbles characteristic of Trinity Peninsula rocks were collected. A comparison with some of the specimens of the Andean Intrusive Suite and Trinity Peninsula Series collected in 1961 by N. Aitkenhead indicates that the source area of these rocks is near the head of Sjögren Glacier, 27 miles (43·4 km.) west of Persson Island (Map 1). Although no representative sampling was carried out from the more massive conglomerates near Hobbs Glacier, it is believed that the pebbles in these rocks were derived from a similar area. Nordenskjöld (1905, p. 240–41) also described blocks from the conglomerate near Hamilton Point and concluded that the plutonic rocks amongst them have Andean affinities. The presence of Andean Intrusive Suite pebbles in these basal conglomerates indicates that the intrusions of Trinity Peninsula had not only been emplaced but uplifted and eroded before the close of the Lower Miocene (cf. Standring, 1956; Hooper, 1962).

There is a similarity between the matrix of the conglomerate from the Croft Bay locality and that from the north side of Hobbs Glacier. The matrix of the tuffaceous conglomerate from west Croft Bay (D.3738.4) is an epiclastic volcanic sandstone (Fisher, 1961), composed predominantly of relatively angular quartz grains and additional grains of plagioclase and alkali-feldspar, small clasts of a quartzo-feldspathic mosaic, minor zeolites and some calcite. The abundant quartz grains and the unusual grains of quartzo-feldspathic material, together with undoubted pebbles from the James Ross Island Volcanic Group, indicate that this rock had a mixed provenance. It is possible that the quartz and quartzo-feldspathic grains have not been re-worked from the Upper Cretaceous sandstones but have been derived from the Upper Jurassic volcanic rocks which occur on the east coast of Graham Land (personal communication from N. Aitkenhead).

Like the rock described above, the tuffaceous conglomerate from the north side of Hobbs Glacier (D.4040.1) also has a sedimentary origin. It is composed essentially of quartz and plagioclase feldspar grains together with olivine-basalt fragments and subordinate tuffaceous material. In addition to these three main constituents, the rock contains individual grains of titanaugite, hornblende, muscovite, biotite, chlorite, iron ore and zircon. Although the titanaugite grains are rounded, as are all the other grains in the rock, they are still fresh. However, there is no fresh olivine in the rock, and even those crystals which were probably olivine in some of the basalt pebbles have been converted wholly (or in one case partially) to chloritic alteration products. The high percentage of quartz grains in this rock points to their derivation from the underlying sandstones as well as from alluvial sand transported with the foreign erratics from north-east Trinity Peninsula. The sandstone fragments themselves were probably derived from the Upper Cretaceous sediments.

The included olivine-basalts are typical of the volcanic group and were probably derived from one of the earliest formed palagonite-breccias. Specimen D.3738.3, an olivine-basalt pebble from the Croft Bay conglomerate, was examined in thin section and found to have a texture very similar to a specimen from the centre of a basalt pillow (D.4078.2; p. 16). Some of the amygdales in this rock are composed of

a carbonate mineral but others are of analcite. There is also some primary interstitial analcite, which, together with the strong purple-pink coloration of the titanaugite, suggests a relatively alkaline basalt (Macdonald and Katsura, 1964, p. 90). The incorporation of James Ross Island Volcanic Group basalt pebbles in conglomerates of the same group was made possible not only by the overlap in time between Lower Miocene sedimentation and the first eruptions (p. 6) but also by the very nature of this vulcanicity, which was often localized in time and place and did not always affect the whole area. Although these tuffaceous conglomerates occur beneath volcanic rocks of phase II (Map 1), they have been included in Map 2A for the sake of clarity. Because the tuffaceous conglomerates are not necessarily the oldest rocks of the volcanic group, they only mark the base of the succession in particular localities.

During this study of the James Ross Island Volcanic Group, the only fossils found were present in the conglomerates on the west side of Croft Bay. They are the white fragmentary remains of a thin-shelled lamellibranch, provisionally identified by B. J. Taylor as *Panope* sp. Since this fossil has a time range from Jurassic to Recent, it is of little value for dating purposes.

2. *Rocks of phase I*

The distribution of the rocks forming phase I is shown in Maps 1 and 2A. Their occurrence is largely confined to a 25 miles (40·2 km.) wide zone trending south-south-west to north-north-east through the centre of James Ross Island. To the east and west of this zone, which is probably a reflection of the pre-James Ross Island Volcanic Group palaeogeography (p. 58), the flow lavas may have been penecontemporaneously eroded and re-deposited nearby as subaqueous tuffs or epiclastic volcanic sandstones. Although the lavas and palagonite-breccias are probably directly related to one another, they have strongly contrasting lithologies, and for this reason they are described separately.

a. *Palagonite-breccias.* The coarsely bedded palagonite-breccias dip at 28–41° with the majority of beds dipping at approximately 35° (Plate VIIc). The bedding becomes less steep and almost asymptotic towards the bases of all the palagonite-breccia units, which have an average thickness of 500 ft. (152 m.). Occasionally, large lenticular masses up to 20 ft. (6·1 m.) long and 10 ft. (3·0 m.) thick occur at the bases of the palagonite-breccia units. They are probably large-scale pillows, indicating that not all the flow lavas brecciated on coming into contact with sea-water.

Lithologically, the palagonite-breccias consist of numerous complete and fragmented pillows of olivine-basalt set in a coarse-grained tuffaceous matrix. The pillows generally range in size from 3 in. (7·6 cm.) to 3–4 ft. (0·9–1·2 m.) in diameter and are often sub-spherical or ellipsoidal in shape. In some cases the pillows have developed a contorted crustal flow structure (Plate IIc); in others, lava drips, still pointing downwards, have been developed from the roofs of pillow cavities. Not all of the pillows are complete and in most examples numerous fragments can be found, probably indicating a late-stage disruption of the cooling masses. The proportion of basalt pillows present in the palagonite-breccias is variable, ranging from 10 to 50 per cent. In some instances it is considerably higher, possibly 80 or 90 per cent, and in these rocks the bedding, which is often ill-defined, may be completely indistinct.

A rhythmic concentric zoning is frequently developed parallel to the margins of the pillows and it may also be observed in many of the olivine-basalt pillow fragments (Plate IId). This zoning, which is best seen on a weathered surface, consists of a series of light bands (weathering rust-red), separated by dark bands with a glassy appearance. The alteration of dark and light bands may be repeated up to five times, a dark glassy band always forming the outer margin of the pillow (Plate VIIIa). The zoning is particularly well developed on the exposed faces of radial cracks in the pillows but it does not appear to form complete concentric shells, because the zones die out approximately 1 in. (2·5 cm.) from the faces of the cracks.

Under the microscope, a thin section across the zoning in a pillow fragment from the Lachman Crags area (D.3749.1) shows that the zoning is due to the local concentration of finely divided iron ore. The dark glassy bands, which are representative of the olivine-hyalobasalt constituting the greater part of the pillow, are effectively chilled selvages. The bands consist of olivine phenocrysts and smaller plagioclase feldspar laths set in a matrix of brown basalt glass (Plate VIIIb). The plagioclase crystals, which are slightly zoned and have an average composition of $Ab_{50}An_{50}$, sometimes carry two small olivine crystals situated in minor indentations on opposite sides of the mid-points of the laths. In this case, the twinning of the feldspars is symmetrical about the mid-point.

However, in the bands which weather to a rust-red colour the same mineral assemblage is set in a

matrix of basalt glass charged with iron ore dust (Plate VIIIc). Modal analyses of these two contrasting bands are given in Table III. The most significant difference between the two zones is the "iron ore" content, which is 19 times greater in the iron-rich band than in the glassy one. Minute iron ore and probable picotite octahedra are present in both zones, but the main bulk of the iron ore in the enriched band consists of finely disseminated dust, which is frequently concentrated around the margins of the phenocrysts and microlites. The greater concentration of olivine and plagioclase crystals in the glassy zone, which is indicated in Table III, may be due to counting errors in the analysis of the iron-rich band. The highest concentration of opaque ore minerals in the iron-rich zone occurs in the areas immediately adjacent to the larger crystals (Plate VIIIc), and could mask some of the smaller microlites visible in the zone containing a clear basalt-glass groundmass. Chemical analyses of "basalt glass" (olivine-hyalobasalt) and a "basalt" from a few inches away (Table VIII, analyses 15 and 16; Prior, 1899) suggest that, in fact, the glassy zones may be slightly more iron-rich than the more crystalline ones. It is suspected that the apparently high concentration of iron ore in some bands of specimen D.3749.1 is due to incipient separation from the glass, indicating a slightly faster cooling rate in the more glassy bands.

TABLE III

MODAL ANALYSES OF TWO CONTRASTING ZONES OF OLIVINE-HYALOBASALT (D.3749.1)

	Glassy Zone (per cent)	*Iron-rich Zone* (per cent)
Glass	58·6	35·3
Olivine	14·3	11·6
Plagioclase	23·8	18·6
Iron ore	1·6	30·3
Others*	1·7	4·2

* Includes small vesicles containing chlorite due to recrystallization of palagonite, and fine palagonite-filled cracks.

The nature of the palagonite-breccia matrix, which encloses the basalt pillows, is clearly revealed by the examination of thin sections. In all the palagonite-breccias studied (D.3302.1, 3726.1, 4068.2) the matrix is composed of olivine-hyalobasalt fragments with a considerable range in size, which are either rimmed by or, if small enough, completely altered to clear yellow isotropic palagonite, the gel-palagonite described by Peacock and Fuller (1928). The fragments are normally cemented together by zeolites (p. 31). The individual olivine-hyalobasalt fragments, which are notably free of vesicles, consist of subidiomorphic, hollow or skeletal olivine phenocrysts and plagioclase microlites set in a matrix of brown basalt glass (Plate VIIId). The percentage and average size of the feldspar microlites vary from one rock to another but they are normally smaller than in associated basalt pillows. The olivines, which contain minute octahedra of picotite and other spinellids, are commonly hollow or skeletal and some isolated fresh crystals, probably the remnants of totally palagonitized olivine-hyalobasalt fragments, occur in the matrix. The olivine phenocrysts (in the composition range Fa_7–Fa_{14}; p. 54), whether surrounded by glass or palagonite, are fresh. In some instances, olivine crystals at the margins of the olivine-hyalobasalt fragments are partially surrounded by glass and partially by palagonite, but they are unaltered and present sharp boundaries to all enclosing material (Plate VIIIe). Contraction cracks, which have developed in the basalt glass around the more equidimensional olivine crystals, are commonly arranged eccentrically around the phenocrysts and they may coincide with a crystal face on one side (Plate VIIIf). They presumably indicate the difference in cooling strain between the basalt glass and the olivine, that in the olivine being the greater. These cracks are similar to the perlitic cracks produced by the hydration of obsidian to perlite, where they are developed around non-hydrated cores of obsidian (Ross and Smith, 1955). The hydrothermal alteration of rocks is commonly believed to produce marked changes in olivine

to intergrowths of chlorite and hematite, sometimes called iddingsite (Smith, 1959). Here, no such changes have resulted and the freshness of the olivine crystals in close proximity to palagonitized olivine-hyalobasalt fragments could mean that the palagonitization process effectively sealed and cemented the rock fragments in a relatively low pressure and temperature environment.

Hollow feldspar microlites with an average composition of labradorite occur in addition to hollow olivine phenocrysts, and it appears that the plagioclase in these rocks is slightly more susceptible to alteration than the olivine. Although isolated plagioclase crystals and those surrounded by palagonite in specimens D.3302.1 and 3726.1 are fresh and unaltered, feldspar crystals similarly situated in specimen D.4068.2 have been altered to a cloudy, slightly birefringent brownish substance, which is possibly fibro-palagonite (Peacock and Fuller, 1928). The alteration of the feldspars and the hyalobasalt fragments has probably been caused by the same agencies.

The basalt glass forming the groundmass of the olivine-hyalobasalt fragments, which are significantly poorer in vesicles or amygdales than those occurring in many palagonite-tuffs (p. 15), is clear, brown and isotropic. Microscopic compositional variations, the presence of crystallites and sometimes abundant vesicles hinder the satisfactory determination of the refractive indices of these basalt glasses by normal immersion methods. In some fragments the compositional variation is so marked that one edge of the fragment has a refractive index lower than that of the liquid, while the opposite edge is higher. This effect was normally observed in fragments containing a plagioclase microlite or part of an olivine phenocryst. The basalt glasses from palagonite-breccias and pillow margins gave the most consistent results, while those from the finer-grained palagonite-tuffs, which are usually highly vesicular, were more difficult to work with. The refractive indices of the James Ross Island Volcanic Group basalt glasses are in the range 1·583–1·598 (Table IV). Olivine-basalt glasses with refractive indices in the range 1·591–1·599 have been reported from the Jones Mountains of western Antarctica (Craddock, Bastien and Rutford, 1964). Muir and Tilley (1964, p. 412) have recently described olivine-hyalobasalts with transitional or alkaline affinities from the Mid-Atlantic Ridge. The refractive index of the basalt glass in these rocks varies from 1·589 to 1·592. The similar refractive indices of all these alkali olivine-basaltic glasses contrast with those of Icelandic tholeiitic basalt glasses, which are in the range 1·604–1·615 (Tyrrell and Peacock, 1926). There appears to be a clear distinction between the refractive indices of alkali-basalt glasses (~ 1·59) and tholeiitic basalt glasses (~ 1·61).

TABLE IV

REFRACTIVE INDICES OF BASALT GLASSES

Specimen Number	*Rock Type*	*Refractive Index*
D.3302.1	Palagonite-breccia (phase I)	1·589±0·002
D.3751.1	Palagonite-tuff (phase ? III)	1·583±0·002
D.3813.2	Palagonite-tuff	1·583±0·002
D.4068.2	Palagonite-breccia (phase I)	1·598±0·002
D.4078.2	Pillow margin (phase II)	1·594±0·002
D.4098.5	Palagonite-tuff	1·592±0·002

Although compositional variations make the determination of basalt-glass refractive indices difficult, more accentuated variations in the gel-palagonite make the precise measurement of its refractive index virtually impossible. Since variations of 0·002 have been observed in the refractive index of a single 85–100 mesh fragment of gel-palagonite, it is meaningless to quote a single refractive index for this material. The refractive indices of James Ross Island Volcanic Group gel-palagonites are in the range 1·500–1·520, which is comparable with that of 1·48–1·52 determined by Tyrrell and Peacock (1926) for Icelandic gel-palagonites. Craddock, Bastien and Rutford (1964) have measured refractive indices as low as 1·404 in palagonite from the Jones Mountains, but they observed that the yellow isotropic

palagonite has a refractive index of 1·51. The zeolites which cement the palagonite-breccias are discussed on p. 31.

b. *Olivine-basalt flow lavas.* The flow lavas differ from the palagonite-breccias in nearly every respect. Twenty-five or more individual flows, from 10 to 20 ft. (3·0 to 6·1 m.) thick and often lenticular in cross-section, have been observed in several cliff exposures. Their attitude is always sub-horizontal. One common feature of the lava flows, particularly of their upper surfaces, is their great vesicularity, probably indicating a high volatile content at the time of eruption. Both their vesicularity and sub-horizontal attitude suggest that most of the lavas were very mobile. Poorly developed columnar jointing has been observed in some of the early flows of phase I but it is an atypical feature. Macroscopic crustal flow structures have been observed only on fallen or ice-transported blocks from the cliffs. Even where access to the cliff tops had been gained, it was impossible to see the surface of any flow because of the snow cover, frost-shattered flags and lichens. Pahoehoe or ropy lava surfaces are typical.

All the lavas are olivine-basalts, ranging in colour from black to pale grey and occasionally red, and in texture from porphyritic and trachytic to uniformly aphanitic. Specimen D.3711.3, from Beak Island, is typical of the dark fine-grained holocrystalline basalts of phase I. It is porphyritic and consists of magnesian olivine ($Fo_{90}Fa_{10}$) and opaque iron ore phenocrysts, often in glomeroporphyritic aggregates, set in a fine-grained groundmass (Plate IXa). The groundmass of this rock, which possesses a fairly marked trachytic texture, is composed of plagioclase microlites, minute stubby clinopyroxene prisms and myriads of opaque ore granules. The groundmass contains many small interstitial crystals of analcite, which is considered to be pyrogenetic in view of the very fresh compact nature of this rock.

Specimen D.3771.1, from the south side of Tail Island, is a rock similar to the basalt from Beak Island, apart from the phenocryst minerals it carries. A characteristic microcrystalline groundmass of plagioclase, pyroxene and iron ore contains individual phenocrysts of magnesian olivine, calcic plagioclase and sparse titanaugite, or glomeroporphyritic clusters of all three minerals together (Plate IXb). The plagioclase phenocrysts sometimes contain minute feathery or rounded inclusions which may be spinel. The plagioclase also shows oscillatory zoning, a feature which is nearly always present in phenocrysts of this mineral. The texture is faintly trachytic. One vesicle containing secondary analcite has been observed, suggesting that other minute interstitial areas and crystals of a colourless isotropic mineral, probably also analcite, may have been formed at a late stage in the crystallization of the rock. The probable occurrence of pyrogenetic analcite in these lavas testifies to the alkaline affinities of all the basalts of this volcanic group (p. 47).

An olivine-basalt from the north coast of Vega Island (D.3722.1) contains approximately 20 per cent of partially crystallized semi-glassy groundmass. The rock consists of magnesian olivine and plagioclase ($Ab_{40}An_{60}$), and second-generation plagioclase in ophitic intergrowth with titaniferous augite set in an ore-rich semi-glassy matrix. The semi-glassy groundmass is composed of zoned feathery titanaugite showing high dispersion and anomalous interference colours, small plagioclase laths, minute hollow olivine crystals and iron ore. The small plagioclase laths in the groundmass evidently crystallized before the glass devitrified, and they have a similar appearance to the feldspar microlites in the olivine-hyalobasalt fragments of the palagonite-breccia. Likewise, the hollow olivine crystals, which are elongated along the *a*-axis (Kuno, 1950), are probably of primary crystallization suggesting that the subsequent partial crystallization has only produced the feathery titanaugite and iron ore dust. There are many vesicles which are either open or lined with minute granular chabazite crystals (p. 32). One or two vesicles contain a lining of an almost isotropic, dusty brown substance. However, a very weak birefringence can be detected in some of this material, which suggests that it is behaving optically as a crystal aggregate. Pockets of layered clay minerals have been deposited in the open vesicles of some palagonite-breccia pillows and it is believed that similar sedimentation sometimes affected the lavas. The brown substance, probably darkened by the presence of iron oxides, has been tentatively identified as a clay mineral aggregate.

c. *Subaerial palagonite-tuffs.* The distribution of these palagonite-tuffs, which are uncommon in comparison with the lavas and palagonite-breccias, is shown in Map 2A. Their bedding dip, which is often difficult to distinguish, is commonly between 10 and 20°. The relatively minor quantities of subaerial tuffs and their frequent lack of bedding make their relationship to the other rocks obscure. It is also difficult to distinguish palagonite-tuffs formed by true subaerial pyroclastic activity from those produced predominantly by the direct interaction of molten lava and water or ice (p. 36). Hyalobasalt fragments

containing considerable quantities of basalt glass or its alteration products are a good indication of the latter type and, where these are absent in palagonite-tuffs of finer grain-size and sub-horizontal stratification, the presence of sedimentary structures commonly associated with subaqueous deposition, e.g. ripple-bedding and small-scale cross-lamination (p. 16), may suggest the mode of origin. A feature believed to be indicative of primary subaerial pyroclastic tuffs is the presence of shards and assorted accidental blocks of pre-consolidated lava in the same rock. However, tuffs formed in such an open environment as that which obviously prevailed in this area will probably have a mixed provenance.

Two palagonite-tuffs from Beak Island are typical of the subaerial type. Specimen D.3713.3 consists of individual olivine crystals and fragments of vesicular basalt containing feldspar microlites approximately 0·1 mm. long set in a groundmass of palagonitized vesicular hyalobasalt fragments and shards. The alteration of the hyalobasalt fragments is relatively far advanced, since nearly all the palagonite has been recrystallized to chlorites and there are many zeolite amygdales. Very little fresh basalt glass remains. This rock is unusual in that there has been some marginal alteration of the isolated olivine crystals in the groundmass. The alteration may have been initially to chlorophaeite but, in keeping with the recrystallization of the palagonite to chlorites, recrystallization has also occurred in the margins of the olivine phenocrysts. They now consist of a core of unaltered olivine immediately surrounded by a thin shell of carbonate mineral, possibly magnesite, and a mantle of chloritic material with a fibrous structure arranged radially to the olivine core. The olivine cores and surrounding alteration products form complex partial pseudomorphs, the overall outlines of which coincide with the original olivine crystal boundaries.

The second palagonite-tuff (D.3714.3) is essentially the same as the previous rock, except in its degree of alteration. Although recrystallized fibro-palagonite is present, the degree of palagonitization is not so extensive and isolated olivine crystals are entirely fresh. This rock is also characterized by the presence of included basalt fragments of various types. One curious feature of the vesicular hyalobasalt fragments in this rock is the development of micro-spiracles from the vesicle walls. In a vesicle of 0·072 mm. diameter, the micro-spiracles have an average length of 0·01 mm. and a tubular cross-section of 0·001 mm. The micro-spiracles are tubular at the vesicle wall but they become more lobate and bifurcating with distance from the wall. It is not known whether these features were formed during the initial consolidation or the subsequent alteration of the rock.

d. *Subaqueous palagonite-tuffs.* There are thought to be two genetically distinct types of subaqueous palagonite-tuff in this volcanic group.

i. Massive palagonite-tuffs, consisting solely of scoriaceous hyalobasalt fragments together with some individual crystals.

ii. Well-stratified palagonite-tuffs of variable grain-size but relatively well sorted, which sometimes contain cognate vesicular olivine-basalt fragments of a single type.

It is believed that these types, which are distinguished from the palagonite-breccias by uniformly finer grain-size, greater vesicularity and an absence of pillows, are due to the direct interaction of very hot basalt lava with water. However, it should be re-emphasized that the clear genetic distinction between one type of palagonite-tuff and another may not be possible, even though there is little doubt as to the nature of the environment in which the individual components of a tuff finally coalesced to form a rock.

The first type of subaqueous palagonite-tuff occurs at the centre of lava and palagonite-breccia volcanoes, where the tuffs form a sub-conical core on which the later palagonite-breccias were deposited. Specimen D.3785.2, from Brown Bluff (Plate IIIa), is typical of these rocks. It consists entirely of palagonitized scoriaceous hyalobasalt fragments, ranging in size from 2 mm. downwards, and olivine phenocrysts ($Fo_{91}Fa_9$) containing many inclusions of picotite and opaque ore octahedra. There is a distinct lack of shards in this tuff. The vesicles and interstices are occupied by zeolites and calcite, which evidently formed later than the zeolites and occasionally fills the cavities of zeolite-lined vesicles. Other rocks of this type occur at Lockyer, Eagle and Red Islands (Plate Id; Map 1).

Other massive subaqueous tuffs of primary deposition are typified by a palagonitized vitric crystal tuff from eastern Croft Bay (D.3729.1; Fig. 1). The hyalobasalt fragments in this rock have been completely altered to a clear yellow palagonite, and a further stage has been reached than in most palagonite-breccias with the development of a rim of cloudy fibro-palagonite around the fragments. The crystals include angular to sub-rounded olivines and tabular plagioclases. The rock is cemented with fibrous phillipsite, which displays an excellent radial structure (Plate XIe).

In contrast, the well-stratified and sorted palagonite-tuffs display several characteristic sedimentary structures, although they are equally fine-grained. The two localities where these rocks are most extensively developed are near Cape Gage and Rink Point. In both of these localities the tuffs are associated with palagonite-breccias of phase I, which are not overlain by flow lavas but are succeeded directly by a second palagonite-breccia unit. The finely laminated bedding of these rocks is almost horizontal (Plate IIIb). Farther north at Tail Island (Map 1) there are some very fine-grained palagonite-tuffs in which ripple-bedding, a characteristic feature, is well developed (Plate IIIc). The inferred current directions suggest that these rocks were deposited in a sedimentary basin between the Egg Island volcanic centre and the centre in north-east Eagle Island (Map 1). Interbedded in the otherwise undisturbed tuffs at this locality is an intraformationally deformed stratum (Plate IIIc, d). The deformation becomes progressively more intense from north-east to south-west (in the direction of the Egg Island volcanic centre) and in approximately 20 ft. (6·1 m.) the uniform laminae are transformed into a completely disrupted bed. Since the underlying tuffs are undisturbed, there was evidently a plane of slip between the deformed bed and those below. It is therefore suggested that the deformation is due to slumping of the tuffs concerned after they had been dislodged by a volcani-seismic disturbance, and that the resultant uneven surface was subsequently levelled by current action. The sub-horizontally bedded tuffs at the west end of Tail Island are overlain by an unusual development of epiclastic volcanic conglomerate, composed of subaqueous palagonite-tuff blocks embedded in a palagonite-tuff matrix. Marine tuffs also occur near Cape Lachman, where Bibby (1966) reported that they are interbedded with pillow lavas.

3. *Rocks of phase II*

The lavas, palagonite-breccias and other rocks of phase II occur nearly everywhere in this area except at Vega Island and the islands in Prince Gustav Channel (Maps 1 and 2B). In some places the phase II lavas and palagonite-breccias rest on those of phase I, but over a large part of this area they rest directly on Upper Cretaceous sediments, at which junction tuffaceous conglomerates have been developed (p. 10). The palagonite-breccias of phase II are up to 1,000 ft. (305 m.) thick where they fill depressions in the pre-Miocene topography (p. 59) but on average they are approximately 500 ft. (152 m.) thick. This is strictly comparable with the thickness of those of phase I, and where phase I and II lavas and palagonite-breccias are superimposed, there is a difference in height of the lava/palagonite-breccia horizons of 500–600 ft. (152–183 m.). An overlap structure, which lowers the lava/palagonite-breccia horizon by 300 ft. (91 m.) and occurs at several localities on James Ross and Jonassen Islands (Map 2B; Fig. 4), is a unique feature of the phase II lavas and palagonite-breccias, which has been used for correlation purposes.

Furthermore, the phase II lava/palagonite-breccia horizon at Jonassen and Andersson Islands becomes progressively lower towards the south until, at the south-west end of Andersson Island, only lavas are visible above sea-level (Map 1). Ashley (1962), in interpreting a magnetic survey of Tabarin Peninsula, has suggested the presence of a southward dipping surface delineating the base of a "lava flow". Since Tabarin Peninsula is immediately to the west of Jonassen and Andersson Islands, it is possible that the structure is continuous from the islands to the peninsula.

a. *Palagonite-breccias.* Lithologically, the palagonite-breccias of phase II are virtually identical with those of phase I. Very similar zoned olivine-hyalobasalt pillows and fragments occur in a strictly comparable matrix of palagonite-tuff.

Two thin sections have been cut from a pillow fragment in the palagonite-breccias at Cape Obelisk (D.4078.2). Section D.4078.2A, cut across the margin of the pillow, shows excellently the gradation from almost clear basalt glass (Table IV) at the edge of the pillow into the adjacent turbid zone (Plate VIIIa). Clear basalt glass, carrying the usual assemblage of olivine phenocrysts ($Fo_{76}Fa_{24}$) and feldspar microlites, gives way to a groundmass rendered almost totally opaque by the incipient crystallization of iron ore and pyroxenic spherulites (Lacroix, 1936).

Both the glassy margin and the inner zone contain some amygdales and an interesting contrast of amygdaloidal material is shown. The vesicles in the inner zone are irregular to sub-spherical in shape and they contain only analcite, which commonly forms a lining on the cavity walls. Occasionally, however, it fills the vesicle completely, although it can be seen that a cavity lining of radiating crystals was formed initially and subsequently more massive crystalline analcite occupied the remainder of the cavity. In the hyalobasalt margin the amygdales are very different from those in the inner zone and more variable.

A common feature is a small zone surrounding the vesicle, composed of hair-like aggregates of crystalline iron ore. If, as is often the case, palagonitization of the basalt glass occurred immediately adjacent to the cavity wall, the clear palagonite zone is followed by the turbid zone. The palagonite itself shows some degree of incipient order into a fibrous radiating crystal structure, probably fibro-palagonite. The first lining inside the cavity wall is composed of radiating phillipsite crystals of low birefringence. There is an inner zone of crystals, which are slightly pleochroic from pale yellow to yellow-green and whose birefringence is of the same order as biotite. These crystals may be a mica, although they are too small for positive identification. Sometimes clear isotropic analcite occurs in the centre of the vesicle.

Although there are many cracks in the rock, some of the amygdales may be composed of crystalline material which was originally present in concentrated aqueous solution. The marginal palagonitization of some of the vesicle walls was probably caused by reaction of the basalt glass with juvenile water.

One immediately apparent feature of the material at the centre of the basalt pillow (D.4078.2B) is the greater size of the feldspar crystals, indicating that crystallization had proceeded to a far more complete stage in the core. Here, the feldspar crystals, which are completely fresh in the hyalobasalt margin, are somewhat sericitized and cracked. Subidiomorphic, embayed, skeletal and hollow olivine phenocrysts are also present but they are no longer than those which occur in other olivine-hyalobasalts. Very much smaller plagioclase crystals, accounting for a large proportion of the groundmass, are sometimes rectangular and hollow.

The interstices are occupied by the usual titanaugite/iron ore intergrowth in which there are platy magnetite crystals. The platy iron ore crystals have a range of preferred orientations depending on their position in the rock and, if this direction is coincident with a feldspar lath, then a high concentration of iron ore will have crystallized along the margins of the feldspar (p. 12). Numerous small intercrystalline cavities are filled with radiating zeolite, possibly thomsonite, and in one case analcite was observed filling a central cavity. These intercrystalline cavities are in marked contrast to the genuine vesicles and they suggest that the minerals they contain may be pyrogenetic.

Specimen D.3745.2, the core of an olivine-basalt pillow from the palagonite-breccias forming Leal Bluff, Vega Island (Map 1), is a remarkable rock in that it contains olivine phenocrysts whose cores have been preferentially replaced by bowlingite. Although it is probably a multi-crystalline aggregate, this mineral behaves optically as though it were a single crystal. It is fibrous, length slow and displays birefringence colours in the second and third orders. It is curious that, although the cores of many of the olivine phenocrysts have been completely replaced, this does not apply to every phenocryst in the thin section. There appears to be a correlation between size of the phenocryst and susceptibility to alteration, the larger phenocrysts being the more commonly and completely altered. However, this appearance could have been produced by the passage of the plane of the thin section tangentially through the unaltered margins of some olivine phenocrysts. The remainder of the rock consists of plagioclase laths, sometimes with associated clusters of small olivine crystals near their mid-points, set in a very dark indeterminate matrix.

Sedimentary rocks composed largely of basalt-glass grains have been found at the base of the palagonite-breccias which form Leal Bluff, Vega Island, and are also interbedded with the palagonite-tuffs at Bibby Point, James Ross Island (p. 22). The macroscopic appearance of the sedimentary rock from the base of Leal Bluff (D.3746.1) is that of a well-indurated shale in which a distinct lamination is visible. Microscopically, it can be seen that the glass fragments are more rounded, much smaller and better sorted than those in the palagonite-tuffs of primary deposition. In one thin section there are three distinct laminae, each of which is slightly graded. The central lamina is composed of basalt-glass grains which are as rounded as those in the other two but are distinguished from them in carrying their own genetically related palagonite rims, evidently developed *in situ* (p. 30). The basalt-glass grains in the other two laminae are fresh to their edges except where a marginal vesicle encloses pre-formed palagonite. The roundness of the basalt-glass grains varies from very angular to sub-rounded (Powers, 1953) as opposed to the uniformly very angular shards in many palagonite-tuffs. The long axes of the basalt-glass grains have a preferred orientation in the plane of the lamination.

In addition to the basalt-glass grains, the rock contains grains of crystalline material and olivine-basalt lava of comparable size and roundness. These include splintered fragments of olivine phenocrysts and clusters of much smaller olivine crystals, quartz grains showing some strained biaxiality and several crystals of pleochroic green hornblende. There are also some bright green patches of glauconite, which

are similar to those occurring in the tuffaceous conglomerate from the Hobbs Glacier area (D.4040.1). The matrix of the laminae containing fresh basalt-glass grains is composed of indeterminate clay-sized material but the lamina which contains the palagonitized grains is more porous. It is this difference in porosity which probably accounts for the selective *in situ* palagonitization of the basalt-glass grains in individual laminae. Although marked temperature gradients over relatively short distances appear to have existed during palagonitization, differences in the degree of palagonitization in this rock are more probably due to differences in the spatial arrangement of the grains. Zeolites, including analcite, thomsonite and chabazite, have been formed interstitially.

This rock (D.3746.1) occurs as a 6 ft. (1·8 m.) thick bed, which is intercalated between palagonite-breccias and the underlying Upper Cretaceous sandstones. It is probably a marine sediment, representing a relatively deep-water (approximately 350 ft.; 106 m.) facies produced as a result of wave attack upon a static or advancing palagonite-breccia slope.

b. *Flow lavas.* Compared with the palagonite-breccias of phase II, the flow lavas show rather more diversity of type than those of phase I. They are approximately 750 ft. (229 m.) thick at Lachman Crags (Map 1), the greatest thickness of flow lavas observed in this area. Some of the lavas south-east of Bibby Point rest directly on Upper Cretaceous rocks (Map 1). It is here that a cylindrically jointed basalt, interpreted as the filling of a lava tunnel (p. 40), occurs immediately beneath the flow lavas. The lavas and the rock filling the tunnel are very similar mineralogically and they are typical holocrystalline ophitic olivine-basalts (D.3759.1, 2). The olivine occurs as individual phenocrysts and also as glomeroporphyritic clusters. The plagioclase, which is ophitically intergrown with titaniferous augite, is slightly zoned but it has an average composition of $Ab_{50}An_{50}$. The titanaugite of specimen D.3759.2 has relatively strong pleochroism, with α = pale pink, β = purple-pink and γ = pale yellow. Small amounts of calcite and biotite occur as accessory minerals adjacent to some of the olivine crystals. Modal analyses of these two rocks are shown in Table V.

A very much more altered lava (D.3753.2) was collected from Lachman Crags nearly 3 miles (4·8 km.) south-east of the last-mentioned locality. It is a pink vesicular lava consisting of intercalated coarse- and fine-grained types. The coarse-grained rock is composed of uralitized olivine and plagioclase together with ophitically intergrown titanaugite and plagioclase. Iron ore rims the olivine crystals and zeolite-lined vesicles are scattered throughout the rock. Some of the olivine crystals contain minute inclusions of picotite and opaque iron ore.

The fine-grained rock, which occurs as a single lamina 10 mm. thick, apparently contains no olivine, although one small very altered crystal was observed. The rock consists of near-idiomorphic feldspar, acicular pyroxene crystals, strings of iron ore grains and iddingsite-like alteration products which may or may not have originated in the rock. The pyroxene is not as titaniferous an augite as usual, which is an indication of a departure from the general characteristics of olivine-basalts. In the groundmass there are many intercrystalline cavities lined with radiating growths of almost isotropic zeolite, whose genesis appears to have been by partial analcitization of the plagioclases. This is the only lava from the James Ross Island Volcanic Group examined so far which does not contain olivine in significant quantity. This rock may be an andesitic derivative.

Segregation veins occur in the coarse lavas approximately 3 miles (4·8 km.) south-west of Cape Lachman (Map 1). Specimen D.3748.1, representative of the coarse-grained ophitic olivine-basalts, consists of large titanaugite crystals up to 3 mm. across ophitically intergrown with plagioclase, and smaller olivine phenocrysts set in a groundmass of feldspar laths, second-generation olivine, iron ore and analcite. The analcite, which is believed to be primary, forms only 1 per cent of the rock (Table V) but its presence is significant. Two inclusions of glass, one of which contains an iron ore octahedron, were observed in an olivine phenocryst. Minute quantities of specular hematite occur in the groundmass.

The finer-grained part of specimen D.3748.3, which occurs immediately adjacent to one of the segregation veins, is characterized by large slightly pleochroic ophitic titanaugite crystals up to 4 mm. in length and plagioclase (approximately $Ab_{36}An_{64}$). The olivine crystals, which are ragged and altered along cracks to iron ore, iddingsite and other alteration products, occur in association with biotite and green fibrous amphibole. Interstitial primary analcite is not uncommon and it sometimes occurs with calcite and a fibrous zeolite, which is probably natrolite.

The segregation vein itself is characterized by an almost total absence of olivine (Bailey and others, 1924, p. 138) and a relatively high content of analcite and natrolite sheaves (Table V). The few olivine

TABLE V

MODAL ANALYSES OF ROCKS FROM THE JAMES ROSS ISLAND VOLCANIC GROUP

	Olivine-basalts		*Olivine-dolerite and Segregation Vein*			*Dykes*		*Volcanic Plugs*					*Dolerite and Dolerite-pegmatite*	
	1	2	3	4	5	6	7	8	9	10	11	12	13	14
Olivine	12·9	15·9	15·4	8·8	0·7	16·3	8·0	8·0	4·7	12·4	6·9	10·0	9·4	3·4
Titanaugite	15·9	14·0	15·3	21·7	18·6	14·7	16·0	18·0	21·0	14·9	12·4	12·6	14·3	5·4
Plagioclase	56·7	61·8	64·2	58·6	42·4	54·5	64·8	58·5	62·1	58·4	64·7	61·0	57·8	15·1
Alkali-feldspar	—	—	—	—	25·0	—	—	tr	tr	tr	tr	tr	6·4	30·3
Analcite and associated zeolites	0·2	0·6	1·0	2·3	6·0*†	0·7	4·1†	5·2†	4·5†	5·1†	5·8†	6·6†	3·4†	30·3†‡
Iron ore	5·5	5·2	3·3	3·3	4·6	7·6	6·1	5·3	4·4	4·0	2·9	3·5	3·8	7·0
Biotite and olivine alteration products	8·8	2·5	0·8	5·3	2·7	6·2	1·0	5·0	3·3	5·2	7·3	6·3	4·9	8·5

* Includes natrolite.
† Includes apatite.
‡ Includes thomsonite, chabazite and indeterminate alkaline mesostasis.

1. D.3759.1 Ophitic olivine-basalt flow lava; approx. 1 mile (1·6 km.) south-east of Bibby Point, James Ross Island.
2. D.3759.2 Ophitic olivine-basalt filling lava tunnel in Upper Cretaceous sediments immediately beneath D.3759.1.
3. D.3748.1 Ophitic olivine-dolerite from the base of north-west Lachman Crags, James Ross Island.
4. D.3748.3a Coarse-grained dolerite occurring immediately adjacent to the segregation vein (D.3748.3b).
5. D.3748.3b Segregation vein in ophitic olivine-dolerite; north-west Lachman Crags, James Ross Island.
6. D.3740.1 Ophitic olivine-dolerite dyke cutting palagonite-breccias at Blancmange Hill, James Ross Island.
7. D.4052.1 Subophitic olivine-dolerite dyke cutting Upper Cretaceous sandstones near Haslum Crag, Snow Hill Island.
8. D.3756.1 Analcite-bearing olivine-dolerite plug; south-west of Lachman Crags, James Ross Island.
9. D.3763.1 Analcite-bearing olivine-dolerite plug; 1 mile (1·6 km.) north-east of Stoneley Point, James Ross Island.
10. D.3800.1 Analcite-bearing olivine-dolerite plug; Humps Island.
11. D.4014.1 Analcite-bearing olivine-dolerite plug; Lonely Rock, off east James Ross Island.
12. D.4052.3 Analcite-bearing olivine-dolerite from a coarse-grained differentiate (probably a plug) adjacent to a dyke (D.4052.1); Haslum Crag, Snow Hill Island.
13. D.4086.1 Analcite-bearing olivine-dolerite typical of the country rock; south-west Palisade Nunatak, James Ross Island.
14. D.4086.3 Dolerite-pegmatite adjacent to specimen D.4086.1.

crystals which are present have ragged embayed outlines and a relatively iron-rich composition (approximately $Fo_{60}Fa_{40}$). They are similar to those occurring in the dolerite-pegmatites of the Palisade Nunatak intrusion (p. 27), but apatite crystals have not been observed inside them. The grain-size is comparatively coarse and some of the pyroxene crystals, which are frequently zoned and twinned, reach 10 mm. in length (Plate IXc). The complex graphic intergrowths of titanaugite and plagioclase, which occur in the dolerite-pegmatites of the Palisade Nunatak intrusion (p. 27), have not been observed in these segregation veins, although skeletal ilmenite occurs in both rock types. In addition to discrete crystals of green augite in the matrix, many of the titanaugite crystals are fringed with green augite or aegirine-augite, which is an indication of the alkalinity of the last stages of cooling of these rocks. The feldspars include labradorite which forms large crystals zoned to more sodic compositions at the margins, and anorthoclase ($2V\alpha \simeq 50°$; optic axial plane perpendicular to (010)). The anorthoclase, which occurs as an epitaxial overgrowth on plagioclase in certain instances, contains many acicular apatite crystals, suggesting the presence of a high proportion of mineralizers which led to the production of a pegmatitoid (Dunham, 1933). Small sheaves of natrolite occur with isotropic analcite in the interstices of the rock. The occurrence of analcite and natrolite is also in contrast to the mineralogy of the dolerite-pegmatites from the Palisade Nunatak intrusion, in which analcite is normally associated with thomsonite (p. 28).

There is a progressive decrease in the olivine content, coupled with a progressive increase in the proportion of analcite and other alkaline mesostasis, from the host rock into the segregation vein (Table V). This is a small-scale trend of alkaline differentiation, which is strictly comparable to the formation of dolerite-pegmatites in the Palisade Nunatak intrusion. However, no felsitic veins, such as those occurring in the Palisade Nunatak intrusion, have been observed in the lavas of phase II.

c. *Palagonite-tuffs.* As in phase I, palagonite-tuffs form only a small proportion of the rocks of phase II (Map 2B). The most interesting occurrence is at Rosamel Island, a steep-sided island in Antarctic Sound composed entirely of these tuffs. On the south-east side of the island there is a shallow embayment backed by steep cliffs, connecting the ends of which is an almost circular reef just beneath sea-level. Viewed from the air, it is clear that this embayment forms part of a crater wall, whose outline is now preserved by the reef. The dip of the tuff beds away from the position of the crater varies between 5 and 10°.

Palagonite-tuffs also occur near the south coast of James Ross Island, and 1 mile (1·6 km.) south of the Hobbs Glacier snout there is a structure which has been interpreted as an ash cone, possibly formed subaerially during the early stages of the phase II eruptions (p. 38). Carlson Island, in Prince Gustav Channel (Map 1), is composed entirely of primary palagonite-tuffs which were probably deposited in sea-water and are associated with lenses of pillow lavas (Plate Va), in which crystalline gypsum has been formed. The tuffs are generally massive orange-weathering rocks but they are very dark on fresh surfaces. They are vitric tuffs, composed largely of palagonitized vesicular basalt-glass fragments up to 10 mm. across and containing numerous amygdales of spherulitic zeolite.

4. *Rocks of phase III*

a. *Lavas and palagonite-breccias.* The distribution of the lavas, palagonite-breccias and palagonite-tuffs of phase III is shown on Maps 1 and 2C, from which it can be seen that they do not occur outside the area of James Ross and Vega Islands. In many localities, particularly near the east coast of James Ross Island, there are no flow lavas overlying the palagonite-breccias. Unlike phase I, where fine-grained palagonite-tuffs are present near palagonite-breccias not overlain by flow lavas, no evidence of similar fine-grained palagonite-tuffs has been found, unless the small thickness of tuffs on top of the dome south-west of Cape Gage is all that remains of a once more extensive development. It is possible that fine-grained palagonite-tuffs were deposited seaward of the palagonite-breccias and have since been removed by erosion. Although the palagonite-breccias of phase III are very similar to those of the earlier phases, more variation has been observed in the olivine-basalt lavas.

Specimen D.4053.1, a fresh olivine-basalt from the south side of Gourdon Glacier (Map 1), is typical of the coarse-grained holocrystalline lavas. It is characterized by the presence of isolated and glomero-porphyritic clusters of olivine phenocrysts, which contain relatively abundant inclusions of picotite and opaque ore minerals. The large, oscillatory zoned calcic plagioclase crystals, which are up to 5 mm. long and also occur as phenocrysts in this rock, are unusually crowded with inclusions, comprising lenticular olivine and rare titanaugite crystals together with many rectangular grains of opaque ore minerals and spinels (Plate IXd). The inclusions are commonly confined to the cores of these phenocrysts, whose

compositions are in the range $Ab_{30}An_{70}$–$Ab_{10}An_{90}$. The phenocrysts are contained in a matrix of relatively coarsely crystalline plagioclase and titanaugite in ophitic intergrowth, and opaque ore minerals. The groundmass plagioclase has a core composition of labradorite and it is often normally zoned at the margins to more sodic compositions. However, the phyric plagioclase is usually more calcic in its composition, frequently lacks well-defined albite or Carlsbad-albite twin lamellae and nearly always displays well-developed oscillatory zoning. The individual zones are not very extensive but many oscillations often occur in a single phenocryst. Large plagioclase phenocrysts, occasionally showing signs of resorption, are characteristic of the majority of phase III lavas.

Specimen D.4053.8, from the same area, is a further example of a basalt with a semi-glassy groundmass. This rock consists of lath-shaped plagioclase phenocrysts ($\sim Ab_{30}An_{70}$), some of which contain small rounded inclusions of olivine and fresh, cracked, occasionally glomeroporphyritic olivines ($Fo_{65}Fa_{35}$) set in a very dark matrix (Plate IXe). The groundmass is composed of myriads of minute hollow olivine crystals, small crystals of titanaugite, zoned plagioclase microlites, iron ore resulting from serpentinization of olivine, minute iron ore octahedra and interstitial basaltic glass which is dusted throughout with iron ore. A fibrous zeolite is present both interstitially and in the vesicles together with later calcite. The hollow olivine crystals in the groundmass are elongated along the *a*-axis and in cross-section the short dimension of the crystal coincides with the *b*-axis (Kuno, 1950). Hollow crystals are a characteristic feature of the more glassy rocks of this group, and in the case of a lava such as this they may be evidence of its partial devitrification.

Specimen D.4053.12, another olivine-basalt from the south side of Gourdon Glacier, is an exception in that it carries no phenocrystic plagioclase. Instead, it contains a relatively large modal percentage of olivine phenocrysts (17·5 per cent) and a few skeletal titanaugite phenocrysts. Although the outlines of the titanaugite crystals suggest subidiomorphism, their very cellular appearance is unusual. The phenocrysts are set in an aphanitic groundmass of pyroxene, plagioclase and opaque ore (Plate IXf). This rock is interpreted as an olivine-rich, oceanitic basalt (p. 48).

Two very altered basalts (D.4053.13, 18) from the same area contain olivine phenocrysts almost completely transformed into iron ore and probably chlorite, which appear in the hand specimen as red spots on a background which is more leucocratic than usual (Smith, 1959). Ragged flakes of titanaugite occur in ophitic intergrowth with plagioclase, which has been analcitized along cleavage planes and cracks. Veinlets of chabazite and other zeolites traverse the rocks and some aragonite or calcite has been deposited in between the pyrogenetic minerals. In these rocks, the titanaugite crystals are rimmed to some extent by green aegirine-augite, which is in keeping with the analcitization of the feldspars and the generally alkaline nature of the alteration.

b. *Palagonite-tuffs.* Apart from the small exposure of tuffs south-west of Cape Gage, the most notable development of these rocks forms Terrapin Hill (Map 2C). They are generally medium- to fine-grained palagonitized crystal tuffs with a highly variable content of vesicular olivine-basalt fragments, weathering brown or yellow depending on whether the content of fragments is high or low. The palagonite-tuffs, which are evenly bedded in some parts and more massive in others (Plate IVa), have been eroded by wind scour into yardangs and pillars (Plate IVb).

Centred approximately 3 miles (4·8 km.) south of Terrapin Hill is a complex of three phase III volcanic centres, whose lavas have been largely removed by erosion (Map 1). The volcanic centres are arranged roughly at the corners of an equilateral triangle with an apex pointing south, and it is clear that the westernmost palagonite-breccia volcano is intermediate in age between the other two. The palagonite-tuffs of Terrapin Hill appear to be associated with the volcano of an intermediate age. The junction between the palagonite-breccias and palagonite-tuffs was observed in the base of an eastward-trending valley 2 miles (3·2 km.) south of Terrapin Hill. Here, the palagonite-tuffs rest conformably on the palagonite-breccias of the volcano and close to the volcanic centre the dip of the palagonite-tuffs follows the rapid change in dip direction of the palagonite-breccias. Towards the north, the palagonite-tuffs take on a gentle easterly dip and the bedding, which is at first massive, becomes increasingly more finely laminated and suggests that the palagonite-tuffs at a greater distance from the volcanic centre have been re-worked. Small-scale faulting, slumping and wash-outs occur near the northern extremity of the outcrop. A small cap of olivine-basalt lava, probably of phase III, occurs at the summit of Terrapin Hill.

22 miles (35·4 km.) west of Terrapin Hill, there is another extensive development of phase III palagonite-tuffs in the area between Lagrelius and Matkah Points (Maps 1 and 2C). Here, the

palagonite-tuffs can be subdivided into yellow-weathering types which are overlain by brown-weathering types. The colour difference is due largely to the difference in the proportions of included vesicular olivine-basalt fragments. The surface slopes of the hill, which are formed entirely of these palagonite-tuffs, are frequently coincident with the dip slopes of the palagonite-tuffs themselves. There is a well-defined radial structure in the bedding of the palagonite-tuffs, which are believed to be the remains of an ash cone. High on the slopes of the hill, the brown-weathering palagonite-tuffs dip radially outwards at 25–30°, while on the lower slopes in the north of the area, the dip of the underlying yellow-weathering palagonite-tuffs becomes progressively less steep at 15–20°.

On weathered surfaces, the blue-black lava fragments stand out sharply against the yellow tuffaceous matrix. Microscopic examination of a specimen of this palagonite-tuff matrix (D.4097.4) reveals that it is composed of wholly and partially palagonitized basalt-glass fragments (most of which are vesicular) and rare pockets of quartz grains. Although there has been some recrystallization of the palagonite, inter-fragmental zeolite cement is rare. The vesicular olivine-basalt fragments and blocks in the palagonite-tuffs are very fine-grained, commonly rectangular in shape and contain well-defined laminae, in which the vesicles are slightly larger and more abundant than elsewhere in the rock. Specimen D.4097.2 contains phenocrysts of olivine and glomeroporphyritic clusters of olivine and plagioclase set in an almost opaque groundmass of feldspar, pyroxene and ore minerals. One banded olivine crystal, which is larger than the other olivine phenocrysts, is probably a xenocryst (Hamilton, 1957). Although the vesicle margins are more opaque than the groundmass elsewhere in the rock and the vesicles appear to be open in the hand specimen, a very narrow lining (0·02 mm.) of chabazite occurs in some of them. The included olivine-basalt fragments and blocks in these palagonite-tuffs bear a resemblance to the vesicular olivine-basalt dykes (p. 24), many of which are strongly banded with vesicles in the vertical plane. It is possible that the included blocks in the palagonite-tuffs at this locality represent material torn from the walls of a vent, where it had cooled and crystallized prior to eruption.

Cross-laminated palagonite-tuffs of phase III also occur at Bibby Point (Map 1; Plate Vc). One of these palagonite-tuffs (D.3751.1) is composed of relatively large fragments of vesicular olivine-hyalobasalt up to 2 mm. across, containing olivine and oscillatory zoned plagioclase phenocrysts, together with rounded pebbles of holocrystalline olivine-basalt up to 7 mm. across. A relatively porous palagonite-tuff (D.3752.1) from a nearby locality contains some laminae which are relatively rich in fragmentary olivine and plagioclase crystals. Palagonitization has been extensive and all the smaller vesicular fragments and shards have been completely hydrated and largely recrystallized. This palagonite-tuff (D.3752.1) occurs with interbedded palagonitic sediments, similar to the ones described from Leal Bluff (p. 17). In contrast to the sedimentary rock from Leal Bluff, the one from Bibby Point (D.3752.2) is strictly an epiclastic volcanic siltstone. It is composed of a few very small fragments of olivine, plagioclase and quartz set in an indeterminate chloritic matrix, in which zeolites have not been recognized. The rock is structureless and has no lamination or basalt-glass grain alignment as in specimen D.3746.1. This rock is black and of low density, has a sub-vitreous lustre and breaks with a conchoidal fracture.

The sedimentary rock forms a bed 0·5–1 ft. (15–30 cm.) thick, which is intercalated with the cross-laminated palagonite-tuffs. If this epiclastic palagonitic siltstone was formed at a depth comparable to the one at Leal Bluff, then either the currents responsible for the cross-lamination of the palagonite-tuffs were active at a depth of 300 to 400 ft. (91·4 to 122 m.) or there was a considerable vertical oscillation in the depth of the basin of deposition in the Bibby Point area.

5. *Lavas and palagonite-breccias of phase IV*

As in phase III, these rocks are restricted to the James Ross and Vega Islands area, although only palagonite-breccias occur at Vega Island. The rocks of phase IV are believed to occur in an almost unbroken sheet, at least marginally to James Ross Island, south-east of a line from Skep Point to Persson Island (Maps 1 and 2D), and they are usually the last observable rock unit beneath the ice-cap margins which occur at the top of the head walls of the large glaciers. They are also present at the top of the cliffs to the south of Croft Bay and are probably responsible for the positive break in slope surrounding Dobson Dome, although exposure is poor in this area. Farther west, lavas and palagonite-breccias of phase IV cap the mesa west of Hidden Lake and form the large mesa to the east. In both of these occurrences "terminal slope" overlap structures have developed (p. 40).

The palagonite-breccias are again composed of pillows and fragments of olivine-hyalobasalt set in

a matrix of coarse-grained palagonite-tuff. The lavas are also very similar to those of other phases, being entirely olivine-basalts. Those from the lava/palagonite-breccia units, which form the mesa east of Hidden Lake are typically grey-weathering holocrystalline basalts, sometimes containing a high proportion of xenoliths (Plate Vb). Although it is difficult to determine whether the xenoliths are cognate or accidental, their similarity to the host rock containing them suggests that they may have been produced by autobrecciation.

A pale red-coloured basalt (D.4085.5) from the mesa east of Hidden Lake contains the usual assemblage of olivine, titanaugite, plagioclase ($\sim Ab_{50}An_{50}$), iron ore and accessory apatite needles. There is one large phenocryst of plagioclase, which contains numerous inclusions of pyroxene and iron ore along crystallographic planes and which is typical of phase IV lavas as well as those of phase III (p. 20). The remainder of the plagioclase occurs in ophitic intergrowth with titanaugite, at the margins of which there is a very thin shell of green augite. The subidiomorphic olivine phenocrysts contain small octahedral magnetite and spinel grains.

Segregation veins have also been found in these olivine-basalts. They commonly form a plane of weakness exploited by weathering agencies and on such an exposed surface the feldspar crystals, a large proportion of which are anorthoclase, weather pink. As in the segregation veins of the phase II lavas, olivine is subordinate and large titanaugite crystals (up to 7 mm. long) are the predominant ferromagnesian minerals. The veins are vesicular in comparison with their host lavas but their vesicularity takes the form of angular intercrystalline cavities, indicating the concentration of volatile constituents in the vein during the last stages of cooling. Acicular apatite prisms are disseminated throughout the alkali-feldspar.

6. *Rocks of phase V*

The distribution of the rocks of phase V is shown on Maps 1 and 2D and, although they are sparsely represented in outcrop, it is probable that considerably more are concealed by the ice cap of Mount Haddington. The palagonite-breccias at the south-west end of Coley Glacier and those west of Rabot Point occur on top of phase IV lavas. The phase V rocks in the cliff south of Croft Bay are composed of a highly complex series of palagonite-tuffs and palagonite-breccias surmounted by almost horizontal flow lavas. The palagonite-tuffs and -breccias form a pseudo-anticlinal structure, which is probably part of a complex strato-volcano formed initially under subaerial conditions. This volcano, together with other large cones, which may have existed near the centre of James Ross Island, probably provided a nucleus around which the marginal lavas and palagonite-breccias were deposited (p. 58).

7. *Cain and Abel Nunataks, Trinity Peninsula*

Cain and Abel Nunataks, which are situated on Trinity Peninsula approximately 8 miles (12·8 km.) north of Egg Island (Map 1), are composed of coarse- and fine-grained stratified palagonite-tuffs. These nunataks were mapped in 1961 by N. Aitkenhead and specimens were collected from one of them. Although these rocks are believed to form a small part of the James Ross Island Volcanic Group, it is not known to which phase they should be assigned. The rocks from Cain Nunatak (D.3813.1, 2) are composed of vesicular olivine-basalt fragments set in a matrix of smaller highly vesicular olivine-hyalobasalt fragments. Glass shards have not been observed. The feldspar laths in the hyalobasalt fragments show a certain amount of alignment, particularly around olivine phenocrysts. However, the phenocrysts in some of the larger microcrystalline olivine-basalt fragments consist of olivine, oscillatory zoned plagioclase and titanaugite, a relatively unusual assemblage which has also been observed in a basalt from Tail Island (p. 14). The palagonite-tuffs are not cemented with zeolites and the hyalobasalt fragments carry only a very narrow rim (0·01 mm. thick) of palagonite. A relatively abundant carbonate mineral, probably calcite, is also present. Abel Nunatak, which is encircled by open crevasses, has not been reached on foot but it is believed to be composed of similar rocks.

B. Intrusive Rocks

Except for the Palisade Nunatak laccolith, the intrusive rocks of this volcanic group are relatively insignificant. The vesicular olivine-basalt dykes and the olivine-dolerite dykes and plugs are small intrusions, which can normally be related to the formation of nearby extrusive rocks. The plugs mark

the sites of central eruptions, and some of the more extensive dykes may have reached the surface and given rise to fissure eruptions. The Palisade Nunatak laccolith is by far the largest exposed intrusion, in which per-alkaline rocks have been produced during the final stages of crystallization.

1. *Dykes*

Dykes form a very small percentage of the James Ross Island Volcanic Group. They may be grouped under three headings, according to their petrographic characteristics and field relations.

i. Black vesicular dykes, which commonly pinch out upwards, have sinuous outlines and are mainly associated with palagonite-tuffs.
ii. Less vesicular dykes, weathering red-brown and having considerable linear extent.
iii. Xenolithic dykes.

Dykes of type (i) occur in scattered and not very dense swarms in the Prince Gustav Channel area. They have been observed at Beak, Eagle, Vortex, Tail and Carlson Islands, where they are always intruded into subaqueous palagonite-tuffs or fine-grained palagonite-breccias (Map 1). The commonest trend of the dykes is parallel to the structural trend of Prince Gustav Channel, although isolated dykes occur almost at right-angles to this. The dykes also occur in the palagonite-tuffs near Bibby Point, James Ross Island, and in the phase III palagonite-breccias of Mahogany Bluff, Vega Island, where they have been injected along minor fault planes (Plate VIId).

These olivine-basalt dykes are always very vesicular, dark and extremely fine-grained. The vesicles may contain a lining of zeolites or occasionally calcite. The groundmass is composed of some basalt glass, which is highly charged with opaque dust. Because the vesicular dykes thin upwards, they appear to have been injected relatively passively.

The dykes of type (ii) are even more uncommon than the first type. Isolated dykes of this type occur at Blancmange Hill and in the low ground south of the snout of Hobbs Glacier (Plate Vd), where it cuts Upper Cretaceous sediments and is believed to have been the feeder for the ash cone exposed in the nearby cliffs (p. 38). The dyke at Blancmange Hill (D.3740.1), which cuts palagonite-breccias of phase I, is a typical ophitic olivine-dolerite (Adie, 1953). It consists of subidiomorphic zoned olivine phenocrysts ($Fa_{27\text{-}37}$), showing a little alteration to serpentine along cracks, set in a matrix of ophitically intergrown plagioclase and strongly coloured titanaugite. There are smaller second-generation olivine crystals ($Fo_{76}Fa_{24}$) in the groundmass and noticeably few apatite needles or other alkaline constituents. The plagioclase ($Ab_{44}An_{56}$) often surrounds the olivine crystals with an indistinct trachytic texture (Plate Xa). This rock contains the highest percentage of olivine of all those examined, assuming that the greater part of the serpentine has replaced olivine (Table V). It also contains the highest percentage of ferromagnesian minerals and almost the largest proportion of iron ore. The mineralogy of this rock suggests that it may be relatively rich in ferrous iron (p. 54).

Several dykes of this type occur at the north-east end of Snow Hill Island (Map 1). They are much harder than the Upper Cretaceous sediments which they intrude and they form pronounced walls exposed in the stream gully 0·5 miles (0·8 km.) from the winter station of the Swedish South Polar Expedition (Nordenskjöld and Andersson, 1905, p. 509). In contrast to the dyke at Blancmange Hill, those of north-east Snow Hill Island are olivine-basalts with pronounced alkaline tendencies. Specimen D.4052.1 (Table V) is relatively rich in subophitic and glomeroporphyritic purple-pink titanaugite, often observed in association with and crystallized around the margins of olivine phenocrysts and clusters. The pyroxene and the cracked, serpentinized olivine contain inclusions of iron ore and spinel. The plagioclase has a core composition of $Ab_{32}An_{68}$ but it is normally zoned to about $Ab_{60}An_{40}$. Analcite, apatite and minor amounts of other zeolites occur interstitially and narrow rims of green augite have been formed around the margins of the titanaugite crystals.

Another dyke rock from north-east Snow Hill Island has been highly carbonatized. Specimens have been examined from the edge and centre of this dyke (D.4051.1, 2), respectively. Specimen D.4051.1 bears a close resemblance to a flow lava from the Gourdon Glacier area (D.4053.8). It consists of glomeroporphyritic aggregates of carbonatized olivine and fresh plagioclase phenocrysts set in a vesicular groundmass of partially crystallized basalt glass. The olivine has been wholly or partially replaced by a carbonate mineral (possibly magnesite) and in the more completely altered crystals there is also some analcite. In contrast, specimen D.4051.2 is a more typical olivine-dolerite. Carbonatization has affected 70–80 per cent of the phenocrystic olivine, in some of which quantities of analcite have been produced,

accentuating the presence of the (010) cleavage which is not normally visible in olivine phenocrysts. Several of the analcite-lined amygdales have been subsequently filled with a carbonate, apparently of the same composition as that replacing the olivine. The plagioclase phenocrysts are unaltered, range in composition from labradorite to sodic andesine and are generally more sodic than those near the margin of the dyke.

It is possible that this dyke, which may be representative of several in this area, owes its carbonatization to the release of carbon dioxide from the calcareous sandstones into which the dyke was injected. However, in view of the high concentration of analcite in some of the olivine phenocrysts, alkalis were also present. In this case, some of the volatiles responsible for the alteration of the dyke may have been of primary volcanic origin.

Xenolithic dykes (type iii) have been observed at three localities: Beak Island, near Dreadnought Point and 1 mile (1·6 km.) north-west of Ekelöf Point (Map 1). The xenoliths in the dykes of Beak Island are composed of altered palagonite-tuff fragments. They are almost colourless but in some instances they have been fractured and invaded by the basalt, which forms veinlets within the xenoliths. The xenolithic dykes of Beak Island occur in association with dykes of type (i). However, the xenolithic dykes at the other two localities are more massive olivine-basalts. At Dreadnought Point, the xenolithic dyke contains many white quartz-rich inclusions (averaging 3 cm. across), one of which has been transformed into dark grey and black banded quartz, possibly jasper. Although some of the xenoliths in this dyke may be incorporated tuff fragments, their quartz-rich composition suggests that they were originally sandstones derived from the underlying Upper Cretaceous strata.

At the third locality a xenolithic dyke (D.4049.3) intrudes Upper Cretaceous calcareous siltstones. The sub-rectangular xenoliths are pale green granular peridotite clusters 5–8 cm. across, which consist of olivine and enstatite together with minor amounts of pale green diopside and dark brown isotropic spinel. They may represent crystal cumulates which formed by gravitational settling in some near-surface magma reservoir prior to the emplacement of the dyke. The olivine ($Fo_{74}Fa_{26}$) is characterized by well-developed banding parallel to (100) (Plate Xb), a feature which is commonly present in the olivines of peridotite nodules (Ross, Foster and Myers, 1954). Hamilton (1957) has deduced that the presence of banding in olivine crystals is diagnostic of xenocrystic, as opposed to phenocrystic, olivine. The undoubted xenolithic nature of the peridotite nodules confirms this conclusion. The spinel, which occurs interstitially amongst the ferromagnesian minerals, could be misidentified as dark brown basalt glass. However, its paragenesis and refractive index ($> 1·70$) support its identification as spinel. No chemical analysis of the minerals constituting these peridotite nodules has been carried out but the spinel and diopside are probably chromium-rich (Ross, Foster and Myers, 1954). The calcareous siltstones in contact with the dyke have suffered low-grade thermal metamorphism or "baking".

2. *Sills*

Recognizable sills are very uncommon in the James Ross Island Volcanic Group, although it is possible that sills injected between flow lavas have not been recognized as such because they are concordant. At station D.3739, 0·5 miles (0·8 km.) south of Dreadnought Point, there is an unusual horizontal lenticular body of basalt which transgresses the bedding of the palagonite-breccias. Although the core of this structure is dark, it is surrounded by a yellow-weathering margin 1–2 ft. (0·3–0·6 m.) thick. Unfortunately, the outcrop occurs halfway up a 200 ft. (61 m.) cliff and is inaccessible. Nonetheless, it is suggested that this structure may have been caused by sill-like intrusion into wet palagonite-breccias, since it bears a resemblance to the intrusive layered lava pods at Unalaska Island, Aleutian Islands, where the intrusion of basalt into saturated sediments has been amply demonstrated by Snyder and Fraser (1963). The yellow-weathering margin is probably a chilled selvage of olivine-hyalobasalt. In addition, dykes of type (i) occasionally have small concordant wedge-shaped ramifications, which are effectively embryonic sills. They have been observed at Cockburn Island (Croft, 1947) and Beak Island.

3. *Volcanic plugs*

In addition to the plug at Haslum Crag in north-east Snow Hill Island, four others have been located. They occur near Stoneley Point, at the south-west end of Lachman Crags, at Humps Island and Lonely Rock, which is a single volcanic plug (Map 1). In all cases, except Lonely Rock which is surrounded by sea, the plugs cut Upper Cretaceous sediments. However, even at Lonely Rock the plug is probably

emplaced in Upper Cretaceous sediments in view of the shoal which connects Lonely Rock with Ula Point only 0·5 miles (0·8 km.) from the nearest Upper Cretaceous outcrop. The plugs are all circular in outcrop and, because they are composed of harder rock than the surrounding terrain, they have formed pronounced knolls or crags (Plate VIIa). Although the Haslum Crag dolerite is located at the edge of a dyke, a field relationship unlike the other plugs, it is included here because of its comparable petrography.

The analcite-bearing olivine-dolerite (Wilkinson, 1955, p. 287) from the plug south-west of Lachman Crags is representative of all these rocks (D.3756.1). It consists of zoned olivine phenocrysts, subidiomorphic titanaugite, plagioclase, analcite and iron ore, with accessory apatite, biotite and zeolite (Plate Xc). The rounded olivine phenocrysts ($Fa_{28\text{-}45}$) are predominantly fresh but they contain small quantities of iron ore and serpentine along cracks. Inclusions of glass are rare. The pale pink titanaugite, which shows both normal and oscillatory zoning, is often twinned on (100). The clinopyroxene has two modes of occurrence, either as large almost idiomorphic crystals showing a slight tendency towards ophitic intergrowth with plagioclase or as smaller crystals which are more rounded and commonly zoned. The smaller titanaugites are occasionally grouped together into glomeroporphyritic clusters in association with biotite and analcite.

The plagioclase, some of which has been analcitized, is strongly zoned from calcic cores to sodic margins. One crystal, ranging in composition from $Ab_{32}An_{68}$ at the core to $Ab_{80}An_{20}$ at the margin, contains numerous randomly orientated apatite needles. Clear isotropic analcite, which has been identified by X-ray analysis, occurs interstitially. It is sometimes associated with apatite prisms, minute flakes of pleochroic biotite and rare calcite. In some of these plugs, particularly the one on Humps Island (D.3800.1), there are secondary zeolites in the vesicles and minute quantities of alkali-feldspar. Modal analyses of five plug rocks are given in Table V.

4. *Palisade Nunatak laccolith*

Palisade Nunatak, situated near the west coast of James Ross Island approximately 2·5 miles (4 km.) south-east of Hidden Lake, is 0·5 miles (0·8 km.) wide and 1·5 miles (2·4 km.) long. Its long axis and crestal ridge are orientated north-west to south-east (Map 1; Fig. 2). The nunatak reaches a height of nearly 1,000 ft. (305 m.) and it is composed of a single columnar-jointed intrusion of analcite-bearing olivine-dolerite (Wilkinson, 1955, p. 287) capped by a small thickness of Upper Cretaceous sandstones (Plate VIa). In view of the shape of the nunatak, its limited lateral extent and the disposition of the

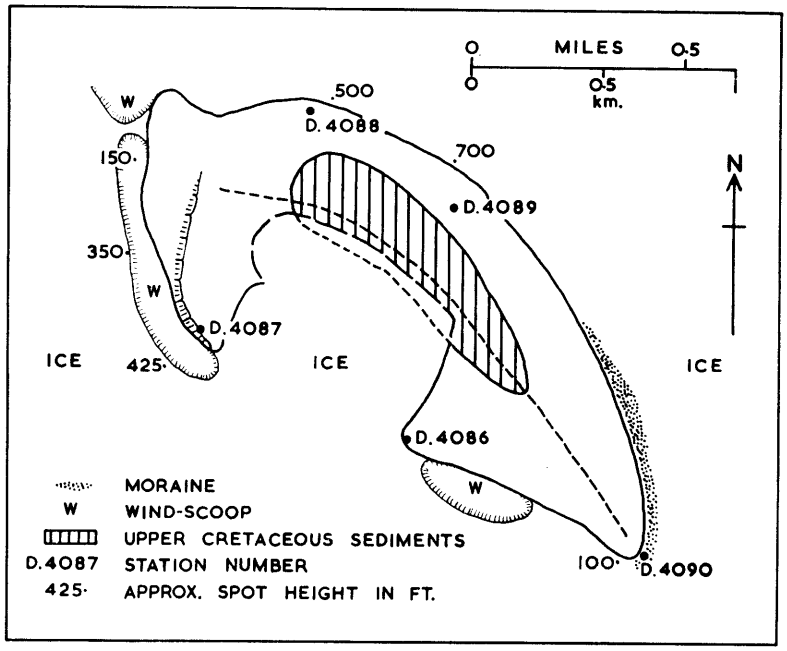

FIGURE 2

Sketch map (based on an aerial photograph) of Palisade Nunatak, James Ross Island.

columnar jointing, it is suggested that the intrusion is a laccolith, which was emplaced during the eruptions of the James Ross Island Volcanic Group. The vertical columns, which are approximately 4 ft. (1·2 m.) across and on the same scale as those at Edinburgh Hill, Livingston Island (Ferguson, 1921), are crossed by jointing and banding which has a shallow southerly dip. During the later stages of crystallization, dolerite-pegmatites and alkali-rich veins and veinlets were formed. Xenolithic pods were incorporated at an unknown stage in the cooling history of this intrusion.

a. *Analcite-bearing olivine-dolerites.* Analcite-bearing olivine-dolerites containing varying proportions of interstitial alkaline minerals form the bulk of the intrusion. They are characterized by the presence of subhedral or rounded olivines up to 3 mm. across, whose compositions lie in the range $Fo_{70}Fa_{30}$–$Fo_{55}Fa_{45}$. Although the olivines are not zoned, unlike those in the analcite-bearing olivine-dolerite plugs (D.3756.1) and more massive dykes (D.3740.1), their subhedral shapes and tendency to occur in "glomeroporphyritic aggregations" (Wilkinson, 1958, p. 5) indicate that they were one of the first minerals to crystallize. In two of the rocks (D.4087.1, 3) second-generation olivines (0·2 mm. across) occur individually in the groundmass. The olivines, which commonly contain minute iron ore and spinel octahedra, are altered marginally and along cracks to bowlingite. In one rock (D.4087.2) iddingsite occurs only in the cracks of the olivines but in another (D.4087.3) rare chlorite has formed as an alteration product. In most of the rocks olivine is associated with pleochroic biotite (straw—dark brown or straw—brownish green), which commonly occurs alongside interstitial titanomagnetite.

Titanaugite, whose varying intensities of purple-pink coloration indicate varying concentrations of titanium, occurs either with plagioclase as ophitic crystals more than 2 mm. across or as discrete 0·2 mm. granular crystals in the groundmass, but it never has both parageneses in the same rock. The titanaugite, which sometimes occurs in the glomeroporphyritic olivine clusters, is commonly zoned and occasionally rimmed by a thin layer of green augite (D.4088.1). The clinopyroxene is always fresh and has relatively constant optical properties: $2V\gamma$ varies between 50 and 60° and $\gamma:c$ has an average value of 45°.

The most abundant feldspar in these rocks is plagioclase, which is normally zoned from about $Ab_{30}An_{70}$ to $Ab_{68}An_{32}$. In one rock (D.4088.1) the plagioclase has a core composition of $Ab_{21}An_{79}$, which is the most calcium-rich feldspar recorded from this intrusion. Oscillatory zoning occurs in the cores of the larger crystals, which contain minute exsolved iron ore grains in one instance (D.4087.4). Although it is not present in some rocks (D.4087.2, 3), alkali-feldspar of the sanidine—anorthoclase cryptoperthite series occurs in most of them. It not only forms minute individual crystals adjacent to the interstitial analcite, but in one rock (D.4086.1) it occurs as a thin epitaxial overgrowth on plagioclase.

Analcite is ubiquitous and typically occurs in wedge-shaped interstices, where it is often associated with slender apatite prisms and biotite flakes. Specimen D.4087.2 is characterized by relatively large interstitial analcite crystals which exhibit slight birefringence, and extensive random analcitization of the plagioclase. Apart from analcite, accessory thomsonite occurs in two rocks (D.4087.2, 4) and in another (D.4086.1) calcite occurs as individual grains in the analcite.

b. *Dolerite-pegmatites and alkali-rich segregations.* Dolerite-pegmatites and the alkali-rich segregations associated with them form coarse-grained schlieren (Walker, 1953) close to the median plane of the intrusion (Plate IVc). They contain a smaller proportion of ferromagnesian minerals than the country rock (Table V), although there is a greater diversity of species. The olivines, whose compositions range from $Fo_{65}Fa_{35}$ to $Fo_{54}Fa_{46}$, are generally more iron-rich than those in the country rock. In marked contrast to the latter, they do not form even rounded crystals but occur interstitially (up to 5 mm. long in the coarsest pegmatites (D.4086.3)) amongst subhedral feldspars. This distinctive subophitic paragenesis, which is one of the features of these rocks, suggests that the iron-rich olivines are of late crystallization (cf. Wilkinson, 1956, p. 446). Stubby apatite prisms occur in the olivine, which may be associated with biotite, ilmenite or apatite, and is often altered marginally to bowlingite or internally to iddingsite (Plate Xd).

Slightly zoned and pleochroic titanaugite is the commonest pyroxene. It occurs as phenocrysts and graphic intergrowths with feldspar which are large (up to 15 mm. across) and complex (Plate Xe). In one rock (D.4086.3) the form of the graphic pyroxene crystals is basically quadribrachial, although the limbs of the structure are composed of many individual parts whose overall shape is ellipsoidal. The elongation of the components in the limbs has an angle of about 26° to a nucleus, whose long axis is parallel to that of the enclosing ellipsoid. The titanaugite, with $2V\gamma = 49$–$64°$ and $\gamma:c \simeq 50°$, normally has a 0·05 mm. rim of green augite ($2V\gamma \simeq 90°$). In two of the rocks (D.4086.3, 4087.9) discrete crystals

of aegirine-augite ($2V\alpha \simeq 60°$) up to 0·2 mm. in diameter are present in the groundmass. In addition to the pyroxenes, specimen D.4087.9 (an alkali-rich segregation) contains basaltic hornblende as individual crystals in the groundmass, and also crystallized alongside titanaugite and olivine. The identification of this amphibole as basaltic hornblende rather than barkevikite, which has been recorded from the Black Jack Sill by Wilkinson (1958, p. 5), is on the grounds of larger $2V\alpha$, and a dispersion of red less than violet as opposed to the red greater than violet dispersion of barkevikite (Deer, Howie and Zussman, 1963*a*). The basaltic hornblende has a pleochroism scheme $\alpha' =$ yellow, $\beta' =$ brown, $\gamma' =$ red-brown, $2V\alpha = 60°$ and $\gamma:c = 9°$.

Alkali-feldspar of the sanidine—anorthoclase cryptoperthite series predominates over plagioclase in the dolerite-pegmatites. It occurs as rare discrete crystals twinned according to the Carlsbad law but largely as zoned epitaxial overgrowths on plagioclase crystals (Plate Xf), whose compositions range from labradorite ($Ab_{34}An_{66}$–$Ab_{43}An_{57}$) at the cores to oligoclase or sodic andesine at the margins (cf. Wilkinson, 1958, p. 17–19). In section, one crystal of alkali-feldspar measured 6 by 3 mm. externally with a 2·5 by 2·0 mm. core of plagioclase. Analcitization of the plagioclase is common. Universal Stage measurements of the optic axial angles of the alkali-feldspars, whose optic axial planes are perpendicular to (010), indicate that they too have a considerable range in composition (Table VI). The predominant alkali-feldspar, particularly that forming the epitaxial overgrowths, appears to have a composition in the range $(Ab+An)_{90}Or_{10}$ to $(Ab+An)_{50}Or_{50}$ with $2V\alpha = 50$–$35°$ (Tuttle, 1952). The smaller and scarcer interstitial Carlsbad-twinned crystals have much lower 2Vs, whose exact measurement is hindered by overlapping

TABLE VI

OPTIC AXIAL ANGLES OF ALKALI-FELDSPARS

Specimen Number	*Measured Values of 2Vα**							
D.4086.2	52·5°	45°	44°	42°	41°	39°	32°	
D.4086.3	53·5°					37°		very low
D.4087.5	50°	49°	48°					very low
D.4087.9		49°	46°		41°		34°	very low
D.4088.5	50°	47°	44°					very low
	(Ab+An) ——— increasing orthoclase ———→							

* These values have an accuracy of ±2°.

D.4086.2 Alkaline segregation associated with dolerite-pegmatite; south-west Palisade Nunatak.

D.4086.3 Dolerite-pegmatite from south-west Palisade Nunatak.

D.4087.5 Dolerite-pegmatite; not as coarse-grained as D.4086.3; west Palisade Nunatak.

D.4087.9 Alkaline segregation associated with D.4087.5; west Palisade Nunatak.

D.4088.5 Alkaline segregation associated with late-stage alkali-rich veins (D.4088.4); north Palisade Nunatak.

of the isogyres. However, their optic axial angles are lower than 32°, suggesting that some of the smaller crystals have compositions approaching that of pure orthoclase with $2V\alpha \simeq 17°$ (Tuttle, 1952). Black Jack Sill anorthoclase has a mean $2V\alpha$ of 52° (Wilkinson, 1958, p. 18).

The interstitial alkaline minerals, which may amount to 30·3 modal per cent (Table V), consist predominantly of analcite. Thomsonite, forming excellent fibrous spherulites, is the commonest zeolite associated with the analcite but chabazite (D.4087.9) and gismondite ((D.4088.5) in which analcite cubes have (111) modifying faces) have been observed as well. Calcite is also present and in addition to the recognizable minerals there is often a very fine-grained matrix of chloritic material. Sizeable acicular apatite prisms occur in most of the rocks. Ilmenite, forming skeletal intergrowths with alkali-feldspar

in many of the rocks, occurs as platy crystals up to 25 mm. long but only 0·5 mm. wide in specimen D.4086.3.

c. *Late-stage veins.* Cross-cutting alkali-rich veins and veinlets occur at many levels in the intrusion. Specimen D.4088.4, from a vein about 10 cm. wide, is representative of the more extensive of these. Microscopic examination of this rock reveals the almost total absence of plagioclase and a sub-parallelism of the alkali-feldspar crystals which constitute its bulk (Plate XIa). The optic axial angles of the majority of these lath-shaped Carlsbad-twinned alkali-feldspars are low, which suggests the predominance of potassium-rich members of the sanidine—anorthoclase cryptoperthite series Occasional irregularly shaped fragments of anorthoclase with a higher $2V\alpha$ are also present. There is probably not more than 1 per cent (modal) of olivine, which is severely altered to iddingsite, and small equidimensional crystals of titanaugite are invariably rimmed with green augite. The sub-parallelism of the alkali-feldspar laths, which have a common orientation throughout the specimen, and their arrangement around the margins of cavities now occupied by analcite, chabazite and thomsonite give the rock a "vesicular trachytic" texture, strictly comparable with that of many flow lavas (Plate XIb). The analcite in the cavities occurs in an unusual hollow form. The overall outlines of the crystals are octagonal but the cores consist of "spokes" of analcite at 45° and separated by empty wedge-shaped cavities.

Veinlets little more than 1 mm. wide occur in addition to the larger felsitic veins. One of these (D.4087.8) is composed largely of analcite and alkali-feldspar, with minor ilmenite, biotite and stubby apatite prisms. The veinlet traverses an average dolerite, whose plagioclases are epitaxially overgrown with anorthoclase next to the veinlet. Although the titanaugite is fresh, olivine crystals incorporated in the veinlet have been marginally altered. However, it is suspected that complete pseudomorphing by bowlingite has occurred in certain instances.

A similar veinlet from the same rock (D.4087.8), which contains far less analcite than the former one, is composed predominantly of alkali-feldspar. Fresh titanaugite, occasionally occurring as a shell around olivine crystals, is marginally rimmed by pale green aegirine-augite. In many places olivine is separated from the vein minerals by titanaugite and where this is present it is unaltered. However, unprotected olivines carry reaction rims of pleochroic brown biotite and iron ore. The mineralogy of the veinlets indicates the late-stage concentration of alkalis and alumina.

d. *Xenolithic pods.* The dark xenolithic pods (D.4088.2), which have been found on the north side of the intrusion, consist of two distinct size groups of minerals. Olivine, plagioclase and colourless augite phenocrysts, and glomeroporphyritic clusters of all three in any combination or alone, occur in a finer-grained holocrystalline groundmass of similar mineralogy except for the absence of olivine. However, the texture is not characteristically porphyritic because analcite, which is present in minute interstitial cavities of some glomeroporphyritic clusters, suggests that the larger-grained clusters have been derived from a source where crystallization was almost complete. It is as though a coarse-grained crystal mush had been rapidly mixed with a melt of nearly the same composition, the resultant quenching of which has produced a textural if not a chemical hybrid.

At a nearby station, more unusual xenolithic pods occur in a matrix of relatively alkali-rich dolerite (D.4087.7). The pods or ocelli, which are up to 20 mm. long and 13 mm. wide, consist of a nucleus of alkali-feldspar, analcite and spherulitic thomsonite, surrounded by a shell of radially arranged titanaugite crystals. The titanaugite ($2V\gamma = 54°$, $\gamma:c = 55°$) occurs in two distinct sizes (0·75 by 0·15 mm. or 0·25 by 0·08 mm.), both of which have been observed in the same ocellus rim. There is a tendency both for the smaller pyroxenes to form one wall of an ocellus and the larger ones the opposite wall, and also for the walls composed of smaller crystals of different ocelli to have a common orientation.

It is suggested that the ocelli represent drops of alkaline residuum which became mixed with unconsolidated country rock, thus forming individual clots of alkaline minerals rather than a vein or stringer, whose formation probably requires intrusion of the residuum into relatively consolidated material.

e. *Contact metamorphism.* The Upper Cretaceous sandstones forming the roof of the intrusion have suffered thermal metamorphism to a distance of 6 ft. (1·8 m.) from the contact. Although the appearance of the quartz, plagioclase and rock fragment sand grains has not been radically changed, alteration of the matrix (originally relatively porous) has transformed the sandstone from a slightly friable grey-green rock to one that is hard, compact and black. The matrix of the sandstone (D.4089.3) contains finely disseminated iron ore granules, which become larger and more prolific in the matrix of the altered rock (D.4089.1, 2) and are responsible for its dark colour. The iron ore grains have a certain amount of

orientation which may be related to the original bedding of the sediment, but no mineralization has been observed.

f. *Summary.* Detailed petrographic study of the Palisade Nunatak intrusion has clearly revealed its alkali olivine-basalt affinities. Wilkinson (1958), describing more alkaline rocks from a Tertiary teschenite sill in New South Wales, classified them into three groups according to textural differences:

i. Porphyritic or basalt type; characterized by conspicuous phenocrysts of fresh olivine and titanaugite, which frequently form glomeroporphyritic clusters.
ii. Ophitic or doleritic type; typically non-porphyritic and with ophitic relationships between olivine and plagioclase. Olivine always serpentinized.
iii. Non-ophitic or gabbro type; where analcite occurs in significant quantities, titanaugite and barkevikite are euhedral. Olivine is serpentinized.

It will be seen that these groups can almost equally well be applied to the Palisade Nunatak rocks, there being "porphyritic" and "ophitic" analcite-bearing olivine-dolerites, although the dolerite-pegmatites are characterized by occasionally strongly ophitic titanaugite and appear to contain basaltic hornblende instead of barkevikite. The trend of differentiation of the Black Jack teschenites is one of initial iron enrichment relative to magnesium, culminating in a sudden increase in the proportion of alkalis (Wilkinson, 1958, fig. 5). Chemical analysis indicates that there is a similar course of crystallization differentiation in the rocks of Palisade Nunatak (p. 50-54).

C. Palagonitization and Zeolites

1. *Hyalobasalt fragments and palagonite rim thicknesses*

One of the major problems connected with the formation of the palagonite-breccias concerns the time at which palagonitization took place. It was originally thought by the author that there would be a relationship between the size of individual hyalobasalt fragments and their associated rims of palagonite, if palagonitization occurred almost simultaneously with brecciation and deposition. If the thermal energy for the palagonitization (corrosion reaction, p. 34) was supplied solely from the cooling of the individual fragments, the thickness of the palagonite rims would probably increase as the size of the basalt-glass fragments increased. If, as now seems more probable, the formation of gel-palagonite is not associated with the initial cooling of the hyalobasalt fragments but with a thermal stress more uniformly applied later in the history of the rock (p. 33), relatively constant palagonite rim thicknesses would be expected.

The cross-sectional dimensions and associated palagonite rim thicknesses have been measured on ten fragments in a thin section of a palagonite-breccia (D.4068.2; Plate VIIId). Although there is a factor of about 100 in the size difference between the largest and smallest hyalobasalt fragments, the range in palagonite rim thicknesses is approximately 3·5. A histogram of the number of fragments having palagonite rims with thicknesses in the range 0·025—0·075—0·125—0·225 mm. gives an approximately Gaussian distribution. The histogram suggests that the average thickness of palagonite rims in specimen D.4068.2 is about 0·10 mm., regardless of the size of the hyalobasalt fragments. A similar thin-section study of other palagonite-breccias reveals that, although there is no consistency from one rock to another, there is a regularity in the thickness of the palagonite rims in any particular palagonite-breccia (Table VII).

The palagonite rim which is 2·0 mm. thick (Table VII) has been measured from the face of a radial crack in an olivine-basalt pillow. This palagonite thickness is nearly ten times as great as any measured under the microscope and occurs at the margin of a pillow about 30 cm. in diameter with an almost holocrystalline core. In this instance, some of the palagonite may have formed during the cooling and crystallization of the pillow, a process which was evidently more protracted than the quenching of hyalobasalt fragments not exceeding 1 cm.^{3} in size.

The narrow interspace between two adjacent hyalobasalt fragments in specimen D.3726.1 is entirely occupied by zeolite, which is separated from the unaltered basalt glass by a film of palagonite only 0·015 mm. thick. The early filling of this interspace by zeolite has evidently inhibited the further formation of palagonite to an average thickness of 0·22 mm. (Table VII). The interdependence of palagonite formation and the formation of zeolites can be deduced from Table VII, where it is generally demonstrated that the thicker the palagonite rim the higher is the grade of zeolitization.

TABLE VII

AVERAGE PALAGONITE RIM THICKNESSES

Specimen Number	*Palagonite Rim Thickness* (mm.)	*Associated Zeolite Grade**
D.3813.1	0·01	1
D.3712.1	0·02	2
D.3302.1	0·04	3
D.4068.2	0·10	3
D.3726.1	0·22	3–4
D.3749.1	2·00	4

* Zeolitization is discussed on p. 31–33.

2. *Zeolites*

Although zeolites occur as primary minerals in many of the analcite-bearing olivine-dolerites and associated pegmatitic rocks, they do not occur as secondary minerals in all rocks of the group. In fact, there is a distinct gradation, which is particularly noticeable in the palagonite-tuffs and breccias (the hydroclastic rocks (Fitch, 1965)), between those rocks which are entirely cemented by zeolites and those with open pore spaces and vesicles. The extrusive rocks and dykes contain chabazite, phillipsite, analcite and natrolite, in order of relative abundance. However, analcite is the most abundant zeolite species in the plugs and the laccolith, where it may be associated with thomsonite, chabazite, natrolite and rare gismondite. Calcite and aragonite have been observed in all rock types. As would be expected, the zeolite assemblage occurring in the James Ross Island Volcanic Group is the one believed to be characteristic of environments that are undersaturated with respect to silica (Coombs and others, 1959).

The optical identifications of chabazite (D.3745.1a, 4068.2, 4087.9), phillipsite (D.3729.1, 3745.1b), thomsonite (D.4088.3), analcite (D.3756.1) and aragonite (D.3725.2) have been confirmed by X-ray powder photography. The optical identification of these minerals in other specimens has been by comparison with those identified by X-ray analysis. It is notable that the two X-ray patterns obtained from phillipsite indicate a structure analogous to that of harmotome, although the optical properties and lack of any other evidence of high barium concentration favour the identification of this zeolite as phillipsite. However, it may be a barium-bearing species similar to wellsite (Deer, Howie and Zussman, 1963*b*). Natrolite and gismondite, which occur in concentrations too low for practicable X-ray powder analysis, have been identified by optical methods only.

a. *Paragenesis of zeolites in the extrusive rocks.* Walker (1960*a*, *b*) has demonstrated that in Iceland and northern Ireland the number of zeolite species present generally increases with the intensity of zeolitization. The same is true in the rocks of the James Ross Island Volcanic Group, in which an additional relationship between the intensities of zeolitization and palagonitization of the hydroclastic rocks has been observed. Four grades of increasing intensity of zeolitization have been recognized, which are very similar to some of those in the lavas of eastern Iceland (Walker, 1960*b*). They are:

Grade 1. Zeolites very rare.
Grade 2. Minor chabazite.
Grade 3. Chabazite and phillipsite.
Grade 4. Analcite.

The higher grades, characterized by mesolite and scolecite, and finally a profusion of zeolites, which occur in the Icelandic lavas (Walker, 1960*b*), have not been observed in rocks of the James Ross Island Volcanic Group. The minerals used in defining the grades are not necessarily the only secondary minerals present at that grade, particularly in the case of analcite which may occur with three other species.

Grade 1. Several of the olivine-basalt lavas and hydroclastic rocks of Tabarin Peninsula and the islands

in Prince Gustav Channel fall into this category. Olivine-basalt lavas from Beak Island and Brown Bluff (D.3711.3, 3787.3) are characterized by open vesicles. These rocks are consequently very fresh, and the analcite occupying minute wedge-shaped intercrystalline cavities in the groundmass of specimen D.3711.3 is believed to be pyrogenetic (p. 14). Although the lavas in the James Ross Island area normally contain some zeolite, vesicles occur in those near Stark Point (Map 1). Vesicles also characterize the highly porous olivine-basalt fragments (D.4097.2) which occur in the palagonite-tuffs south of Lagrelius Point (p. 21), even though the matrix of the rock (D.4097.4) consists of wholly and partially palagonitized olivine-hyalobasalt fragments cemented by a little zeolite (grade 2).

The palagonite-tuffs forming Cain Nunatak (D.3813.1, 2), an outlier of the James Ross Island Volcanic Group on Trinity Peninsula, are distinguished by the almost entire absence of zeolite and palagonite (Table VII). Indeed, they bear a resemblance to a very fresh hyaloclastite from Donald Nunatak, Seal Nunataks, in that they contain moderate amounts of secondary calcite. Fine-grained palagonite-tuffs from Tail Island (D.4101.3, 4), composed almost entirely of shards, are also characterized by relatively abundant calcite but only minute quantities of zeolite.

Grade 2. Many of the lavas of James Ross and Vega Islands contain vesicles only lined with chabazite about 0·02 mm. thick. The chabazite, which is occasionally associated with small calcite crystals, has a granular habit and a low birefringence. At the highest point of the west end of Beak Island and overlying a compact fresh olivine-basalt lava (D.3711.3), there is a palagonite-tuff composed of scoriaceous basalt-glass fragments and shards (D.3712.1). Most of the shards have been completely altered but palagonitization, which has not been very intense (Table VII), has produced a coating of chabazite only 0·01 mm. thick on the glass fragments.

Grade 3. Most of the rocks containing well-developed zeolites come under this heading, and the index minerals are occasionally accompanied by natrolite, calcite or aragonite. The chabazite, which invariably has a low birefringence, forms interlocking granular crystals which may either fill the vesicles and pore spaces or not (Plate XIc). The phillipsite, an occasionally fibrous zeolite, normally forms minute incomplete spherulites but sometimes it has a bladed habit. The refractive indices and birefringence of the fibrous phillipsite normally vary with distance from the centre of the spherulites (Plate XIe). The bladed phillipsite, which always exhibits interpenetrant or complex twinning, may form complete amygdales (Plate XIf) or interlocking aggregates of minute crystals (Plate XId). Although calcite occurs interstitially amongst the zeolites and is evidently of late formation, aragonite occasionally forms spherulites up to 30 mm. in diameter.

In some rocks, either of the index minerals can occur to the virtual exclusion of the other, but when the two occur together the phillipsite, whose spherulites are nucleated around the margins of vesicles and hyalobasalt fragments, frequently appears to have formed first. In some cases the formation of phillipsite seems to have ceased relatively quickly and the bulk of the zeolite is chabazite. An example of this is a palagonite-breccia from southern James Ross Island (D.4068.2), in which phillipsite is confined to minute spherulites about 0·01 mm. in radius formed on the palagonite rims of the hyalobasalt fragments, while the remainder of the rock is cemented with chabazite. In contrast, chabazite occurs only as subordinate interstitial grains in a palagonite-breccia from Seven Buttresses (D.3302.1), which is cemented predominantly with much larger spherulites of bladed phillipsite. The earlier formation of phillipsite than chabazite can also be observed in amygdales of the olivine-basalt lavas, which are rarely complete and normally contain a central cavity. The amygdales in a typical lava from the north end of Persson Island (D.4077.1) consist predominantly of phillipsite spherulites. In this rock the phillipsite is occasionally succeeded by chabazite exhibiting faint multiple lamellar twinning, and calcite which sometimes occurs against the amygdale wall.

Grade 4. Zeolitization of this grade, the essential feature of which is the presence of analcite perhaps accompanied by any or all of the other zeolites, is not common or extensive in the extrusive rocks of this volcanic group. Significant amounts of analcite have been recorded from only three localities: Carlson Island, west Croft Bay and Cape Obelisk. Minor amounts occur in the rocks at two other localities. First, a palagonite-breccia from the Stark Point area (D.3726.1) contains minute crystals of analcite and natrolite next to the palagonite, although bladed phillipsite and chabazite constitute the bulk of the zeolite. Secondly, a palagonite-tuff from east Croft Bay (D.3729.1) also contains subordinate analcite.

At Carlson Island analcite and other zeolites occur in a palagonite-tuff which forms a matrix between pillow lavas (D.4098.5). The analcite occurs as amygdales in the hyalobasalt fragments, either alone

or with various combinations of other zeolites, including chabazite and phillipsite, and secondary calcite. However, the interfragmental pore spaces are characterized by the absence of analcite and the presence of only phillipsite. Chabazite and phillipsite, in the absence of analcite, occur in a palagonite-tuff (D.4098.6) underlying the horizon of pillow lavas.

Above the tuffaceous conglomerates near the west coast of Croft Bay, there is a palagonite-tuff in which analcite has an interesting paragenesis. Specimen D.3738.6 consists of a central lamina of tuff, containing dark yellow, partially recrystallized palagonite, 0·04 mm. thick, intercalated between two laminae containing clear yellow isotropic palagonite, 0·10 mm. thick. The original porosity of the central lamina (20 per cent) was less than that of the adjacent ones (40 per cent) but the pore spaces are now filled by zeolite. The abundant zeolite matrix of the marginal laminae includes chabazite, phillipsite and minor natrolite, together with calcite that has replaced some of the plagioclase microlites. However, the chabazite, phillipsite and calcite in the central lamina are accompanied by analcite, which is often the predominant species. There is a rapid change in the abundance of analcite from maximum to zero across the planes bounding the central lamina. It is, perhaps, significant that the limits of dark recrystallized palagonite do not coincide with these planes but occur within the central lamina itself.

The analcite and phillipsite, which occur as amygdale minerals in a basalt pillow from the Cape Obelisk area, have been described on p. 16. However, it is notable that the analcite frequently occurs as the only amygdale mineral in this rock (D.4078.2). A zeolite of extremely low birefringence, probably analcite, lines nearly all of the vesicles to a depth of 0·03 mm. and cements the shards of a brick-red altered palagonite-tuff from the Massey Heights area (D.3760.1).

b. *Distribution and origin of zeolites in the extrusive rocks.* The distribution of zeolite grades in the lavas and hydroclastic rocks of the James Ross Island Volcanic Group is included in Map 1. Most of the plotted localities occur between sea-level and an altitude of 1,000 ft. (305 m.) and, although there are far too few stations to reach any definitive conclusions, there is a general tendency for the lower grades of zeolitization to occur in the Tabarin Peninsula area and the islands of Prince Gustav Channel, and the higher grades to be confined to the James Ross and Vega Islands area. In fact, except in the tuffs of Carlson Island and the carbonatized dykes of Snow Hill Island, analcite has not been observed outside the area of James Ross Island (except the Seal Nunataks).

Walker (1960*a*, *b*) has demonstrated that the zeolite zones or grades in the lavas of northern Ireland and eastern Iceland form well-defined horizons which transgress the bedding of the lavas. He has suggested that zeolitization took place some considerable time after eruption of the flows in which the zeolites now occur, and probably after about 1,000 ft. (305 m.) of lavas had accumulated (Walker, 1960*a*, p. 523). He envisaged the steady rise of geo-isotherms in a lava pile which was gradually thickening by successive eruptions (Walker, 1960*b*, p. 519), and believed that at those levels where the appropriate temperature was attained, the ground water would begin to react with the basalts to produce zeolites. Walker (1951, p. 789; 1960*a*, p. 524) has considered that the heat necessary for the formation of zeolites came partly from exothermic hydration reactions (including the hydration of olivine), which occurred between the basalts and the ground water. He has suggested that the intrusion of dykes or some other agency could have provided sufficient local overheating to initiate the reactions, and that having once started they would have become self-generating and only ceased when all the water had been used up. In Iceland, Walker (1960*b*) has collected evidence indicating that the original top of the lava pile once stood about 2,000 ft. (610 m.) above the top of the analcite zone and that zeolites evidently disappear completely about 1,300 ft. (396 m.) above the top of this zone, leaving 700 ft. (213 m.) of zeolite-free lavas.

Although no detailed collecting has been carried out, it is notable that zeolites are generally better developed in the hydroclastic rocks than in the lavas of the James Ross Island Volcanic Group. It is believed, therefore, that the zeolitization of these rocks should be considered under two separate but related headings. Zeolitization of olivine-basalt lavas probably depends on the hydration of their constituent minerals (Walker, 1951, 1960*a*, *b*). However, extensive zeolitization up to grade 3 has occurred in hydroclastic rocks of the James Ross Island Volcanic Group, in which extensive palagonite has been formed without alteration of the crystalline material. For example, a palagonite-breccia (D.3302.1; p. 13), in which isolated olivine and plagioclase crystals are fresh, contains well-developed phillipsite that has probably formed entirely as a result of palagonitization. The greater instability of basalt glass probably leads to zeolitization under conditions of lower stress than would be necessary to accomplish the same degree of zeolitization in a holocrystalline basalt lava.

In a study of the aqueous corrosion of soda-lime glass rods, Charles (1958, fig. 1) has illustrated sharp boundaries separating corroded and fresh glass, which are very similar in appearance to the palagonite/basalt-glass boundaries in the hydroclastic rocks. Charles (1958) contended that two factors are of importance in the corrosion of glass: first, the unending silica network, and secondly, the terminal structures associating the alkali ions to the silica network. He suggested that the terminal structures are more important in the initial stages of corrosion and illustrated this by the following reaction:

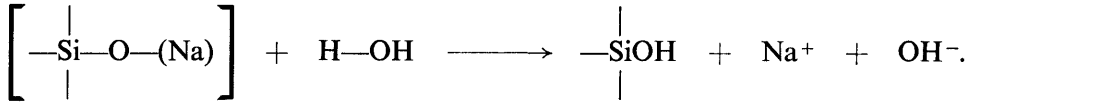

He considered that the production of a free hydroxyl ion can lead to a second step, in which the very strong Si—O—Si bond is broken:

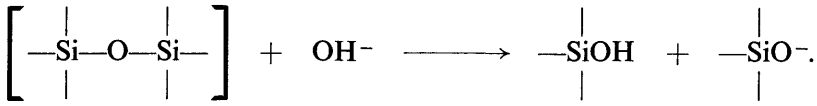

One of the end structures produced in this stage is capable of dissociating another water molecule as follows:

Charles noted that, as these reactions proceed, excess hydroxyl ions will be produced in equal proportions to the alkali ions that are no longer associated with silica in the corrosion products. This increase of pH in the corrosion layer tends to make the process autocatalytic, although there will probably be a limit to the pH build-up, because the tendency to form silicate ions and the consequent removal of free hydroxyl ions from solution will increase. In the palagonitization of basalt glass this tendency to form silicate ions will probably result in the crystallization of zeolites. Charles (1958) concluded that the "dissolution of multicomponent silica glasses is greatly enhanced in basic solutions". If the deposition of the James Ross Island Volcanic Group hydroclastic rocks took place largely in sea-water of about pH 8, the initiation of these reactions may have been relatively easily accomplished. It is for future experimental work to discover whether the rate of formation of zeolites is greater during the corrosion of basalt glass by sea-water than by fresh water (pH 7).

Unfortunately, no information is available regarding the vertical distribution of zeolites in a single palagonite-breccia unit. However, at Tabarin Peninsula and north-east of Stark Point, vesicular lavas overlie palagonite-tuffs or breccias in which zeolites of grade 3 have been developed. The analcite in the lowermost palagonite-breccias near Stark Point (D.3726.1) only about 700 ft. (213 m.) below vesicular lavas (p. 31) suggests that little more than half the thickness of strata than in Iceland intervenes between the top of the analcite zone and the disappearance of zeolites (p. 33). It is possible that this is also due to the greater reactivity of basalt glass compared with crystalline silicates such as feldspar and olivine.

Apart from the two local occurrences of analcite in the tuffs at Carlson Island and west Croft Bay, the general low intensity of zeolitization and the absence of the two higher zeolite grades which occur in the basalts of Iceland suggest that the depth of burial of the James Ross Island Volcanic Group has not been very great. Indeed, it is possible that the present overall shape of James Ross Island is very much as it was at the close of vulcanicity.

c. *Zeolites in the intrusive rocks.* Analcite is the predominant zeolite species in the olivine-dolerite plugs and the Palisade Nunatak intrusion. Although considerable amounts occur in analcitized plagioclase, in which the analcite is obviously secondary to the crystallization of the feldspar, significant amounts also occur interstitially. Since the interstitial analcite is often associated with alkali-feldspar of the sanidine—anorthoclase cryptoperthite series, biotite and calcite, and it frequently contains minute prisms of apatite, it is probably pyrogenetic. The analcitization of the plagioclase and the formation of other zeolite species may have taken place during a period of secondary zeolitization long after the consolidation of the rocks (cf. Walker, 1960*a*). Their formation could equally well have occurred syngenetically as a result of the late-stage concentration of alkalis during crystallization. This explanation is preferred in

view of the large proportion of alkali-feldspar in the dolerite-pegmatites of the Palisade Nunatak intrusion, which, together with the geochemistry (p. 50), is strong evidence favouring the late-stage concentration of alkalis.

IV. STRUCTURAL GEOLOGY

A. Cone Structures

Seen in vertical section the lavas and palagonite-breccias are unmistakably different. While the lavas are characterized by well-defined sub-horizontal stratification, the palagonite-breccias nearly always dip at 30–40°, with an average dip of 35°. In addition to the relative steepness, the dip direction of the palagonite-breccias varies in an ordered and radial sense and was commonly followed through a change in direction of almost 180° of arc, and in one instance through 360° of arc (Egg Island; Map 1). It has been deduced that the bedding structure of the palagonite-breccias is in the form of complete or partial cones and, although it was thought for some time during the present work that the lavas and palagonite-breccias were distinct units separated from each other by an angular unconformity (p. 4), it is now suggested that the two units are effectively one.

The attitude of the sub-horizontal lavas, which frequently have very vesicular upper surfaces, is not difficult to explain. Highly mobile basalt lavas (suggested by their vesicularity and the presence of olivine phenocrysts, indicative of the former presence of volatile constituents and relatively high temperature) would have been able to flow on a very low-angle slope. However, it is a little more difficult to account for the attitude of the palagonite-breccias, although there is no doubt that their present attitude is their original one. The following possible explanations of the structure in the palagonite-breccias will be considered.

i. That the palagonite-breccias have been symmetrically folded and that the folds were subsequently planed by erosion.
ii. That the palagonite-breccias are the bases of razed subaerial strato-volcanoes.
iii. That the lavas and palagonite-breccias are the components of discoidal volcanoes analogous to tuyas (Mathews, 1947).
iv. That the palagonite-breccias were produced from large lava streams in a deltaic manner.

Explanations (i) and (ii) are untenable on several counts.

i. Although an isolated pseudo-anticlinal structure, e.g. the one in the north coast cliffs of Vega Island (Map 1), may be interpreted as a fold (Bibby, 1966), this explanation cannot account satisfactorily for the structures in three superimposed units of steeply dipping palagonite-breccias separated by sub-horizontal flow lavas. A fold may explain the structure in the lowermost palagonite-breccias, but to invoke any further folding for the succeeding palagonite-breccia units would be to ignore completely the horizontal attitude of the intervening flow lavas.

ii. The second possible explanation can be discounted, because the attitude of the palagonite-breccia beds is atypical of the rocks in subaerial strato-volcanoes. In the palagonite-breccia section in the north coast cliffs of Vega Island, which is typical of all such palagonite-breccias of this volcanic group, the relatively high dip of the beds ($\simeq 35°$) is maintained from the approximate position of the centre to the periphery of the cone structure, a distance of at least 4 miles (6·4 km.). In a typical subaerial strato-volcano it has been found that, at any one level in the cone, the dip of the volcanic rocks decreases with distance from the erupting centre. In fact, it is normal for the rocks high on the slopes of the volcano, near the crater, to dip more steeply than those lower on the flanks and consequently farther from the crater. However, in the palagonite-breccias of the James Ross Island Volcanic Group this has not been observed, although all the palagonite-breccia beds, whether near or at a distance from their centre of eruption, are asymptotic to the base of the unit, e.g. the cliffs west of Cape Gage and the cone south of Terrapin Hill (Plates IIIb and VIb).

There is a further serious objection to the "base of a cone" theory, which concerns the relative volumes of the original and residual volcanoes. Unless the tops of all the volcanoes were removed by Krakatao-like explosions, there would probably be some evidence of the waste products of the planed-off volcanoes

amongst the remainder of the primary volcanic rocks. No such evidence has been found, at least on the scale necessary to confirm this hypothesis.

Explanations (iii) and (iv), which are preferable to either of the first two, both involve the aqueous brecciation of molten basalt and the production of fragmentary olivine-hyalobasalt rocks: the palagonite-tuffs and breccias, or hydroclastic rocks (Fitch, 1965). Both of these explanations have application in this context, explanation (iv) accounting for many of the structures near the middle of James Ross Island, and explanation (iii) being applicable in the areas farther away. The lavas and palagonite-breccias are distinct and can never be confused in the field; in fact, they are so dissimilar that their possible genetic relationship was not at first suspected. However, in the cliff section at Cape Broms (Plate VIIc), a brecciated lava flow can undoubtedly be followed from a level where it is above the plane of apparent unconformity separating the two types of rocks through a series of downward steps into the palagonite-breccias. This structure can be seen in several other sections and it is important to note that in all cases the direction in which lava flows are cut out by the downward transgression of succeeding flows is in the same sense as the dip direction of the underlying palagonite-breccias. It would seem, therefore, that there is some genetic connection between the two stratigraphic units.

The flow lavas are sub-horizontal, holocrystalline and vesicular, whereas the palagonite-breccias always dip at about 35°, contain a high percentage of basalt glass and are cemented by zeolites. While the lavas show all the features to be expected of a basalt which has flowed, cooled and crystallized in a subaerial environment, the basalt glass in the underlying palagonite-breccias is evidence of the drastic quenching of molten basalt. The probable explanation of these contrasting characteristics is that the palagonite-breccias have been derived by the aqueous brecciation of olivine-basalt lava, which also formed the overlying sub-horizontal flow lavas. It was argued by Fuller (1931) that "a fluid lava on encountering a local body of water would tend to granulate like molten slag and would thus form a fine breccia, which would accumulate to a depth approximately equal to that of the water". When molten blast-furnace slag is poured into the sea, so much steam is produced by boiling that the granulating slag forms a floating fan. If the slag is tipped into the sea after a coherent crust has formed in the bucket, 10 per cent of the blocks so formed suffer explosive disruption but the rest sink quietly. The analogy is that the finer-grained palagonite-breccias have probably been formed by the granulation of relatively mobile basalt lava and that the basalt pillows, which either remain entire or are mechanically disrupted at a late stage in their cooling, have been formed from basalt with higher viscosity.

iii. Some of the lavas and palagonite-breccias evidently form discoidal volcanoes, analogous to the tuyas described by Mathews (1947) from northern British Columbia. These tuyas were formed as a result of the subglacial initiation of basaltic central eruptions and, in British Columbia, the water levels of the intra-glacial lakes (produced by volcanic melting of the ice sheet) were the planes at which most of the lava brecciation took place (Mathews, 1947). In the James Ross Island area the evidence favouring a marine environment is scarce. It includes the ophiuroids discovered by Bibby (1966), and it is also suggested by the geographical location of this volcanic group off the north-east coast of Graham Land. Apart from those described by Watson and Mathews (1944) and Mathews (1947), lava/palagonite-breccia volcanoes have been recorded in Iceland, where they were named "tablemountains" by Van Bemmelen and Rutten (1955). Palagonite-breccias have also been recovered from a seamount off the coast of Washington State, U.S.A., suggesting a closer similarity to a lava/palagonite-breccia volcano than a guyot (Nayudu, 1961).

At five localities within the James Ross Island area the lava/palagonite-breccia volcano cores are composed of fine-grained relatively structureless palagonite-tuff (p. 15). The tuff, which consists of palagonitized vesicular hyalobasalt fragments and individual olivine crystals, evidently represents the complete granulation of the emergent basalt magma when submarine eruption was initiated. These palagonite-tuffs are in marked contrast to the palagonite-breccias, which lack shards and contain clasts with very few vesicles. Here, the contrasting characteristics may be accounted for by the loss of volatile material while the lava was flowing subaerially, so that the viscosity would have been higher, the temperature would have been lower and the size of the resultant fragments would have been greater when the final brecciation took place (Fig. 3).

The sequence of events during the early stages of formation of these lava/palagonite-breccia volcanoes was probably similar to the initial activity of Surtsey, the new marine volcano south-west of Iceland (Dollar and Guest, 1963; Walker, 1964). The initial activity of Surtsey, which began erupting from the

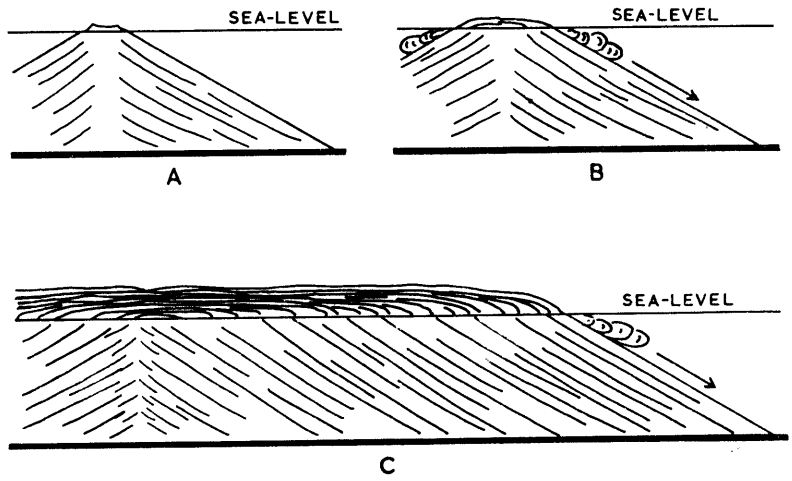

FIGURE 3

Diagram showing three stages in the development of a lava/palagonite-breccia volcano.

A. The initial submarine cone of finely divided hyalobasalt fragments.
B. The first few lava flows issuing from a subaerial vent and forming submarine "palagonite-breccia" talus slopes.
C. The mature lava/palagonite-breccia volcano.

sea bed at a depth of approximately 300 ft. (91·4 m.) was extremely violent. Volumes of ash-laden steam were produced for several weeks, at the end of which time a substantial complex cone of finely divided scoriaceous basalt fragments had been built up above the surface of the sea. Three coalescing craters could be discerned at this stage. After about 2 months of quiescence, activity re-commenced from one of the craters with the development of a small lava lake, from which braided flows drained across the ashy surface to the surrounding sea. Relatively quiet brecciation, where the molten lava met the sea-water, occurred in the manner which has been suggested for the formation of palagonite-breccias. The quiet effusion of basalt, which at one stage drained from the lava lake through a tunnel (p. 40), has since formed a substantial fan-shaped lava field seaward of the crater. It is believed that "palagonite-breccias" underlie the lava field and that sustained activity of this nature will result in a type lava/palagonite-breccia volcano (personal communication from G. P. L. Walker).

In plan, lava/palagonite-breccia volcanoes are capable of attaining as great a degree of eccentricity as is sometimes developed in subaerial strato-volcanoes. The large phase I volcano, which occurs in the centre of Vega Island and is exposed in the cliffs trending west from Cape Well-met, probably has "radii" ranging from 3·5 to 7 miles (5·6 to 11·3 km.) in length. Similarly, the phase I lava/palagonite-breccia volcano exposed in Seven Buttresses on Tabarin Peninsula measures between 1 and 4 miles (1·6 and 6·4 km.) from the eruptive centre to the periphery (Map 1).

Two occurrences of relatively steeply dipping fine-grained laminated tuffs, which have been interpreted as ash cones, occur in the head wall of Gourdon Glacier and in the cliffs 1 mile (1·6 km.) south of the snout of Hobbs Glacier. In view of the relationships between the ash cones and the surrounding rocks (Plate VIIb), they were probably formed subaerially, although their bases may have been submerged in water (Plate IIb). Although the structures are not so well displayed, other similar developments of tuffs have been interpreted as ash cones.

iv. In areas where the dip directions of the palagonite-breccias cannot be followed through 360° of arc, a modified type of lava/palagonite-breccia structure has been formed. In the localities where this is common, e.g. the coastal strips along the southern side of James Ross Island (Map 1), the dip of the palagonite-breccias is nearly always away from the centre of the island. There are indications that there was an island near the site of the present Mount Haddington during the greater part of the formation of the James Ross Island Volcanic Group, suggesting that the central area of James Ross Island was the site of a volcanic island similar to those of the Hawaiian type. Some of the flows from this volcano may be supposed to have reached the surrounding sea, as has happened in some of the Pacific islands Anderson, 1910) and Réunion (Lacroix, 1936). If the points of outflow of certain lava streams were

maintained for some time, then on being brecciated by sea-water, palagonite-breccia fans would probably be built out seaward in a manner comparable to deltaic sedimentation at the mouth of a river. However, it should be stressed that there are many localities around the margins of this area, where the dip of the palagonite-breccias is *towards* the location of this hypothetical island, and where it is unlikely that the palagonite-breccias were derived from such a source. Seven Buttresses, Egg and Vega Islands are three such localities.

By closely following the dip directions of the palagonite-breccias, particularly those of phase I, it has been possible to locate many centres from which palagonite-breccias have apparently been built out. These positions may represent the true centres of eruption or, alternatively, points where lava streams, having flowed from a large volcano situated near the centre of James Ross Island, entered the sea and built palagonite-breccia deposits in a deltaic fashion. It is notable that some centres of eruption appear to have been re-opened during a subsequent phase, an effect which has been recorded in Iceland (Van Bemmelen and Rutten, 1955). Those centres for which there is sufficient evidence, together with the locations of ash cones and volcanic plugs, have been plotted in Map 1. The distribution of the centres is apparently random and it reveals no significant structural trend, although it may reflect the underlying Upper Cretaceous structure in north-west James Ross Island and the structure beneath Prince Gustav Channel in the area south of Duse Bay. There is, however, a probable connection between the distribution of some apparent centres of eruption and the pre-James Ross Island Volcanic Group palaeogeography (p. 58).

Although the junction between lavas and palagonite-breccias may appear to be an unconformity, it is important to stress that it is a constructional, not destructional, horizon (Fig. 3). Seen in section, the sub-horizontal contact between lavas and palagonite-breccias is a good indication of the position of sea-level at the time of formation of the structure. By observing the relative heights and lateral relationships of several contacts, it is possible to determine the sequence and amounts of epeirogenic movements during the formation of the volcanic group. It has been found that this area underwent progressive depression relative to sea-level, although it was of an oscillatory nature and several temporary re-emergences occurred. An unusual overlap structure of palagonite-breccias against lavas, which has been seen at two localities only, suggests that the rate of eruption of flow lavas was, in rare instances, precisely balanced against the rate of sinking of a volcano beneath the sea (p. 40).

B. Overlap Structures

1. *Cone surface overlap structures*

The burial of pre-existing ash cones or palagonite-breccia slopes by the products of subsequent eruptions has led, in certain instances, to the development of cone surface overlap structures. The clearest example is the overlap structure formed against the surface of the ash cone 1 mile (1·6 km.) south of the snout of Hobbs Glacier (Plate VIIb), where flow lavas of a phase II lava/palagonite-breccia volcano overlap against the ash cone surface. The period of erosion which evidently intervened between phase II eruptions and those of phase III is demonstrated by the positive break in slope of the cone surface approximately 150 ft. (45·7 m.) above the top of the phase II flow lavas, and the lenticular body of tuff within the negative break in slope, consisting of the top surface of the lavas and the slope of the partially buried cone. At the close of phase II volcanic activity the negative break in slope was probably a land form which was subsequently buried by talus from the eroded ash cone. The eroded cone was finally buried completely beneath a palagonite-breccia of phase III.

Other examples of this type of structure occur in the head wall of Gourdon Glacier valley and in the large mesa east of Hidden Lake.

2. *Overlap structures probably due to sea-level changes*

In the cliffs 3 miles (4·8 km.) west of Cape Gage, St. Rita Point, the cliffs due west of Hamilton Point, the north end of the cliff 13 miles (20·8 km.) east-north-east of Cape Obelisk and the north coast cliffs of Jonassen Island, the contact between phase II lavas and palagonite-breccias occurs at two distinct but related levels, the altitudes of which are separated by 300 ft. (91·4 m.). (Fig. 4; Map 2B). In the occurrences at James Ross Island, the change in altitude is from approximately 1,100 to 800 ft. (336

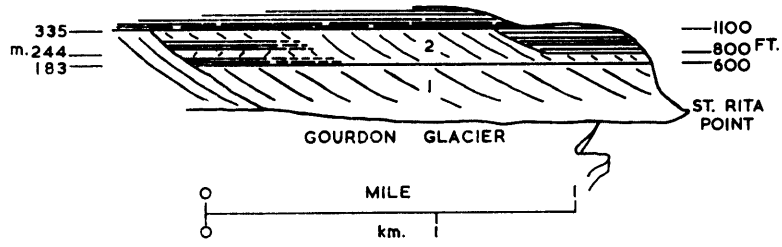

FIGURE 4

Field sketch of the overlap structures in the cliffs west of St. Rita Point. The horizontal shading represents olivine-basalt flow lavas.

1. Palagonite-breccias of phase I.
2. Palagonite-breccias of phase II.

to 244 m.) above sea-level, whereas at Jonassen Island the change is from 1,000 to 700 ft. (305 to 213 m.) above sea-level. The slope of the plane of overlap is parallel to the bedding of the palagonite-breccias immediately adjacent to it, and the continuity of the underlying palagonite-breccia units demonstrates that the structure is not due to faulting (Fig. 4).

Similar structures have been described in a tuya of northern British Columbia by Mathews (1947, p. 563), who attributed the stepped nature of the base of the flow lavas to progressive and sudden depressions of the level of the lake into which the tuya was erupted. In the case of the overlap structures in the James Ross Island Volcanic Group, the cause is more likely to have been a relative change in the position of sea-level at the time of their formation. In view of the instability of this area at the time of volcanicity, this probably resulted from a temporary 300 ft. (91·4 m.) elevation of the landmass. This type of overlap structure, which appears to be unique to the phase II lava/palagonite-breccia volcanoes, has been used as a means of correlation (p. 8).

Approximately 1 mile (1·6 km.) west of the exposure of the overlap structure on the south side of St. Rita Point, the two palagonite-breccia units and their associated flow lavas are truncated against older palagonite-breccias along a cone surface overlap structure (Fig. 4). The sequence of events which gave rise to these intercalations is reasonably clear. The palagonite-breccias forming the cone surface of the overlap structure in the west were evidently deposited first, when sea-level was at least at the present 1,100 ft. (336 m.) horizon. Subsequently, phase I lavas and palagonite-breccias were probably deposited in the deltaic manner described on p. 38, but later erosion removed most of the flow lavas, the remains of which immediately overlie the phase I palagonite-breccias adjacent to the cone surface overlap structure. At this stage sea-level had apparently been relatively lowered by at least 500 ft. (152 m.). A second unit of flow lavas, of limited lateral extent, occurs above the remnants of the phase I lavas and it is separated from them by a thin layer of palagonite-breccias (Fig. 4). These rocks were probably formed after a relative 250 ft. (76·2 m.) rise in sea-level and they represent a minor outburst of activity between the more prolonged volcanism of phases I and II.

Overlying all the previous rocks are the lavas and palagonite-breccias of phase II, in which the overlap structure probably due to a change in relative sea-level has been formed. Since the lava/palagonite-breccia contact in these rocks is initially at 1,100 ft. (336 m.) and is lowered to 800 ft. (244 m.) above sea-level farther to the east, it is evident that more sea-level fluctuations took place at the time of their formation. The apparent changes of sea-level with time have been plotted in Fig. 5 from which it will be seen that

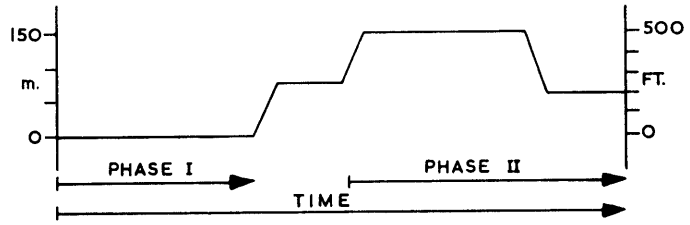

FIGURE 5

Graphical representation of the probable changes of relative sea-level during the formation of the overlap structures in the cliffs west of St. Rita Point.

approximately 800 ft. (244 m.) of relative lowering (approximately 500 ft. (152 m.) prior to phase I plus 300 ft. (91·4 m.) during phase II) and 500 ft. (152 m.) of relative elevation of sea-level (between phases I and II) took place during the formation of these structures.

3. *"Terminal slope" overlap structures*

There is an unusual overlap structure in the cliffs 2·75 miles (4·4 km.) south of Kotick Point and in the north-facing cliffs of the large mesa east of Hidden Lake. The flow lavas overlap against palagonite-breccias but the plane of overlap transgresses the bedding of the palagonite-breccias (Fig. 6). To the west of the "terminal slope" overlap structure in the mesa east of Hidden Lake, the lavas overlap against an older set of palagonite-breccias on a plane of cone surface overlap. Although the plane of a "terminal slope" overlap structure is ill-defined compared with a cone surface overlap, in the exposure 2·75 miles (4·4 km.) south of Kotick Point the flow lavas rest unconformably on palagonite-breccias, ruling out the possibility that the lavas fill a valley carved through the flank of a lava/palagonite-breccia volcano.

It is deduced that the palagonite-breccias beneath the cone surface overlap structure in the mesa east of Hidden Lake were erupted from the same centre that was subsequently responsible for the formation of the lavas. In view of the probable causality of sea-water in the brecciation of the lava flows, it is suggested that the development of a "terminal slope" overlap structure is evidence of a precise balance between the rate of eruption of lavas and the sinking of a volcano beneath the sea. In this way each successive lava, having descended the cone surface, flowed just above sea-level, brecciated at its distal end and formed "terminal slopes" which are steeply dipping palagonite-breccias of a modified form of lava/palagonite-breccia volcano. This explanation, summarized diagrammatically in Fig. 7, must remain tentative.

C. Lava Tunnels

Structures resembling filled lava tunnels occur in the cliffs 1 mile (1·6 km.) south-east of Bibby Point and in the north wall of the Gourdon Glacier valley. In both localities the structures appear as sub-circular cliff sections of coarse-grained lava, in which a system of cylindrical and radial joints has been developed. In the first one, the floor of the tunnel is probably composed of Upper Cretaceous rocks, in which there may have been a small valley. However, the Gourdon Glacier example is completely surrounded by flat-lying flow lavas. In both cases the tunnels are approximately 20 ft. (6·1 m.) high but their lengths are unknown.

D. Faults

1. *Minor faulting*

In the James Ross and Vega Islands area a few small penecontemporaneous faults have been observed (Plate VIId) but farther north in the islands of Prince Gustav Channel faulting is more significant.

There is a small fault in the west end of Beak Island, which brings palagonite-breccias of phase I against horizontally bedded palagonite-tuffs and has an unknown downthrow to the east (Map 1). A similar fault with an unknown downthrow to the west has been inferred in the structure of Eagle Island, where palagonite-breccias have been brought into juxtaposition with horizontal tuffs. In addition, it is possible that the difference in height between the lavas in north-east Eagle Island and those which cap the western end of Beak Island is due to displacement by a fault located in the channel separating the two islands. If this is a correct interpretation, the fault has a downthrow to the east of approximately 1,000 ft. (305 m.) (Map 1).

Preliminary determinations of olivine compositions (Table IX) has suggested that they can be used for stratigraphic correlation, providing the rocks of each phase carry olivine phenocrysts of relatively constant and characteristic composition. It is believed that the olivine phenocrysts of phase I are distinctly more magnesian than those of phase II and that the olivine phenocrysts become progressively more iron-rich with each succeeding phase. Although no systematic testing of this hypothesis has been possible, it suggests that the rocks of Brown Bluff and Seven Buttresses belong to the same phase (p. 8; Map 1). The 500 ft. (152 m.) difference in height between the lava/palagonite-breccia horizons in these two areas

indicates a fault with a downthrow to the west somewhere between Brown Bluff and Seven Buttresses. Geomagnetic evidence suggests extensive faulting in the rocks of Trinity Peninsula to the north (Allen, 1966). It is probable that faulting also affects the rocks of the James Ross Island Volcanic Group in close proximity to Trinity Peninsula.

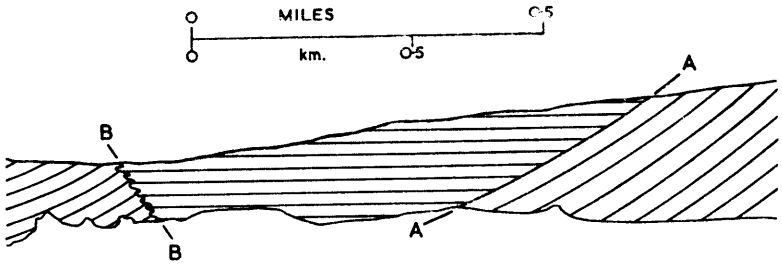

FIGURE 6

Diagram of the cone surface and "terminal slope" overlap structures exposed in the northern cliffs of the mesa east of Hidden Lake, James Ross Island; drawn from a photograph. The horizontal shading represents lavas and the diagonal shading represents palagonite-breccias.

A—A. Line of cone surface overlap structure.

B—B. Line of "terminal slope" overlap structure.

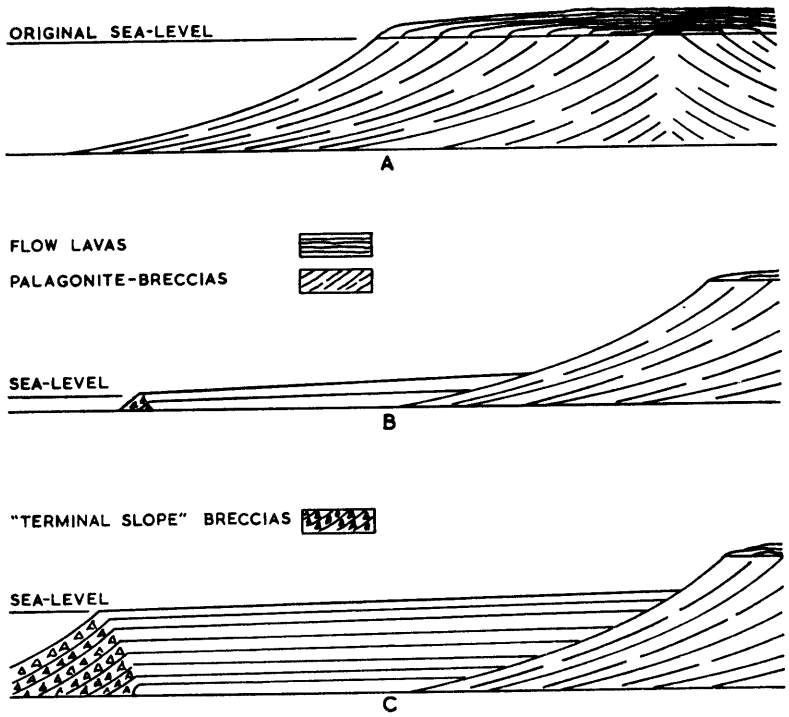

FIGURE 7

Diagram showing the suggested mode of formation of a "terminal slope" overlap structure.

A. The original volcano, probably a lava/palagonite-breccia volcano.

B. The original volcano and the first few flows after submergence has commenced.

C. The final composite volcano when submergence has been almost completed.

TABLE VIII

CHEMICAL ANALYSES OF ROCKS FROM THE JAMES ROSS ISLAND VOLCANIC GROUP

	1	2	3	4	5	6	7	8	9	10	11	12	13	14	15	16	
SiO_2	48·85	49·02	50·39	48·81	49·50	48·52	47·65	48·49	49·30	43·69	52·60	49·53	58·58	57·06	50·22	48·97	SiO_2
TiO_2	1·84	1·61	1·76	1·83	1·71	1·77	2·26	2·07	1·90	1·54	2·98	1·56	0·76	1·19	1·95	1·62	TiO_2
Al_2O_3	15·58	15·59	16·71	15·77	17·01	17·32	17·14	14·68	18·23	13·48	14·68	16·95	19·23	18·19	16·20	16·12	Al_2O_3
Fe_2O_3	1·76	2·59	1·71	2·01	1·85	3·38	3·51	3·52	5·00	5·10	2·19	3·49	2·26	2·75	3·13	1·90	Fe_2O_3
FeO	8·83	8·89	7·76	9·73	7·89	6·68	6·52	7·08	4·22	6·26	7·69	6·09	2·04	2·50	8·07	9·63	FeO
MnO	0·15	0·17	0·15	0·16	0·16	0·17	0·15	0·16	0·14	0·15	0·16	0·15	0·06	0·09	tr	tr	MnO
MgO	8·62	8·56	5·91	6·65	6·20	6·07	5·17	9·27	4·68	8·61	2·55	6·22	0·75	1·30	8·57	8·73	MgO
CaO	8·15	8·16	8·58	9·66	9·87	9·26	8·85	8·42	8·28	8·07	6·47	9·08	2·52	2·91	7·54	7·64	CaO
Na_2O	3·76	3·45	3·72	3·66	3·52	3·48	3·64	3·45	3·64	2·43	5·20	3·70	6·36	5·69	3·36	2·99	Na_2O
K_2O	1·17	0·94	1·16	0·73	0·96	1·09	1·34	1·31	1·71	0·69	3·05	1·12	4·91	4·46	1·38	1·21	K_2O
H_2O+	0·39	0·38	1·22	0·85	1·22	1·67	2·04	0·70	2·13	9·75	1·06	1·10	2·16	3·10	0·22*	1·39*	H_2O+
H_2O-	0·16	0·64	0·21	0·16	0·18	0·20	0·82	0·35	0·20		0·09	0·56	0·13	0·10			H_2O-
P_2O_5	0·47	0·39	0·45	0·36	0·34	0·42	0·56	0·62	0·54	0·19	1·09	0·34	0·08	0·28	—	—	P_2O_5
CO_2	0·65	0·05	0·05	0·14	0·07	0·14	0·13	0·12	0·13	0·57	0·13	0·08	0·13	0·12	—	—	CO_2
TOTAL	100·38	100·44	99·78	100·52	100·48	100·17	99·78	100·24	100·10	100·53	99·94	100·08	99·97	99·74	100·64	100·20	TOTAL
	ANALYSES LESS TOTAL WATER (Recalculated to 100)																
SiO_2	48·93	49·31	51·23	49·05	49·96	49·36	49·17	48·88	50·43	48·12	53·25	50·32	59·97	59·11	50·01	49·56	SiO_2
TiO_2	1·84	1·62	1·79	1·84	1·73	1·80	2·33	2·09	1·94	1·70	3·02	1·69	0·78	1·23	1·94	1·64	TiO_2
Al_2O_3	15·61	15·68	16·99	15·85	17·17	17·62	17·69	14·80	18·65	14·85	14·86	17·22	19·69	18·85	16·13	16·31	Al_2O_3
Fe_2O_3	1·76	2·61	1·74	2·02	1·87	3·44	3·62	3·55	5·12	5·62	2·22	3·55	2·31	2·85	3·12	1·92	Fe_2O_3
FeO	8·85	8·94	7·89	9·78	7·96	6·79	6·73	7·14	4·33	6·90	7·78	6·19	2·09	2·59	8·04	9·75	FeO
MnO	0·15	0·17	0·15	0·16	0·16	0·17	0·15	0·16	0·14	0·16	0·16	0·16	0·06	0·09	tr	tr	MnO
MgO	8·64	8·61	6·01	6·68	6·26	6·17	5·33	9·35	4·77	9·48	2·58	6·32	0·77	1·35	8·53	8·84	MgO
CaO	8·16	8·21	8·72	9·71	9·96	9·43	9·13	8·49	8·47	8·89	6·55	9·23	2·58	3·01	7·51	7·73	CaO
Na_2O	3·77	3·47	3·78	3·68	3·55	3·54	3·76	3·48	3·72	2·68	5·26	3·76	6·51	5·89	3·35	3·03	Na_2O
K_2O	1·17	0·95	1·18	0·73	0·97	1·11	1·38	1·32	1·75	0·76	3·09	1·14	5·03	4·62	1·37	1·22	K_2O
P_2O_5	0·47	0·39	0·46	0·36	0·34	0·43	0·58	0·62	0·55	0·21	1·10	0·35	0·08	0·29	—	—	P_2O_5
CO_2	0·65	0·05	0·06	0·14	0·07	0·14	0·13	0·12	0·13	0·63	0·13	0·08	0·13	0·12	—	—	CO_2
	NORMS																
Q	—	—	—	—	—	—	—	—	0·27	—	—	—	—	—	—	—	Q
or	6·89	5·62	6·95	4·28	5·73	6·56	8·12	7·78	10·34	4·50	18·24	6·73	29·69	27·24	8·34	7·23	or
ab	31·86	29·34	31·96	30·23	30·03	29·92	31·75	29·40	31·44	22·64	40·40	31·75	49·36	49·78	28·30	25·68	ab
an	22·21	24·38	25·88	24·57	28·02	28·82	27·33	20·88	29·02	26·24	7·84	26·74	9·67	11·37	25·02	26·69	an
ne	—	—	—	0·48	—	—	—	—	—	—	2·19	—	3·07	—	—	—	ne
di	8·98	10·96	11·43	16·71	15·25	11·46	10·90	13·09	6·66	9·90	14·50	13·01	1·38	0·77	14·12	13·63	di
hy	0·80	5·31	8·07	—	1·40	4·55	2·45	2·54	9·50	20·75	—	4·47	—	2·97	4·55	2·22	hy
ol	20·65	16·42	8·49	16·07	12·55	8·83	8·67	15·37	—	2·56	5·16	7·87	1·44	0·39	11·78	16·58	ol
mt	2·55	3·78	2·53	2·92	2·71	4·99	5·27	5·15	7·45	8·17	3·22	5·15	3·36	4·13	4·64	2·78	mt
il	3·50	3·09	3·40	3·50	3·30	3·42	4·44	3·98	3·69	3·24	5·75	3·22	1·49	2·34	3·80	3·04	il
ap	1·11	0·91	1·07	0·84	0·81	1·01	1·38	1·48	1·31	0·50	2·59	0·84	0·20	0·67	—	—	ap
cc	1·48	0·11	0·14	0·32	0·16	0·32	0·30	0·27	0·30	1·43	0·30	0·18	0·30	0·27	—	—	cc
	CATION PERCENTAGES																
Si^{+4}	22·87	23·05	23·95	22·93	23·35	23·07	22·98	22·85	23·57	22·49	24·89	23·52	28·03	27·63	23·36	23·15	Si^{+4}
Al^{+3}	8·26	8·30	8·99	8·39	9·08	9·32	9·36	7·83	9·87	7·86	7·86	9·11	10·42	9·97	8·54	8·63	Al^{+3}
Fe^{+3}	1·23	1·83	1·22	1·41	1·31	2·41	2·53	2·48	3·58	3·93	1·55	2·48	1·61	1·99	2·18	1·34	Fe^{+3}
Mg^{+2}	5·21	5·19	3·63	4·03	3·77	3·72	3·21	5·64	2·88	5·72	1·56	3·81	0·46	0·81	5·15	5·33	Mg^{+2}
Fe^{+2}	6·88	6·95	6·13	7·60	6·19	5·28	5·23	5·55	3·37	5·36	6·05	4·81	1·62	2·01	6·23	7·58	Fe^{+2}
Na^{+1}	2·79	2·57	2·80	2·73	2·63	2·63	2·79	2·58	2·76	1·99	3·90	2·79	4·83	4·37	2·49	2·25	Na^{+1}
Ca^{+2}	5·83	5·87	6·23	6·94	7·12	6·74	6·52	6·07	6·05	6·35	4·68	6·59	1·84	2·15	5·37	5·52	Ca^{+2}
K^{+1}	0·97	0·79	0·98	0·61	0·81	0·92	1·15	1·09	1·45	0·63	2·56	0·95	4·17	3·84	1·14	1·01	K^{+1}
Ti^{+4}	1·10	0·97	1·07	1·10	1·04	1·08	1·40	1·25	1·16	1·02	1·81	1·01	0·47	0·74	1·16	0·98	Ti^{+4}
Mn^{+2}	0·12	0·13	0·12	0·13	0·13	0·13	0·12	0·13	0·11	0·13	0·13	0·13	0·05	0·07	tr	tr	Mn^{+2}
P^{+5}	0·20	0·17	0·20	0·16	0·15	0·19	0·25	0·27	0·24	0·09	0·48	0·15	0·03	0·13	—	—	P^{+5}
O^{-2}	44·54	44·18	44·68	43·97	44·42	44·51	44·46	44·26	44·96	44·43	44·53	44·65	46·47	46·29	44·38	44·21	O^{-2}
Position $[(\frac{1}{3}Si+K)-(Ca+Mg)]$	−2·45	−2·59	−0·90	−2·72	−2·30	−1·85	−0·92	−3·00	+0·38	−3·95	+4·61	−1·61	+11·21	+10·09	−1·59	−2·12	Position $[(\frac{1}{3}Si+K)-(Ca+Mg)]$
Fe	60·9	62·8	66·9	69·1	66·5	67·4	70·7	58·7	70·7	61·9	83·0	65·7	87·5	83·2	62·0	62·6	Fe
Mg	39·1	37·2	33·1	30·9	33·5	32·6	29·3	41·3	29·3	38·1	17·0	34·3	12·5	16·8	38·0	37·4	Mg
Fe	47·5	50·7	49·8	55·0	51·0	51·4	52·0	46·3	49·5	52·7	48·7	49·1	25·5	30·7	48·9	50·9	Fe
Mg	30·5	29·9	24·6	24·6	25·6	24·9	21·5	32·5	20·5	32·4	10·0	25·7	3·6	6·2	30·0	30·4	Mg
Alk	22·0	19·4	25·6	20·4	23·4	23·7	26·5	21·2	30·0	14·9	41·3	25·2	70·9	63·1	21·1	18·7	Alk
Ca	60·8	63·6	62·2	67·5	67·4	65·5	62·3	62·3	59·0	70·8	42·0	63·8	17·0	20·7	59·7	62·9	Ca
Na	29·1	27·8	28·0	26·6	24·9	25·6	26·7	26·5	26·9	22·2	35·0	27·0	44·5	42·2	27·6	25·6	Na
K	10·1	8·6	9·8	5·9	7·7	8·9	11·0	11·2	14·1	7·0	23·0	9·2	38·5	37·1	12·7	11·5	K

* Total loss on ignition including CO_2

1. D.3302.1 Fresh olivine-hyalobasalt from palagonite-breccia; Seven Buttresses, Tabarin Peninsula.
2. D.3740.1 Ophitic olivine-dolerite dyke; Blancmange Hill, James Ross Island.
3. D.3756.1 Analcite-bearing olivine-dolerite plug; south-west end of Lachman Crags, James Ross Island.
4. D.4052.3 Analcite-bearing olivine-dolerite associated with olivine-dolerite dyke; Haslum Crag, Snow Hill Island.
5. D.4053.1 Coarse olivine-basalt with xenocrystic plagioclase; Gourdon Glacier, James Ross Island.
6. D.4053.7 Coarse olivine-basalt with phyric plagioclase; Gourdon Glacier, James Ross Island.
7. D.4053.8 Olivine-basalt with hemi-hyaline groundmass; Gourdon Glacier, James Ross Island.
8. D.4053.12 Olivine-rich basalt; Gourdon Glacier, James Ross Island.
9. D.4053.18 Altered olivine-basalt; Gourdon Glacier, James Ross Island.
10. D.4068.2 Palagonite-breccia cemented with chabazite; south of Tait Glacier, James Ross Island.
11. D.4086.4 Dolerite-pegmatite schlieren; Palisade Nunatak, James Ross Island.
12. D.4088.1 Analcite-bearing olivine-dolerite; Palisade Nunatak, James Ross Island.
13. D.4088.4 Alkali-segregation; Palisade Nunatak, James Ross Island.
14. D.4088.5 Late-stage felsitic vein; Palisade Nunatak, James Ross Island.
15. "Basalt glass"; Cockburn Island (Prior, 1899). Probably an olivine-hyalobasalt from pillow margin.
16. "Basalt"; Cockburn Island (Prior, 1899). Probably an olivine-basalt from the same pillow as analysis 15.

Analyses 1–14 by P. H. H. Nelson.

[face page 42

2. *Absence of evidence for major faulting*

In all the cliff sections of volcanic rocks examined on James Ross and Vega Islands, not one fault of any consequence has been observed. This is negative evidence but it is believed that if faulting is present then somewhere in approximately 240 miles (386 km.) of cliff sections large faults would be observable. However, there are 19 examples of the various types of overlap structures, and many more rock relationships at present obscured by ice may be explained by extrapolation of the structures. The occasional absence of some units, particularly flow lavas, is probably due to the very open subaerial and shallow subaqueous nature of the environment of formation. The structural arrangement of the James Ross Island Volcanic Group rocks is believed to be almost the same now as it was at the end of their formation, and it is unnecessary to invoke large-scale faulting to explain it.

V. GEOCHEMISTRY

FOURTEEN new chemical analyses of rocks from the James Ross Island Volcanic Group are presented in this report (Table VIII, analyses 1–14) and for the purposes of discussion, two analyses carried out by Prior (1899) have been included (Table VIII, analyses 15 and 16). The range and distribution of the rocks types are given in the explanation to Table VIII. The selection of specimens for analysis has been carried out as follows:

i. Rocks from phases I, II and III (p. 8) have been analysed to study the chemical variation in the lavas, olivine-hyalobasalts, plugs and dykes, and to afford a chemical basis for their classification.

ii. In order to obtain a preliminary definition of the chemical changes involved in the palagonitization and cementation of a palagonite-breccia with zeolite (p. 33), a well-cemented palagonite-breccia of phase I has been selected.

iii. Four rocks from the analcite-bearing olivine-dolerite intrusion of Palisade Nunatak have been selected to define the late-stage course of differentiation, which is characterized by the abundance of alkalis and volatile constituents (p. 27).

iv. The selection of extrusive rocks and those from Palisade Nunatak has been carried out with a view to demonstrating the inter-relationship of the two rock groups.

A. VARIATION TRENDS

C.I.P.W. norms and cation percentages are also given with the chemical analyses in Table VIII. Ternary variation diagrams of the James Ross Island Volcanic Group rocks have been plotted on the co-ordinates (Fe″+Fe‴)—Mg—Alk and Ca—Na—K (Fig. 8). Ternary variation diagrams of the feldspathic normative constituents have been plotted on the co-ordinates an—ab—or and ne—kp—SiO_2 (Figs. 9 and 10). Two linear variation diagrams are also included (Figs. 11 and 12). Fig. 11 shows the variation of the cations and oxygen in relation to the function $[(\frac{1}{3}Si+K)-(Ca+Mg)]$, which is the modified Larsen function used by Nockolds and Allen (1953), and Fig. 12 relates the change in total iron (Fe″+Fe‴) to magnesium (Mg), expressed as cation percentages.

All the analysed rocks are plotted in each variation diagram and curves have been drawn relating the late-stage rocks of the Palisade Nunatak intrusion to the lavas and plug rocks. Because the analcite-bearing olivine-dolerite from the Palisade Nunatak intrusion plots in a central position within the changes demonstrated by the lavas (Figs. 8 and 11) and because of the association of the two rock groups, it is believed that the chemical changes in both the lavas and the rocks of Palisade Nunatak can be taken in conjunction with each other. However, it is very important to note that the last stages of differentiation have been recorded in the Palisade Nunatak intrusion only and they have not been encountered as surface flows or other extrusive bodies.

Fig. 8 shows the variation of the James Ross Island Volcanic Group rocks plotted on the co-ordinates (Fe″+Fe‴)—Mg—Alk. The main differentiation curve is characterized by initial moderate iron enrichment culminating in a marked increase in the relative proportion of alkalis. The ratio (Fe″+Fe‴) : Mg and the relative proportion of alkalis increase steadily from the start, but where the rate of increase in the relative proportion of alkalis is greatest, the increase in the (Fe″+Fe‴) : Mg ratio is least (Table VIII).

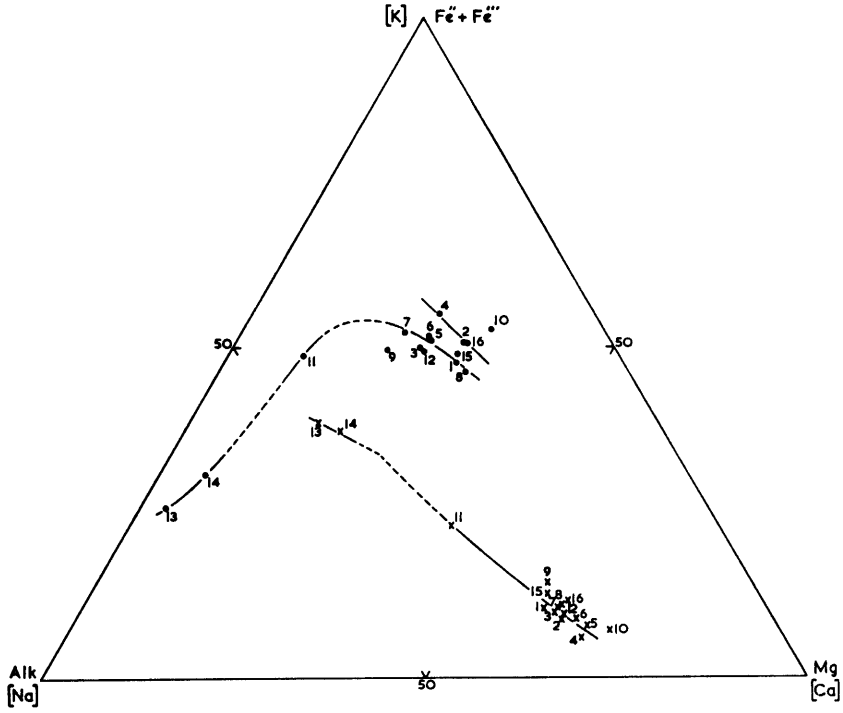

FIGURE 8

Triangular variation diagrams for the James Ross Island Volcanic Group rocks, plotted on the co-ordinates (Fe''+Fe''')—Mg—Alk (upper curves) and Ca—Na—K (lower curve). The numbers refer to the chemical analyses in Table VIII.

The smaller curve, which lies nearer to the (Fe''+Fe''') apex in Fig. 8, relates the dyke rocks (Table VIII, analyses 2 and 4) and possibly the basalt from Cockburn Island (Prior, 1899; Table VIII, analysis 16). This curve, drawn as a straight line originating at the Mg apex of the diagram, represents an increase in the ratio (Fe''+Fe''') : Mg at a constant (Fe''+Fe''') : Alk ratio. The plot of a palagonite-breccia (Table VIII, analysis 10) is isolated in a position nearer the (Fe''+Fe''')—Mg boundary than any other analysed specimen.

All the analysed rocks appear to belong to a single trend when plotted on the co-ordinates Ca—Na—K, with the probable exception of the palagonite-breccia (Table VIII, analysis 10), which is closer to the Ca apex than any other analysed specimen (Fig. 8). The greater part of this trend is characterized by an increase in Na and K relative to Ca, and an increase in the K : Na ratio. The last part of the trend, the starting point of which is not known precisely, is characterized by an increase in Na and K relative to Ca but at a constant K : Na ratio. An interesting feature is shown by the early part of this trend. If the course of differentiation is shown correctly by the curves of (Fe''+Fe''')—Mg—Alk variation (Fig. 8), i.e. analysis 1 is earlier than analyses 5 and 6, and analysis 2 is earlier than analysis 4, it will be seen that early rocks are relatively poorer in Ca than those immediately following them. Although these plotted positions are so close together that they may not be statistically significant, it suggests that very early in the trend Ca becomes enriched relative to Na and K (cf. Fig. 9).

The relative proportions of the an, ab and or molecules occurring in the norms have been plotted on the co-ordinates an—ab—or (Fig. 9). Where it occurs, ne has been recalculated as ab. Although the calculation of C.I.P.W. norms represents an "idealized mineral assemblage", it is believed that the alumino-silicates, above all, are relatively faithfully represented. The "critically undersaturated" nature (Yoder and Tilley, 1962) of nearly all the norms also suggests that changes in bulk feldspar composition may be justifiably considered in terms of normative an, ab and or. This diagram reveals a similar overall trend to that plotted on the co-ordinates Ca—Na—K. In the later stages of the trend there is a marked depletion in the an molecule at the expense of the ab and or molecules, and the or : ab ratio rises. In the final stages of the trend (Fig. 9, analyses 11, 14, 13) there is a sudden increase in the relative proportion of the or molecule, followed by an increase in the ab and or molecules at a constant or : ab ratio (or_{35} :

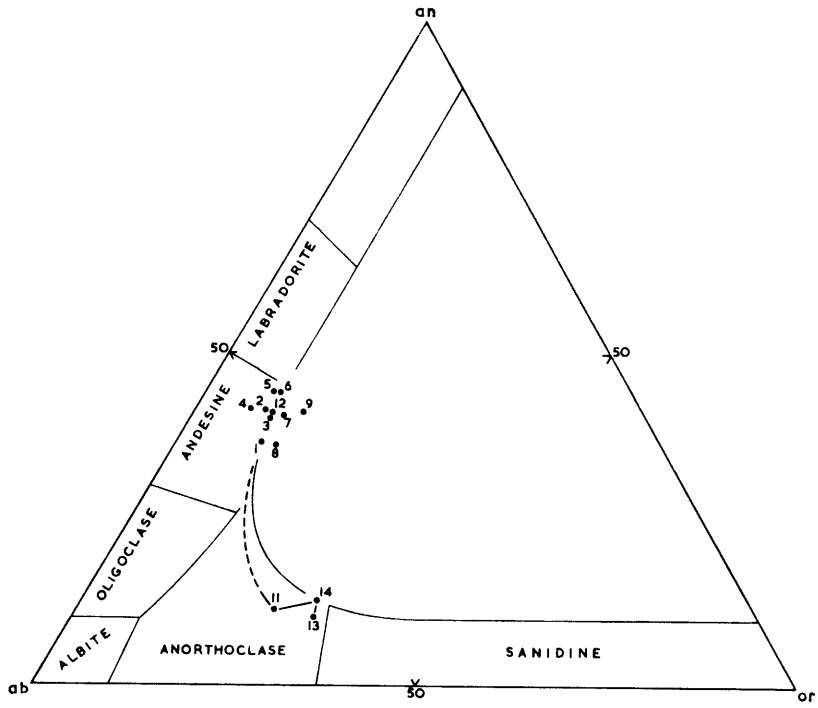

FIGURE 9

Triangular variation diagram of normative feldspar compositions in rocks of the James Ross Island Volcanic Group, plotted on the co-ordinates an—ab—or. The numbers refer to the chemical analyses in Table VIII. The suggested limits of solid solution in the feldspars (Deer, Howie and Zussman, 1963*b*) are also shown.

ab_{65}). The last two rocks (Table VIII, analyses 14 and 13) contain 88·39 and 94·38 per cent of normative feldspar (including ne as ab), respectively.

In the early stages of this trend (Fig. 9) there are indications of a similar relative increase in the proportion of the an molecule to the apparent increase in total Ca with respect to Na and K in Fig. 8. Yet again, the grouping of these plotted points may be too close to be of statistical significance. However, in view of the difference of nearly 8 per cent between the normative an content of analysis 1 and analyses 5 and 6, and the consistency of the direction of this change in both variation diagrams (Figs. 8 and 9), the trend is believed to be real. Moreover, it can be accounted for by the mineralogy of the rocks. Nevertheless, it should be noted that the norm can indicate plagioclase that is more calcic than the modal mineral, due to entry of alumina into modal pyroxene (Yoder and Tilley, 1962, p. 420). Except for analyses 8 (an olivine-rich basalt) and 9 (a rock in which zeolite veinlets occur), the plotted bulk normative feldspar compositions all lie close to the estimated limit of solid solution in the feldspar series (Deer, Howie and Zussman, 1963*b*).

Only the last two rocks of the trends revealed in Figs. 8 and 9 can be considered in terms of the co-ordinates ne—kp—SiO_2 (Fig. 10). Bowen (1937), who first described this system in relation to natural rocks, excluded from his considerations all rocks in which the total of ne, kp and SiO_2 occurring in the norm was less than 80 per cent. The totals of ne (and ab recalculated as ne), kp (or recalculated as kp) and SiO_2 (the excess SiO_2 derived by recalculating ab and or) in analyses 14 and 13 are 77·05 and 84·74 per cent of the norm, respectively. Strictly speaking, analysis 14 should be excluded. However, its total ne, kp and SiO_2 content is nearly 80 per cent, and it has been retained in order to illustrate the precise coincidence of the plotted positions of analyses 13 and 14 in this system (Fig. 10). This fact has governed the plotting of the late-stage course of differentiation in the previous variation diagrams (Figs. 8 and 9), in which the final stages of alkali enrichment relative to Ca have been deduced to be at a constant Na : K ratio. In addition, the plotted positions of analyses 13 and 14 fall within the low-temperature trough on the ab—or tie-line, very close to the plotted positions of the averages of 19 alkaline trachytes and 32 alkaline syenites (Bowen, 1937).

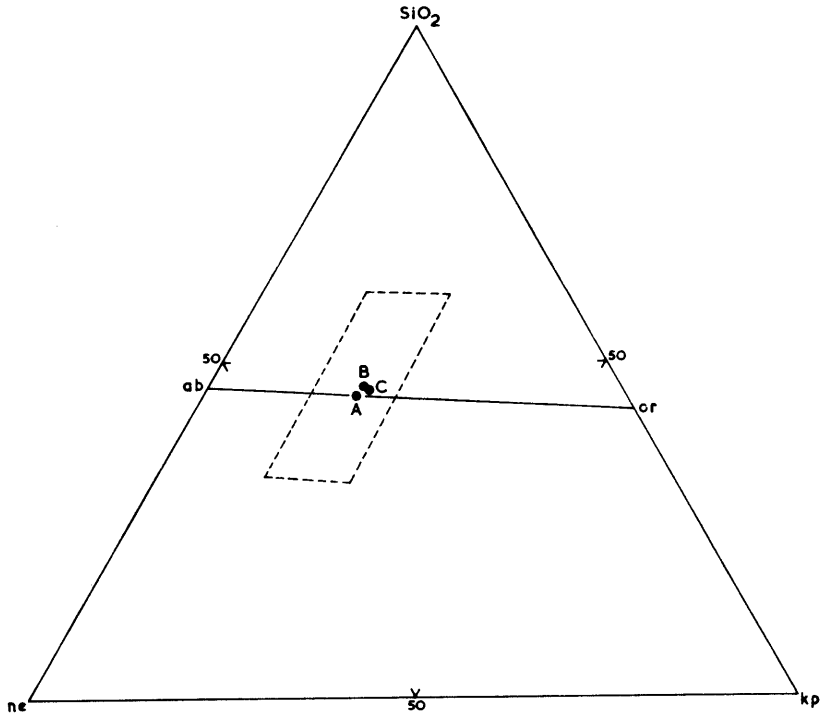

FIGURE 10

Triangular variation diagram of an alkaline segregation and felsitic vein from Palisade Nunatak, James Ross Island, plotted on the co-ordinates ne—kp—SiO_2. The pecked line indicates the approximate limits of the low-temperature trough (Bowen, 1937).

A. Alkaline segregation and felsitic vein from Palisade Nunatak, James Ross Island (Table VIII, analyses 13 and 14).
B. Position of 19 alkaline trachytes (Bowen, 1937).
C. Position of 32 alkaline syenites (Bowen, 1937).

In Fig. 11 cation percentages have been plotted against the function $[(\frac{1}{3}Si+K)-(Ca+Mg)]$, *the position* (Nockolds and Allen, 1953), in preference to the plotting of oxides against the ratio $(FeO+Fe_2O_3)/(FeO+Fe_2O_3+MgO)$ (Walker, 1953; Wilkinson, 1958). The former representation can reveal relative and total iron enrichment and it is better suited to the last stages of the differentiation trend, where an increase in Si becomes important. It has been found that the shapes of the first part of the curves, i.e. at low values of the position or the ratio $(FeO+Fe_2O_3)/(FeO+Fe_2O_3+MgO)$, are the same in both diagrams.

Si rises steadily with increase in the value of the position (Fig. 11). After an initial rise, however, O and Al fall to a distinct minimum with further increase in the value of the position. Analysis 11, which plots on the minima of these trends, is a dolerite-pegmatite from the Palisade Nunatak intrusion. Finally, O and Al rise to values which are higher than at any previous stage, although there are too few "control" points in this critical part of the differentiation. With increase in the value of the position, Mg falls rapidly at first but it then diminishes more gradually, until it reaches a minimum value in the last rock of the trend. In contrast, Ca behaves in an opposite manner to Mg at the start, but having rapidly reached a maximum at a low value of the position, it falls steadily to the critical point (analysis 11), where it is believed that there is a rapid decrease in Ca, a downward trend which is continued less severely to the end.

The main total iron trend is characterized by virtual constancy of the total iron value with increase in the value of the position until the critical point is reached (Fig. 11, analysis 11), after which there is a significant depletion to the end. Although by no means proven, it is suggested that there is a slight absolute enrichment in iron before the critical point is reached (Figs. 11 and 12). The dykes (analyses 2 and 4) and perhaps the rocks from Cockburn Island (analyses 15 and 16) appear to form part of a separate group with a total iron content significantly higher than that of the other rocks. A small horizontal trend line has been drawn through them. The behaviour of P and Ti is somewhat similar to that of total iron.

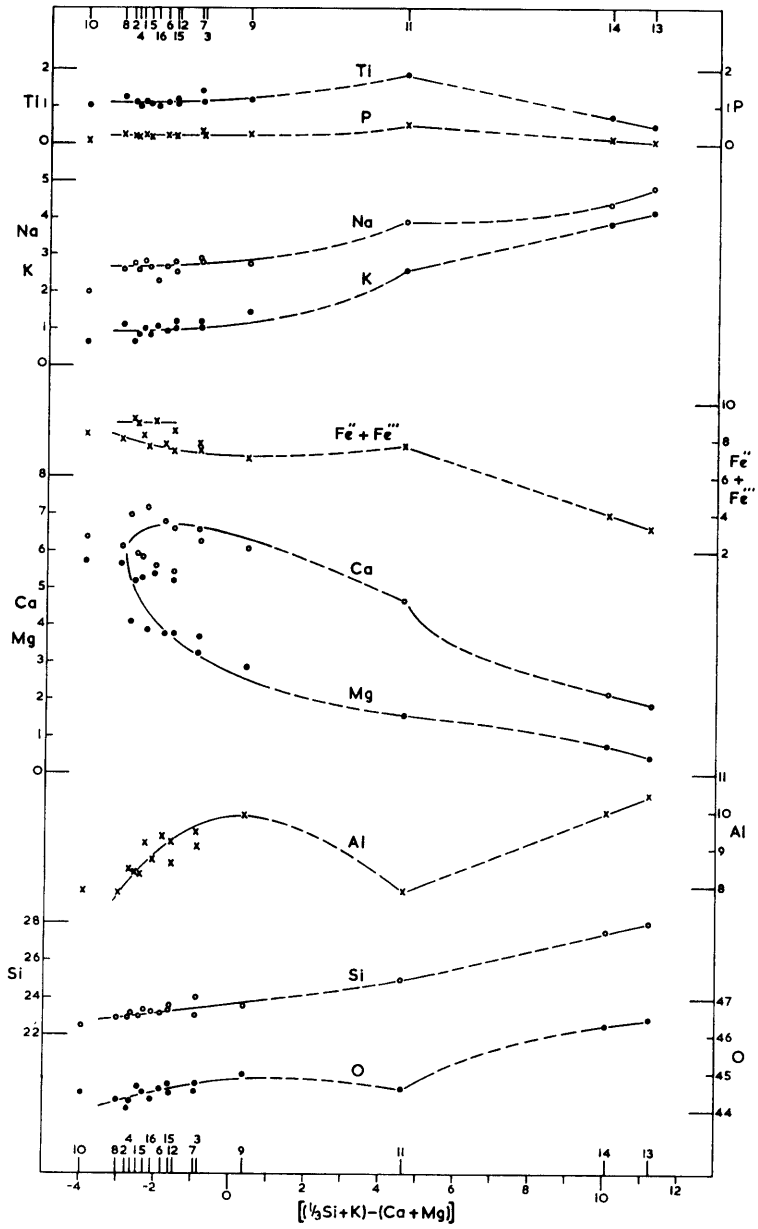

FIGURE 11

Variation diagram of cations (per cent) and oxygen (per cent) for the James Ross Island Volcanic Group rocks, plotted against the function [(⅓Si+K)—(Ca+Mg)]. The numbers refer to the chemical analyses in Table VIII.

Between the start of the trend and the critical point, the amounts of P and Ti double. However, these two cations fall significantly during the last stages of the trend to about one-half their original values.

Throughout the whole trend, the alkalis follow courses of continual enrichment but until the very last stages, at high values of the position, K becomes enriched at a greater rate than Na. During the very last stages the rate of enrichment is probably the same for both alkalis (Figs. 8, 9 and 10). In this particular context the degree of absolute enrichment of each alkali is the same both before and after the critical point (Fig. 11, analysis 11), i.e. about 1 per cent for Na and 1·5 per cent for K.

This graphical representation of the variation in cation percentages against the function [(⅓Si+K)—(Ca+Mg)] reveals the apparently anomalous characteristics of analysis 11 at the critical point. Here, Al and O are at a minimum when P, Ti and possibly total iron have just attained a maximum. It is this feature in particular, which is probably more typical of the differentiation of intrusive dolerites

(Nockolds and Allen, 1956) than of a series of related volcanic rocks (Nockolds and Allen, 1954). Nockolds and Allen (1956, figs. 42h, i, 43h, i) have shown that in the case of the Dillsburg sill and the Skaergaard intrusion minima in O and Al coincide with a maximum in total iron, although Si rises continually throughout the trends. In their papers Nockolds and Allen (1953, 1954, 1956) have shown that in most series of related volcanic rocks O tends to rise steadily with Si as the value of the position increases to a maximum, but there is no evidence of a minimum in the Al trend.

In order to ascertain still further the validity of analysis 11 (Fig. 11), cation percentages have been calculated for some of the analyses of dolerite-pegmatites and associated dolerites quoted by Walker (1953, fig. 2), who has demonstrated that the dolerite-pegmatites are more differentiated rocks than their parent dolerites. This conclusion was borne out when the oxygen percentages of the dolerite-pegmatites and dolerites were plotted against the position, and it was found that four out of six dolerite-pegmatites (Walker, 1953) are poorer in oxygen than their parent dolerites. It is therefore concluded that the unusual characteristics of analysis 11 (Fig. 11) are probably real.

In Fig. 12 the cation percentages of total iron have been plotted against a scale of diminishing percentages of Mg. The main trend suggests once again that an initial relative enrichment in iron is followed by a

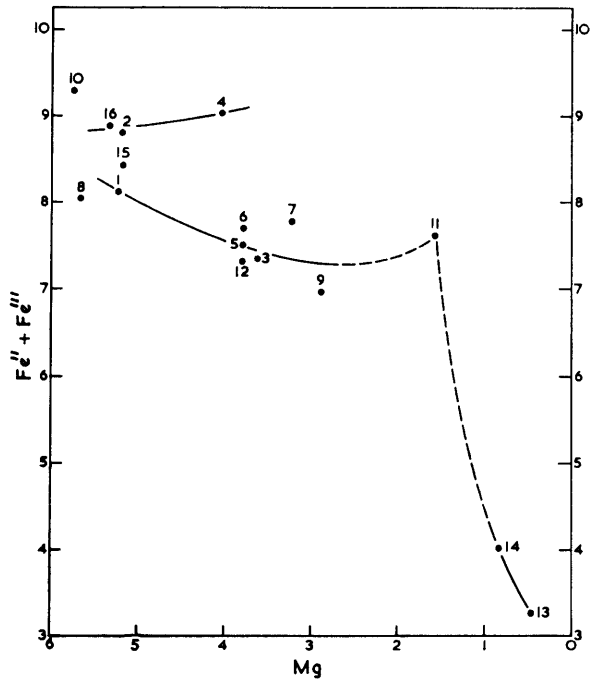

FIGURE 12

Variation diagram of (Fe″+Fe‴) (cation per cent) plotted against Mg (cation per cent) for rocks of the James Ross Island Volcanic Group. The numbers refer to the chemical analyses in Table VIII.

small absolute enrichment until a critical point is reached (analysis 11), where there is a sudden depletion in total iron. The ratio (Fe″+Fe‴) : Mg rises throughout this trend but it rises only slightly between analyses 11 and 14 (cf. Fig. 8). In addition, plotting total iron against magnesium effectively separates the dykes (analyses 2 and 4) from the rocks which lie on the main trend. Here also, analyses 15 and 16 probably correlate with the dyke rocks. The plotted position of a palagonite-breccia (analysis 10) is isolated, with a higher total iron content than any other rock.

B. Discussion

1. *Chemical classification*

Macdonald and Katsura (1964, fig. 1) have shown that, in the case of basalts from Hawaii, plotting (Na_2O+K_2O) against SiO_2 reveals a distinct population minimum separating tholeiitic from alkalic

basalts. The distinction between tholeiitic and alkalic basalts is otherwise drawn on the basis of mineralogical differences, and they have noted that when it is present titanaugite is diagnostic of alkalic basalts (Macdonald and Katsura, 1964, p. 90). The James Ross Island Volcanic Group lavas, plug and dyke rocks have been plotted on a total alkali oxides—silica diagram (Fig. 13), in which they all lie within the field of alkalic basalts as defined by Macdonald and Katsura (1964). The ubiquitous occurrence

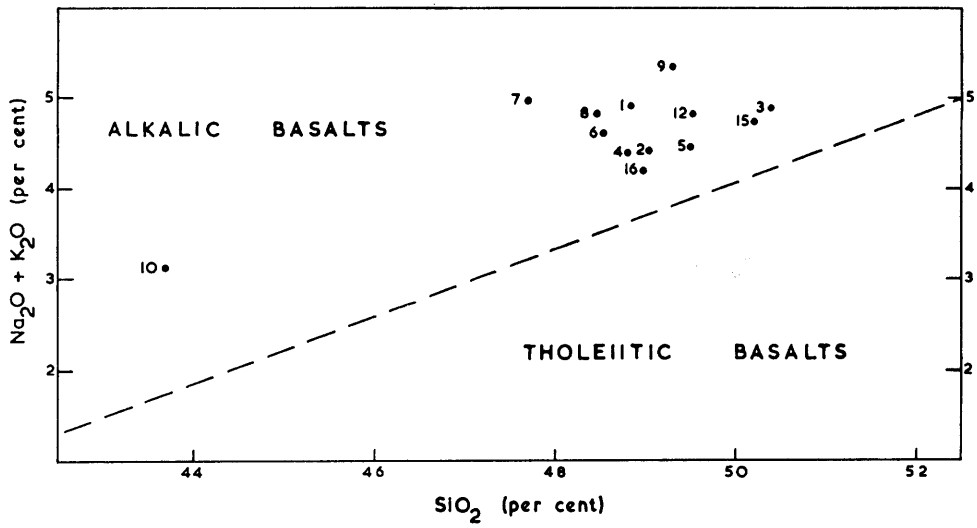

FIGURE 13

Graphical representation of total alkalis plotted against silica for rocks of the James Ross Island Volcanic Group. The fields of alkalic and tholeiitic basalts as defined by Macdonald and Katsura (1964) are also shown. The numbers refer to the chemical analyses in Table VIII.

of olivine, the frequent occurrence of titanaugite and the associated "undersaturated" assemblage of zeolites (p. 31) suggest that the field of alkalic basalts, which has been defined by Macdonald and Katsura (1964) with reference to Hawaii, has application in this context. In spite of the absence of nepheline in many of the norms and the presence of a little quartz in one of them, factors which would have led Yoder and Tilley (1962) to class most of these rocks as olivine-tholeiites, it is concluded that the James Ross Island Volcanic Group is composed entirely of alkalic (olivine-) basalts and their derivatives. Although the nomenclature of Macdonald and Katsura (1964) has been adopted for the basalts of this group, it should be emphasized that the majority of the rocks lie close to the plane of "critical undersaturation" in the simplified basalt system of Yoder and Tilley (1962, fig. 2). Moreover, all the extrusive rocks of the James Ross Island Volcanic Group are characterized by a high Al_2O_3 content, which places them near the field of high-alumina basalt. Yoder and Tilley (1962, p. 420–21) have noted that: "For critically undersaturated basalts, the alumina content would . . . be expected to be high in the normal course of fractionation." It is believed that the geochemistry of the James Ross Island Volcanic Group is also consistent with these conclusions.

2. *Differentiation in the extrusive rocks*

The extrusive rocks (Table VIII, analyses 1, 5, 6, 7, 8 and 9) examined here are all confined to the early part of the differentiation trend and they lie between position values of −3·0 and +0·4 (Table VIII). The palagonite-breccia (Table VIII, analysis 10) has been extensively altered and is therefore considered separately (p. 54). The plotted position of analysis 8 in most of the variation diagrams suggests that it is the least differentiated of the extrusive rocks but its position is probably anomalous. This is an olivine-rich basalt, which contains approximately 17·5 modal per cent of olivine phenocrysts; thus it is probably a cumulite type containing an abnormally large amount of magnesium for its stratigraphic position (phase III) and its place in the differentiation sequence as revealed in Figs. 8 and 11.

The fresh olivine-hyalobasalt from Seven Buttresses (Table VIII, analysis 1) is believed to approximate to the composition of the parental basalt of this volcanic group. Its low position in the stratigraphic sequence (phase I) and the magnesium-rich nature of its phenocrystic olivines ($Fo_{91}Fa_9$) support this

suggestion. Its chemical composition compares closely with the deduced chemical composition of the alkali olivine-basalt parental magma of Japan and Korea (Table X). The unusually high CO_2 content of this rock (Table VIII) is probably due to the incomplete mechanical separation of fresh olivine-hyalobasalt from its mantling shell of palagonite prior to analysis. It is suspected that palagonitization has the effect of introducing the CO_3^{-2} ion in abundance (p. 56). However, the thickness of the palagonite rims is not very great in this rock (0·04 mm.; Table VII) and the average size of the fragments is comparatively large (10–20 mm. and more in diameter), so it is believed that anomalies in the values of the other constituents, notably Na_2O and K_2O, will be only slight, even if a minor amount of palagonite has been included in the analysis sample. Because specimen D.4053.18 (Table VIII, analysis 9) has probably suffered minor hydrothermal alteration and it contains zeolite veinlets, the early course of differentiation will be considered in terms of analyses 1, 5, 6 and 7 (Table VIII). However, analysis 9 plots close to most of the differentiation curves, suggesting that its composition approximates to that of a fresh rock.

As is usual in basaltic differentiation, the first stage is characterized by the significant depletion of Mg and the resultant increase or virtual steadiness of every other constituent (Fig. 11). This is attributed to the initial crystallization of magnesian olivines which are, significantly, the only phenocryst minerals in the hyalobasalt fragments of phase I palagonite-breccias, and in the completely fragmented tuffs representing the first products of submarine eruption (p. 36). It is possible that early crystallization of magnesian pyroxenes occurred as well, although clinopyroxene phenocrysts in the lavas are very rare.

The second stage of differentiation is characterized by the depletion of Ca and a drop from the high value it had attained due to the early fractionation of magnesium-rich ferromagnesian minerals alone. As is normally the case, ferromagnesian fractionation continued and, because of the absence of a reaction relation between olivine and the magma (Wilkinson, 1956; Yoder and Tilley, 1962), both olivine and probably clinopyroxene became more iron-rich (p. 54). The steady depletion of Ca in this second stage of differentiation was most probably due to the start of calcium-rich plagioclase crystallization. Indeed, the phase III lavas (Table VIII, analyses 5, 6, 7 and 9) are characterized by the presence of large prismatic anorthitic plagioclase crystals, in addition to glomeroporphyritic clusters of olivine. Although the large feldspar crystals occasionally show signs of resorption, they are often subidiomorphic. It is believed that they are just as much phenocrysts (as opposed to xenocrysts) as the olivines and that these two minerals represent the crystalline phases existing in the basalt liquid before extrusion. However, it is possible that feldspar-rich basalt types have been developed giving rise to similar anomalies as olivine-rich oceanitic basalts, inasmuch as they may reveal an abnormally high Ca content due to the presence of anorthitic plagioclase crystals. The increase in Ca relative to Na and K (Fig. 8) and the increase in the an molecule relative to the ab and or molecules (Fig. 9) is due to the existence of large anorthitic plagioclase crystals in specimens D.4053.1, 7 (Table VIII, analyses 5 and 6). The anomalies shown by the olivine-rich and feldspar-rich basalts illustrate the difficulties arising from an attempt to define a course of differentiation on the basis of the chemical analyses of phyric rocks. Aphyric basalts would have revealed a closer approximation to the liquid line of descent but the phyric rocks are of sufficient interest and abundance in the field to justify their inclusion.

The probable order in which the crystalline silicate phases have separated from the magma is important. The early hyaloclastites of phase I contain only olivine phenocrysts (Fa_{7-9}), which are joined after extrusion by myriads of lath-shaped plagioclase microlites. A more protracted cooling period, such as in basalt pillows, has led to the additional development of "pyroxenic spherulites" (Lacroix, 1936), which may be large enough to be identified as titanian augite. Rocks from phase II or early phase III are characterized by the presence of slightly more iron-rich olivine phenocrysts (Fa_{25-28}) and very rare clinopyroxenes. Granular aggregates of olivine ($Fo_{74}Fa_{26}$), enstatite and minor diopside and spinel occur as cumulite pods in a dyke which is possibly associated with phase II eruptions (D.4049.3, p. 25), but the occurrence of clinopyroxene as phenocrysts is very rare. A few small fragmentary oscillatory zoned calcium-rich plagioclase crystals also occur in the rocks of phase II.

Rocks from phase III and later phases are characterized by the presence of even more iron-rich olivine phenocrysts ($Fo_{65}Fa_{35}$) and large complete plagioclase phenocrysts in the composition range $Ab_{10}An_{90}$–$Ab_{40}An_{60}$. The significance of these various associations of phenocryst minerals probably lies in the observations that (a) except in one instance (D.3771.1; p. 14), no clinopyroxene phenocrysts have been found in lavas bearing phyric olivine and anorthitic plagioclase, and (b) with the same exception, plagioclase phenocrysts are absent from rocks bearing phyric olivine and clinopyroxene.

Before an explanation of the variations in mineralogy, composition and associations of the phenocryst minerals can be attempted, it is necessary to ascertain whether water was present in the parental magma. Although all the analysed rocks contain H_2O+, it is believed that an approach to this problem via chemical analyses of the rocks as they are now is invalid. There is abundant evidence of the loss of volatile constituents in the form of vesicles in the hyaloclastites and upper surfaces of lava flows. This suggests that the H_2O+ content revealed by analysis is lower than the original water content of the magma. Walker and Poldervaart (1949, p. 676), in pursuing a similar line of enquiry with regard to the parental magma of the Karroo Dolerites, deduced that the approximate initial water content of the magma was 5 per cent. Yoder and Tilley (1962, p. 464) have concluded that the water content of basalt liquid probably increases from about 3 to 11 per cent with decreasing temperature at 5,000 bars water pressure, but they also noted (1962, p. 465) that: "A basaltic magma which crystallizes at or near the surface as basalt must have lost its water during its course to the surface or was essentially dry initially." Although there is no direct evidence, the initial water content of the James Ross Island Volcanic Group parental magma may have been approximately 3 per cent; at least, there is little doubt that water was present.

Bowen and Tuttle (1950), Yoder (1954, 1958) and Yoder and Tilley (1962), amongst others, have demonstrated the progressive lowering of the melting temperatures of silicates with increase in the water-vapour pressure (P_{H_2O}). In the system diopside—anorthite—water at 5,000 bars the liquidus temperature of anorthite (1,230°C) is lower than that of diopside (1,290°C), and the eutectic composition is moved from 42 per cent anorthite in the "dry" system to 73 per cent anorthite in the "wet" system (Yoder, 1954). In the "dry" system anorthite has a higher melting temperature (1,550°C) than diopside (1,391°C) (Yoder, 1954). Furthermore, Yoder and Tilley (1962, figs. 28 and 29), in their hydrothermal experiments on examples of naturally occurring high-alumina and alkali basalts, have shown convincingly that at low P_{H_2O} and temperatures of approximately 1,150°C olivine accompanied by plagioclase can exist in equilibrium with basaltic liquids of the compositions they have considered. At increased water pressures (approximately 500–2,000 bars) and at equivalent temperatures to those considered before, olivine accompanied in this case by clinopyroxene has been observed to be in equilibrium with the basalt liquids.

It is suggested, therefore, that decreasing temperature and variations in the water-vapour pressure could have been the dominating influences in determining whether the basalts carry phyric olivine alone, phyric olivine and clinopyroxene, phyric olivine and plagioclase or, critically, phyric olivine plus clinopyroxene and plagioclase. Although the magma reservoir which fed the volcanoes of this group may have been of substantially uniform temperature, it was probably of sufficient vertical extent to transgress a critical plane of pressure (assuming $P_{load} \propto P_{H_2O}$), above which olivine was accompanied by plagioclase with decreasing temperature and below which olivine was accompanied by clinopyroxene. The rare occurrence of clinopyroxene and olivine as an association of phenocrysts in the lavas may be explained by the greater likelihood of the upper part of the magma reservoir being tapped during eruptions. Thus, the low P_{H_2O} association (olivine and plagioclase) is more likely to have been emitted at the surface after the temperature had fallen enough to allow a second silicate phase to join olivine. Great care must obviously be exercised when considering basaltic crystallization in these terms, particularly with respect to the assumption that P_{H_2O} is proportional to P_{load}. Yoder and Tilley (1962, p. 465–67) have observed that, if P_{H_2O} is less than P_{total}, the liquidus temperatures are raised relative to those "when the water pressure is the total pressure of the system". Even if $P_{total\ (load)}$ was greater than P_{H_2O} at all levels in the magma reservoir, providing the reservoir transgressed a critical plane of P_{H_2O} at which pressure clinopyroxene and plagioclase began to crystallize simultaneously (Yoder and Tilley, 1962, figs. 28 and 29), the two contrasting phenocryst associations of olivine and plagioclase, and olivine and clinopyroxene, may still be accounted for in this manner.

Perhaps it should be re-stated that the differentiation which has been observed in the extrusive rocks is not very extensive. No extreme differentiatiates such as alkaline trachytes have been observed, although they may occur high in the stratigraphic sequence.

3. *Differentiation in the intrusive rocks*

a. *Main trend.* This aspect of the differentiation is largely concerned with the Palisade Nunatak analcite-bearing olivine-dolerite intrusion and, in addition, the plug rocks. The intrusion is considered first. The analysis of a representative specimen of the analcite-bearing olivine-dolerite from Palisade Nunatak plots centrally within the changes demonstrated by the lavas (Figs. 8 and 11), and the Palisade

Nunatak intrusion is probably associated with the extrusive rocks of the James Ross Island Volcanic Group. It is suggested that the course of differentiation immediately following analysis 12 (Table VIII) is essentially the same in the intrusion as the last part of the differentiation demonstrated by the lavas, i.e. from position values −1·6 to +0·4 (Fig. 11). Between position values +0·4 and +11·2, the most differentiated rock defined by the analyses, the course of differentiation is believed to follow the paths indicated in Figs. 8 and 11. Discussion of that part of the differentiation between the most differentiated of the lavas and the dolerite-pegmatite (Table VIII, analysis 11) will be necessarily speculative due to the lack of "control" analyses (Fig. 11).

The genesis of the dolerite-pegmatite (Table VIII, analysis 11) was due largely to the creation of a hydrous partial magma by the crystallization events which preceded it, but the chemical composition of the dolerite-pegmatite as it is now may not be truly representative of the original liquid composition from which it began to crystallize, for reasons which will be explained. In the majority of the lavas and in each analcite-bearing olivine-dolerite specimen from Palisade Nunatak, anhydrous silicate minerals are much more abundant than hydrous ones. Nonetheless, the dolerites from Palisade Nunatak all carry analcite, which occurs in significant amounts as an interstitial phase and is occasionally accompanied by other zeolites. This is compatible with the presence of water in the original basalt magma (p. 50). The conclusion of Walker and Poldervaart (1949) and Walker (1953) that, because of the initial crystallization and fractionation of anhydrous silicate phases, water and other volatiles will be concentrated in the last liquids to crystallize in a dolerite intrusion, appears to be fully justified. It is therefore concluded that the concentration of volatile constituents in the partial magma, which *began* to crystallize as the dolerite-pegmatite, was relatively high. Referring once more to the deductions from experimental evidence of Yoder and Tilley (1962, p. 464), it is suggested that the concentration of volatiles would have been about 11 per cent at this stage. Shepherd (1938) has concluded that water constitutes about 80 per cent of the volatile constituents dissolved in basaltic magma, indicating that approximately 8 per cent of the partial magma which gave rise to the dolerite-pegmatite was water. The other volatile constituents probably included carbon dioxide, fluorine, chlorine and oxides of sulphur. Additional important features of the differentiation prior to the formation of the dolerite-pegmatite are as follows:

i. Sodium, potassium, phosphorus, titanium and possibly total iron had been concentrated as a result of the crystallization of high-temperature anhydrous silicates (Fig. 11).
ii. Magnesium, calcium (and possibly aluminium) had been considerably depleted for the same reasons.

The structure of the graphic intergrowths of titanaugite and plagioclase in the dolerite-pegmatite suggests that the crystallization of these two minerals was simultaneous and that they were the first two crystalline phases to separate from the liquid during the formation of this rock (p. 27). It is considered important that the crystallization and fractionation of titanaugite at an early stage will accelerate the abstraction of Ca from the hydrous partial magma. Wilkinson (1956) has demonstrated the almost constant CaO content of the clinopyroxenes of an alkali olivine-basalt magma, although the FeO : MgO ratio of these minerals increases during crystallization differentiation. Thus the comparatively limited quantity of Ca in this rock (Table VIII, analysis 11) will have been removed at an early stage from the melt. The formation of the anhydrous titanaugite—plagioclase intergrowths will have had the additional effect of raising the water content of the residual liquid still further (the large size of the graphic intergrowths being attributed to the hydrous nature of the melt, a condition often believed to be conducive to the growth of large crystals).

In addition to increasing the water content of the residual liquid, the formation of the graphic intergrowths will have further concentrated P, Fe‴, Na and K. K will have been concentrated to a greater extent than Na, due to the removal of Na and the limited entry of K into the plagioclase structure (Sen, 1959). Fe‴ will have been concentrated to a greater extent than Fe″, due to absorption of Fe″ into titanaugite. At some time during the formation of the graphic intergrowths, probably in the final stages of their development, the precipitation of Ti—Fe ore minerals probably became inevitable. Wager and Deer (1939, p. 228–29) have suggested that a TiO_2 content in excess of 2·5 per cent and an Fe_2O_3 content in excess of 3·5 per cent will result in the primary crystallization of ilmenite and magnetite, respectively. Although skeletal ore crystals in the dolerite-pegmatite have been identified as ilmenite, a precise identification of the phases present cannot be made in the absence of ore microscopy. However,

it is concluded that ilmenite is a primary crystalline phase in the dolerite-pegmatite (Plate Xe), in view of the TiO_2 content of nearly 3 per cent in this rock (Table VIII, analysis 11). Wager and Deer (1939, p. 227) also noted that the conditions favouring the separation of P_2O_5 as a primary phase from a basic magma are similar to those for TiO_2, and they have suggested that a P_2O_5 content in excess of 1·5 per cent will result in the formation of primary apatite. The mineralogy and chemistry of this dolerite-pegmatite point to the almost simultaneous abstraction of Fe‴, Ti and P at a critical stage or stages during the development of the titanaugite—plagioclase intergrowths. The relatively large sizes of the ore and apatite crystals are also consistent with the high concentration of water at this stage.

From textural considerations, it has been suggested that the separation of the relatively iron-rich olivine ($Fo_{54}Fa_{46}$) occurred comparatively late in the crystallization sequence of the dolerite-pegmatites (p. 27). The apatite crystals which have been enclosed in olivine crystals also indicate the late formation of the olivine. Because of the analysed P_2O_5 content of just over 1 per cent in the dolerite-pegmatite (Table VIII, analysis 11), it is likely that a certain amount of crystallization would have taken place before the critical value of 1·5 per cent P_2O_5 had been exceeded. It seems that the effective P_2O_5 content of the residual liquid was increased by the formation of the graphic intergrowths, because no apatite crystals have been observed within them. The evidence suggests that plagioclase and clinopyroxene preceded olivine in the order of separation of the anhydrous silicate phases from a partial magma of such advanced fractionation, which is in direct contrast to the sequence of crystallization in less differentiated basalts and dolerites of this volcanic group (p. 49).

The probable role of Na and K in the crystallization of the dolerite-pegmatite will now be discussed. It will be seen that the deduced sequence of crystallization effectively removes all the major constituents of the melt, with the exception of the alkalis together with some Al_2O_3 and SiO_2. The precipitation of iron and titanium oxides will effectively concentrate SiO_2 and the relatively limited quantity of plagioclase will ensure that Al_2O_3 is still present, and yet this rock is apparently deficient in Al as a whole (Fig. 11; p. 46). The rapid transition from plagioclase to anorthoclase in the epitaxially overgrown crystals has already been described (p. 28) but it has also been observed that there is a distinct paucity of individual potassium-rich alkali-feldspars in the interstices of the dolerite-pegmatites. It is suggested that when the Ca content of the residual liquid became critically low (due to the simultaneous crystallization of plagioclase and titanaugite) the resultant course of crystallization may be considered in terms of the ternary feldspar system at 5,000 bars water pressure (Yoder, Stewart and Smith, 1957). The absence of leucite from any of the late-stage rocks of the Palisade Nunatak intrusion justifies the assumption that the water pressure was high at this stage. It has been shown by Yoder (1958) that high sanidine, the inverted form of which occurs as individual crystals in the late-stage rocks of this intrusion, melts to a water-rich liquid at water pressures exceeding 3,000 bars, whereas at lower P_{H_2O} the field of leucite intervenes between those of high sanidine and liquid. In addition, the leucite field in the "dry" ternary feldspar system (Franco and Schairer, 1951) is replaced by a smaller field of potassium-rich alkali-feldspar in the P_{H_2O} = 5,000 bars ternary feldspar system (Yoder, Stewart and Smith, 1957).

Although low-temperature terminations in the three-feldspar system are complex (Stewart and Roseboom, 1962), it is believed that just before anorthoclase began to crystallize epitaxially around the dolerite-pegmatite plagioclase, i.e. when the calcium content of the liquid became critically low, a second potassium-rich alkali-feldspar would have joined the sodium-rich anorthoclase, and two alkali-feldspars would have crystallized from and been in equilibrium with the liquid (Yoder, Stewart and Smith, 1957). At this stage in the crystallization, the K content of the liquid, which had probably risen to a high value due to its limited entry into the plagioclase structure at these temperatures (? 800°C; Sen, 1959), began to diminish due to the precipitation of potassium-rich sanidine crystals. With increasing fractionation, the anorthoclase became more potassium-rich (Table VI) and the sanidine may have become more sodium-rich (Stewart and Roseboom, 1962). There is good optical mineralogical evidence for the zoning in the anorthoclase but, although the latter potassium-rich to sodium-rich zoning may have occurred in the sanidine crystals, its study by optical methods is not easily accomplished for two reasons:

i. Overlapping of the isogyres at low values of 2V limits the scope of Universal Stage measurements (p. 28).

ii. Compared with the large and abundant anorthoclase crystals, individual potassium-rich sanidine crystals are small and uncommon.

The second reason is considered to be petrogenetically significant, although two explanations can be offered to account for the scarcity of sanidine crystals. At the stage when the rapid zonal transition (labradorite—andesine—oligoclase—anorthoclase) occurred at the plagioclase margins, the composition of the residual liquid may have effectively reached the cotectic boundary curve of the ternary feldspar system (Yoder, Stewart and Smith, 1957). In this case, it is suspected that the potassium-rich alkali-feldspar, which would have begun to crystallize as well as anorthoclase at this stage (Yoder, Stewart and Smith, 1957), would constitute a modal percentage of the dolerite-pegmatite of the same order as that of the anorthoclase. That it evidently does not, may be due either to the failure of the residual liquid composition to reach the two-feldspar boundary curve until very late in the crystallization, or to the mechanical separation of the potassium-rich alkali-feldspar which had formed from the remainder of the rock. It is also of interest that the predominant interstitial hydrous phase, analcite, is a sodium alumino-silicate and that Na, rather than K, is the alkali cation in many others, e.g. thomsonite, aegirine and the oxyhornblendes (p. 28). Potassium occurs only in sparse biotite.

The alkali-rich rocks (Table VIII, analyses 13 and 14), which were probably formed at the temperature minimum of the main trend (Fig. 10), will now be considered. Although the chemistry of these two rocks is very similar, their respective mineralogies and textures are distinct (p. 29). Several features of the felsitic vein (Table VIII, analysis 13) are considered significant in the discussion of their origin. They are (a) the predominance of potassium-rich sanidine over every other mineral, (b) the absence of plagioclase, (c) the sub-parallel arrangement of the sanidine crystals which is indicative of flow during or soon after crystallization, and (d) the "vesicular" nature of the rock. Walker and Poldervaart (1949, p. 612) considered that the thin irregular acid veins, which they discovered in the Karroo Dolerites, represent late injections of a highly differentiated partial magma. Their studies were hampered by the weathered nature of the material examined and the difficulty of recognizing veins produced by rheomorphic injection of the surrounding sediments. However, the freshness of the vein from Palisade Nunatak provides good evidence to support a similar explanation of its genesis to that of Walker and Poldervaart (1949). The intrusion mechanism of the felsitic vein and the probable inter-relationship between it and the dolerite-pegmatite will now be considered.

Morey (1922) and Yoder (1958) have suggested that, in a univariant system, continued crystallization of a silicate phase with decreasing temperature from a "wet" melt will have the effect of raising the P_{H_2O} enormously. Yoder (1958) has noted that the condition of univariancy may be encountered in the final stages of cooling of a complex magma. Morey (1924, p. 295), however, concluded that: "In natural magmas critical phenomena [of water] probably play no part." Morey contended that the presence in the liquid of constituents with lower volatility than water would tend to hold water in solution. These other constituents include the borates, phosphates, silico-fluorides, fluorides and chlorides (Morey, 1924, p. 294). However, many of these constituents will probably have been removed from the liquid by the precipitation of primary apatite at a relatively early stage in the crystallization of the dolerite-pegmatite. It is suggested that water was the only volatile constituent remaining in the liquid, when two alkali-feldspars began to crystallize in equilibrium. It is further suggested that at this final stage of cooling (Yoder, 1958) the precipitation of two co-existing alkali-feldspars occurred essentially as in a univariant system, thus greatly raising the P_{H_2O} in the liquid. In short, the partially consolidated dolerite-pegmatite probably became explosive and caused the surrounding dolerite to yield along planes of weakness. It is not difficult to envisage a process of filter-pressing, by which only the remaining liquid and some of the smaller crystals would be expelled from the site of dolerite-pegmatite generation to end the consolidation sequence as felsitic veins. The absence of chilled edges on these veins is to be expected because of the likelihood that the bulk of the intrusion, though solid, was still at an elevated temperature.

The contrasting mineralogies and textures of specimens D.4088.4, 5 (Table VIII, analyses 13 and 14) have already been mentioned. Although a process of mechanical fractionation and injection can account satisfactorily for the formation of the felsitic veins, specimen D.4088.5 appears to have been formed by a process of more passive segregation. This rock may be connected with the last stages of dolerite-pegmatite crystallization, which had been preceded by gravitational settling of the large titanaugite—plagioclase graphic intergrowths. Release of water pressure in this instance may have been achieved by the more extensive development of hydrous phases (Yoder, 1958), e.g. analcite, thomsonite and gismondite (p. 28). Faint birefringence in analcite, similar to that which has been observed in many of these late-stage rocks, has been attributed by Wilkinson (1962) to a type of unmixing of a potassium-rich

analogue. But analcite is known to have a high-pressure polymorph (Yoder, 1958), the inversion of which from high to low pressures may have caused the birefringence.

The differentiation of the main intrusive trend may be summarized as follows:

i. Prolonged separation of anhydrous silicates from the olivine-dolerite parental magma led to concentration of alkalis and volatile constituents in the final liquids.
ii. When volatile concentration exceeded a certain limiting value, crystallization of dolerite-pegmatites was initiated.
iii. At some critical stage in the crystallization of the dolerite-pegmatites, separation of the final liquids, which were extremely rich in alkalis, took place with varying degrees of violence. The abnormally low Al content of the dolerite-pegmatite (Fig. 11, analysis 11) may be due to the extreme fractionation of liquids rich in alkali alumino-silicates.

The zoned olivines (Fa_{28-45}), the interstitial analcite associated with apatite and the small biotite crystals suggest that the plug rock (Table VIII, analysis 3) is a condensed version of the differentiation sequence observed in the Palisade Nunatak intrusion. In the variation diagrams (Figs. 8 and 11) analysis 3 plots in a position indicative of relatively advanced differentiation (phase III or younger) and yet the core composition of its olivines and its field relations suggest that it is associated with phase II. Its chemical analysis, therefore, probably indicates the algebraic sum of a complete differentiation sequence.

b. *Dyke rocks.* The chemical analyses and variation diagrams suggest that the dyke rocks (Table VIII, analyses 2 and 4) and possibly the rocks from Cockburn Island (Table VIII, analyses 15 and 16) belong to a separate but related trend of initial absolute iron enrichment. It has already been observed that cumulite aggregates of magnesian olivine, enstatite, diopside and chrome spinel occur as nodules in a dyke believed to be associated with phase II. The possibility that pressure variations in the magma reservoir were responsible for the difference between olivine—plagioclase and olivine—clinopyroxene phenocryst associations has also been discussed. If this is a justifiable conclusion, it will be seen that prolonged precipitation and accumulation of several magnesium-rich ferromagnesian silicates low in the magma reservoir will increase the Fe content of the liquid considerably. It is therefore suggested that the non-vesicular iron-rich dykes may have been injected along fissures, which originated lower in the magma reservoir than the conduits which fed the central volcanoes. Thus the dykes would probably have been committed to a trend of absolute iron enrichment at their source.

However, the sinuous vesicular dykes, none of which has been analysed, are probably related to the central eruptions.

4. *Crystallization and sequence of eruptions*

Universal Stage determinations of the olivine 2Vs in several extrusive rocks have given tentative support to the stratigraphic sequence, which was originally determined from structural considerations alone (p. 8). It has been found that the unzoned olivines in the lavas and hyaloclastites become progressively more iron-rich from phase I onwards (Table IX).

Although the changes in olivine composition parallel those revealed by the chemical analyses of whole rocks (Tomkeieff, 1939), there are distinct compositional gaps between olivines believed to be associated with one phase and those of the next (considering only the core compositions of zoned olivines). Allusion has also been made to a magma reservoir, which fed the volcanoes and gave rise to the dykes (p. 50). Such a reservoir, once emplaced at an intermediate level in the Earth's crust (O'Hara, 1965), would undergo slow but steady cooling, which, if equilibrium crystallization was maintained, would result in the gradual change of olivine from forsteritic to more fayalitic compositions. Fractionation crystallization would presumably produce more pronounced changes. It is concluded that the time interval between phases indicated by the field relations and the time interval indicated by the "missing" olivine compositions can be correlated, although the figures compiled in Table IX are hardly a statistical analysis. It is suggested that, after the first relatively widespread series of eruptions, the timing of each successive phase may have been governed to a large extent by the degree of cooling and crystallization in the magma reservoir.

5. *Palagonitization*

Very little chemical analysis has been carried out in connection with this problem. The one total analysis of a palagonite-breccia (Table VIII, analysis 10) suggests that the ideas propounded by Charles

TABLE IX

OPTIC AXIAL ANGLES AND COMPOSITIONS OF OLIVINES

*Average 2Vα**	*Composition* (from Deer and Wager, 1939, fig. 1)	*Specimen Number*
93°	Fa_7	D.4068.2 (phase I)
92°	Fa_9	D.3302.1 (phase I)
92°	Fa_9	D.3785.2 (phase II or ? I)
90°	Fa_{14}	D.3726.2 (phase I)
84·5°	Fa_{26}	D.4049.3 (associated with phase II)
84–79°	Fa_{27-37}	D.3740.1 (associated with phase II)
83–75°	Fa_{28-45}	D.3756.1 (phase II)
80°	Fa_{35}	D.4053.8 (phase III)

* The measured angles have an accuracy of ±2°, but they are probably 1–2° too small (Munro, 1963).

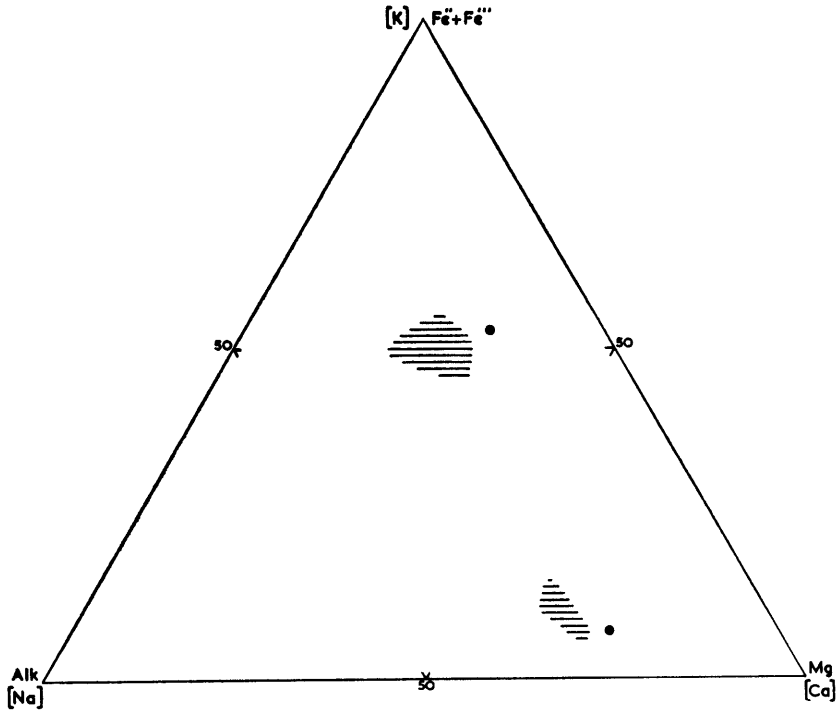

FIGURE 14

Triangular variation diagrams for the undifferentiated olivine-basalts (horizontal shading) and a palagonite-breccia (solid circle; D.4068.2) of the James Ross Island Volcanic Group, plotted on the co-ordinates (Fe''+Fe''')—Mg—Alk (top centre) and Ca—Na—K (bottom right).

(1958; p. 34) may be applicable in this context. In Fig. 14, analysis 10 has been plotted in relation to the field occupied by the other extrusive rocks within the co-ordinates (Fe''+Fe''')—Mg—Alk and Ca—Na—K. It can be seen that analysis 10 lies on the alkali-deficient and calcium-rich sides of the fields of the

extrusive rocks. The calcium-rich nature of this rock is easily accounted for by the abundant chabazite cement (p. 32). However, if the rock were merely rich in Ca, its relative proportions of total Fe, Mg and alkalis would be unaffected. Assuming that the composition of the fresh hyalobasalt in this rock is similar to analysis 1 (Table VIII), analysis 10 should plot within the field occupied by the remainder of the fresh extrusive rocks. The fact that it falls on the alkali-deficient side of this field is believed to represent a real depletion of Na and K, which is attributed to the palagonitization process.

If the fragments of olivine-hyalobasalt comprising specimen D.4068.2 (Table VII) are considered as perfect spheres with an average diameter of 2 mm., then palagonitization to an overall depth of 0·1 mm. (Table VII) will have the effect of corroding more than one-quarter of the hyalobasalt present (27·1 per cent assuming perfect sphericity). If the low Na_2O and K_2O contents of this palagonite-breccia are due to the effects of palagonitization, it is interesting to note that the Na_2O and K_2O contents of analysis 10 (Table VIII), plus one-third, result in figures very close to the mean values in the lavas of this volcanic group (Table X),

i.e. $2{\cdot}68+0{\cdot}89 = 3{\cdot}57$ per cent Na_2O,
$0{\cdot}76+0{\cdot}25 = 1{\cdot}01$ per cent K_2O.

Determinations of total H_2O and CO_2 in the olivine-hyalobasalt and palagonite from a palagonite-breccia pillow margin (D.3749.1) suggest that 2·5 per cent of water and 1·5 per cent of carbon dioxide have been absorbed during the transformation of hyalobasalt into palagonite. The fresh olivine-hyalobasalt contained 1·53 per cent of total H_2O and 0·14 per cent of CO_2, whereas the palagonite, which was extracted from the pillow margin immediately adjacent to the hyalobasalt, contained 4·07 per cent of total H_2O and 1·69 per cent of CO_2. Unfortunately, a very limited amount of palagonite was available for these determinations, which should be considered as only an indication of the changes involved.

6. *Comparison with other alkaline rock series*

a. *Composition of parental magmas.* In Table X the suggested composition of the parental magma of the James Ross Island Volcanic Group is compared with the deduced composition of the alkali olivine-basalt parental magma of Japan and Korea (Kuno, 1960) and the average composition of 28 alkalic basalts from Hawaii (Macdonald and Katsura, 1964).

The suggested parental magma composition of the James Ross Island Volcanic Group is very similar to that for Japan and Korea with respect to every constituent except Na_2O which is higher, and CaO which is lower in the James Ross Island Volcanic Group. These two parental magma compositions are unlike the average Hawaiian alkalic basalt, which is lower in SiO_2, Al_2O_3, Na_2O and K_2O, and higher in TiO_2, total iron oxides and CaO. The dissimilarity between continental and oceanic rock types has been discussed by Macdonald (1960), who observed that: "the calc-alkaline suite characteristic of orogenic regions of the continents—basalt, hypersthene-andesite, hornblende-andesite, dacite, rhyodacite, and rhyolite—appears to be completely absent within the true Pacific Ocean basin, defining the latter simply as the area west of the continental slopes of the Americas and east of the outermost island arcs of the Pacific margin of Asia."

Tertiary andesites occur at Anvers Island (Hooper, 1962), about 180 miles (290 km.) west of James Ross Island (Fig. 1), more recent andesites occur at Deception Island (Hawkes, 1961), about 120 miles (193 km.) north-west of James Ross Island (Fig. 1), and there is a general association of calc-alkaline rocks in the Graham Land area. It is reasonable, therefore, to expect a closer similarity between the suggested parental magma compositions of the James Ross Island Volcanic Group and the volcanic rocks of Japan and Korea, than between the James Ross Island Volcanic Group and the alkalic basalts from Hawaii.

b. *Differentiation trends.* Variation trends for the rocks of the James Ross Island Volcanic Group, Deception Island (Hawkes, 1961), Réunion and Hawaiian volcanic suites (Nockolds and Allen, 1954) have been plotted together on the co-ordinates (Fe″+Fe‴)—Mg—Alk and Ca—Na—K (Fig. 15). The variation in the rocks from Piton de Neiges, Réunion, follows an identical path to that of the rocks from Mauritius (Walker and Nicolaysen, 1953). The shapes of these variation trends plotted on the co-ordinates (Fe″+Fe‴)—Mg—Alk are very similar to one another, and indeed they are almost coincident during the latter part of their courses. Although the start of each trend is evidently determined by the initial relative alkali content, it is tempting to suggest that marked relative alkali enrichment begins at a total iron : magnesium ratio which is common to all groups of alkali olivine-basalt magmas. The close coincidence of the early parts of the James Ross Island Volcanic Group and Deception Island

TABLE X

COMPARISON OF ALKALI OLIVINE-BASALT COMPOSITIONS

	I	II	III	IV
SiO_2	49·01	48·85	48·11	46·46
TiO_2	1·84	1·84	1·72	3·01
Al_2O_3	16·50	15·58	15·55	14·64
Fe_2O_3	2·88	1·76	2·99	3·27
FeO	7·34	8·83	7·19	9·11
MnO	0·16	0·15	0·16	0·14
MgO	6·73	8·62	9·31	8·19
CaO	8·83	8·15	10·43	10·33
Na_2O	3·60	3·76	2·85	2·92
K_2O	1·15	1·17	1·13	0·84
P_2O_5	0·45	0·47	0·56	0·37
TOTAL	98·49	99·18	100·00	99·28

I. Alkali olivine-basalt from the James Ross Island Volcanic Group (average of 10 analyses).

II. Earliest member of the James Ross Island Volcanic Group differentiation series (D.3302.1; Table VIII, analysis 1).

III. Suggested composition of the alkali olivine-basalt parental magma of Japan and Korea (Kuno, 1960, p. 141).

IV. Alkalic basalt of the Hawaiian Islands (average of 28 analyses; Macdonald and Katsura, 1964).

trends suggests an inter-relationship which is more apparent than real. Because the variations shown by these two groups when plotted on the co-ordinates Ca—Na—K are very different, it is conceivable that the large relative potassium increase in the James Ross Island Volcanic Group trend is more characteristic of alkali olivine-basalt differentiation in a single intrusion. It is closely comparable with the potassium enrichment which occurred in the Black Jack teschenite sill of New South Wales (Wilkinson, 1958).

VI. GEOLOGICAL HISTORY AND CONCLUSIONS

AFTER the deposition of the Upper Cretaceous Snow Hill Island Series, folding and uplift took place in the whole of the James Ross Island area. Although the folding of the Upper Cretaceous sediments is never very intense, it becomes progressively weaker south-eastwards, away from the structural feature of Prince Gustav Channel (Bibby, 1966). It is probable that a major part of the faulting, which is postulated to have taken place along Prince Gustav Channel, occurred during and towards the end of these post-Cretaceous earth movements. It is considered that the movement was probably confined to the Oligocene and Lower Miocene, because erosion products from the rising landmass in the Trinity Peninsula area were transported by a drainage system across the James Ross Island area and deposited as a coastal facies to the south-east. The Lower Miocene sediments, which occur only at Cockburn and Seymour Islands, are believed to be all that remains of this period of deposition. Further evidence of the timing of these relative movements is provided by the presence of pebbles of Andean Intrusive Suite rocks in the tuffaceous conglomerates at the base of the James Ross Island Volcanic Group (p. 10). If the Andean Intrusive Suite of north-east Graham Land had been emplaced before the close of the Eocene, then the

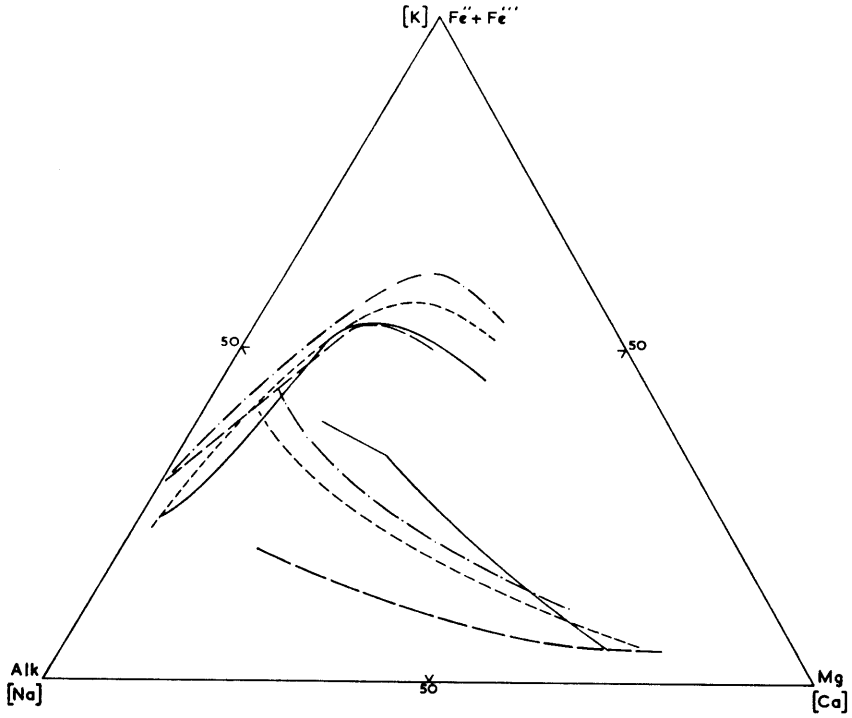

FIGURE 15

Triangular variation diagrams for the James Ross Island Volcanic Group and other volcanic suites, plotted on the co-ordinates (Fe″+Fe‴)—Mg—Alk (upper curves) and Ca—Na—K (lower curves). Chemical variations in the Mauritius volcanic suite are almost identical to those of Piton de Neiges, Réunion (Walker and Nicolaysen, 1953).

Solid lines.	James Ross Island Volcanic Group.
Long-dash lines.	Deception Island volcanic suite (Hawkes, 1961).
Short-dash lines.	Hawaiian alkali-basalt—trachyte series (Nockolds and Allen, 1954).
Dot-dash lines.	Piton de Neiges, Réunion (Nockolds and Allen, 1954).

intrusions had evidently been uplifted and eroded before the Middle Miocene. The present relative positions and heights of the Trinity Peninsula and James Ross Island areas may have been roughly established during this early Tertiary period of earth movements.

When volcanic activity commenced in the Lower or Middle Miocene, a mature undulating landscape formed on Upper Cretaceous sediments existed in the area of James Ross Island. This landscape formed the foothills of the more elevated mountain chain of Trinity Peninsula. Solid outcrops of Upper Cretaceous sediments attain their highest and most extensive development in north-west and south-east James Ross Island, and the phase I James Ross Island Volcanic Group rocks are largely confined to a north-north-east to south-south-west trending zone between these two areas (Maps 1 and 2A). At present, the sea-level during the eruptions of phase I is at approximately 500 ft. (152 m.) above sea-level, whereas the buried pre-Miocene topography occasionally reaches 1,000 ft. (305 m.) above sea-level, e.g. near Kotick Point (north-west James Ross Island; Map 1). If the most important centre of eruption was situated near the site of Mount Haddington (Adie, 1953), the relatively high ground to the east and west of this site would have formed a barrier, beyond which lavas could not flow during the eruptions of phase I. The bulk of the lavas, therefore, would have been obliged to flow either to the north-east or south-west. Those that flowed south-westwards may have formed the "deltaic" lava/palagonite-breccia structures now exposed in the coastal cliffs between Röhss Bay and Jefford Point (Map 1). The profusion of apparent centres in this area may represent the variation with time of the terminal position of the lava stream or streams, which flowed from one major centre of activity. To the north-east, particularly in the Vega Island area, the dip directions of the palagonite-breccias towards James Ross Island and the greater distances between apparent centres of eruption suggest that these phase I centres approximate to the real eruption sites. However, the occurrence of phase I palagonite-breccias at Rink Point (north-west James Ross Island), at St. Rita Point and north of the Coley Glacier snout (south-east James Ross Island) indicates that the

pre-Miocene topographic barriers were not entirely impassable, *if* these palagonite-breccias were formed from lava flows which issued from the main volcanic centre. If, alternatively, these palagonite-breccias were derived from nearby centres, they may owe their asymmetrical outward-dipping structure to the siting of the vents on the flanks of pre-Miocene hills.

The fact that 500 ft. (152 m.) thick palagonite-breccias form the first recognizable phase of volcanic rocks suggests that the James Ross Island area had been submerged beneath the surrounding sea to a depth of at least 500 ft. (152 m.) before the first eruptions. However, it should be pointed out that phase I of the James Ross Island Volcanic Group does not necessarily include all the earliest-formed volcanic rocks (p. 9). Ashley (1962) and A. Allen (personal communication) have obtained magnetic evidence from Tabarin Peninsula and the islands in Prince Gustav Channel which suggests that highly magnetized rocks, possibly lava flows, occur to a considerable depth below present sea-level. Nevertheless, phase I volcanic rocks certainly rest on a surface composed of the Snow Hill Island Series in both James Ross and Vega Islands.

After the rocks of phase I had been erupted from the centres indicated on Map 1, the lavas from the lava/palagonite-breccia volcanoes near the east and west coasts of James Ross Island were evidently removed by erosion. Possibly, this indicates that there was some crustal warping which elevated the eastern and western margins of the James Ross Island area after the close of phase I volcanic activity. However, this does not necessarily follow, because marine plantation would proceed along the original lava/palagonite-breccia contact if the rocks suffered prolonged exposure to wave action (p. 39). During the interval between phases I and II, ash cones such as the one south of the snout of Hobbs Glacier may have been deposited subaerially on the phase I flow lavas.

Phase II volcanic activity was preceded by increased subsidence of the James Ross Island area, which had evidently been submerged a further 500 ft. (152 m.). This indicates that a total subsidence of approximately 1,000 ft. (305 m.) had occurred before the commencement of the phase II eruptions. From the evidence of overlap structures (p. 38) it is deduced that during the period of phase II vulcanicity there was a comparatively rapid 300 ft. (91·4 m.) elevation relative to sea-level which may have been confined to the margins of this area. A further overall subsidence of this area intervened between the vulcanism of phases II and III, during which the eruptions again gave rise to lava/palagonite-breccia volcanoes. Because of the absence of phase III flow lavas in the Hobbs and Coley Glacier areas, it is possible that minor re-elevation followed the close of phase III activity, although prolonged wave action could have been responsible for their total removal. During phase IV a similar pattern of subsidence and lava/palagonite-breccia formation was followed. The existence of cone surface and "terminal slope" overlap structures in the cliffs of western James Ross Island (p. 40) suggests that there may have been a subsidence of the landmass of approximately 1,000 ft. (305 m.) in this area. It is deduced that the volcanic activity of phase V was preceded by a further overall subsidence of the order of 500 ft. (152 m.). Field relations and olivine phenocryst compositions suggest that the analcite-bearing olivine-dolerite intrusion of Palisade Nunatak was emplaced either during phase III or phase IV.

Although there are no further rock exposures above an altitude of 3,000 ft. (914 m.), there are breaks in slope of the James Ross Island ice cap at approximately 4,000 and 5,000 ft. (1,219 and 1,524 m.) above sea-level. It is believed that there are at least two more phases of volcanic rocks buried beneath the ice cap, which rises to a distinct peak at Mount Haddington (Plate Ia). If the ice-covered volcanic rocks possess structures similar to those of the exposed rocks, as the physiographic evidence suggests, it is conceivable that the James Ross Island area underwent a total subsidence approximately equal to the thickness of the volcanic group (5,000 ft.; 1,524 m.).

The absence of thick interbedded clastic sediments in the James Ross Island Volcanic Group and the probable termination of relative vertical movement between the James Ross Island and Trinity Peninsula areas prior to the Lower—Middle Miocene vulcanism suggest that the Trinity Peninsula area simultaneously underwent this overall subsidence. Nichols (1960) has suggested that the plateau of Trinity Peninsula was probably formed in the Middle or late Tertiary and he has quoted Ashley (1931), who has reported that most high-level erosion surfaces in the world are of this age. The fact that the height of the Trinity Peninsula plateau to the north-west of James Ross Island is approximately the same as the height of the island itself therefore suggests that the formation of this plateau occurred towards the end of the Miocene, which is assumed to be the end of the formation of the James Ross Island Volcanic Group.

Since the end of the Miocene, it is evident that elevation of the landmass has proceeded steadily up

to the present day. If the Pecten Conglomerate of Cockburn Island is Pliocene in age, then it is feasible that at least 4,000 ft. (1,219 m.) of re-emergence of the area had taken place before the close of the Pliocene. Further uplift, which has occurred in the geologically recent past, is demonstrated by the elevated wave-cut benches and raised beaches in various parts of this area (Bibby, 1965).

There are indications that an island existed near the centre of James Ross Island during the whole period of formation of the James Ross Island Volcanic Group (p. 10). It is stressed, therefore, that in the lower levels at least the stratigraphical sequence and geological history should be considered essentially marginal to James Ross Island.

Alkalic olivine-basalt lavas and hyaloclastites, which show some crystallization differentiation, form the entire volcanic group. Although no per-alkaline differentiates, such as trachytes, have been recorded in this area either as plugs or surface flows, crystallization differentiation has produced dolerite-pegmatite schlieren and per-alkaline veins in the Palisade Nunatak analcite-bearing olivine-dolerite intrusion. The olivine-dolerite dykes evidently form part of a separate but related differentiation trend which is characterized by initial total iron enrichment. It has been found that palagonitization of basalt glass in the hydroclastic rocks results in the removal of alkalis from the basalt glass and the formation, at least at low intensities of alteration, of a calcium zeolite cement. Finally, it is concluded that the alkalic olivine-basalts of the James Ross Island Volcanic Group are geochemically more closely related to those of alkalic basalts from orogenic regions than from oceanic environments.

VII. ACKNOWLEDGEMENTS

THE field work was carried out from the British Antarctic Survey station at Hope Bay during 1960–62. I am grateful to all the members of the station for their assistance, in particular K. Allen, Dr. R. H. C. Catty, J. Cheek and J. M. Smith, for their enthusiastic companionship while sledging with me. I also gratefully acknowledge the help of Captain R. H. Graham, R.N., of H.M.S. *Protector*. The laboratory work was carried out in the Department of Geology, University of Birmingham, with facilities made available by Professor F. W. Shotton. I wish to thank Dr. R. J. Adie for guidance with the laboratory work and invaluable assistance in the preparation of the manuscript. I am also grateful to my colleagues and other members of the Department of Geology, University of Birmingham, for a great deal of fruitful discussion. Finally, I wish to thank Dr. G. P. L. Walker, Imperial College of Science and Technology, for his encouragement and criticism.

VIII. REFERENCES

ADIE, R. J. 1953. *The Rocks of Graham Land.* Ph.D. thesis, University of Cambridge, 259 pp. [Unpublished.]

————. 1957. Geological Investigations in the Falkland Islands Dependencies before 1940. *Polar Rec.*, **8**, No. 57, 502–13.

————. 1958. Geological Investigations in the Falkland Islands Dependencies since 1940. *Polar Rec.*, **9**, No. 58, 3–17.

AITKENHEAD, N. 1965. The Geology of the Duse Bay—Larsen Inlet Area, North-east Graham Land (with Particular Reference to the Trinity Peninsula Series). *British Antarctic Survey Scientific Reports*, No. 51, 62 pp.

ALLEN, A. 1966. A Magnetic Survey of North-east Trinity Peninsula, Graham Land: II. Mount Bransfield and Duse Bay to Victory Glacier. *British Antarctic Survey Scientific Reports*, No. 49, 32 pp.

ANDERSON, T. 1910. The Volcano of Matavanu in Savaii. *Q. Jl geol. Soc. Lond.*, **66**, No. 264, 621–39.

ANDERSSON, J. G. 1906. On the Geology of Graham Land. *Bull. geol. Instn Univ. Upsala*, **7**, 19–71.

ASHLEY, G. H. 1931. Our Youthful Scenery. *Bull. geol. Soc. Am.*, **42**, 537–45.

ASHLEY, J. 1962. A Magnetic Survey of North-east Trinity Peninsula, Graham Land: I. Tabarin Peninsula and Duse Bay. *Falkland Islands Dependencies Survey Scientific Reports*, No. 35, 35 pp.

BAILEY, E. B., CLOUGH, C. T., WRIGHT, W. B., RICHEY, J. E. *and* G. V. WILSON. 1924. Tertiary and Post-Tertiary Geology of Mull, Loch Aline, and Oban. *Mem. geol. Surv. U.K.*, 445 pp.

BEMMELEN, R. W. VAN *and* M. G. RUTTEN. 1955. *Tablemountains of Northern Iceland.* Leiden, E. J. Brill.

BIBBY, J. S. 1965. Some Observations on Sea-level Changes in the James Ross Island Group. *British Antarctic Survey Bulletin*, No. 6, 67–75.

————. 1966. The Stratigraphy of Part of North-east Graham Land and the James Ross Island Group. *British Antarctic Survey Scientific Reports*, No. 53, 37 pp.

BOWEN, N. L. 1937. Recent High-temperature Research on Silicates and Its Significance in Igneous Geology. *Am. J. Sci.*, Ser. 5, **33**, No. 193, 1–21.

———. *and* O. F. TUTTLE. 1950. The System $NaAlSi_3O_8$—$KAlSi_3O_8$—H_2O. *J. Geol.*, **58**, No. 5, 489–511.

CARLISLE, D. 1963. Pillow Breccias and Their Aquagene Tuffs, Quadra Island, British Columbia. *J. Geol.*, **71**, No. 1, 48–71.

CHARLES, R. J. 1958. Static Fatigue of Glass. I. *J. appl. Phys.*, **29**, No. 11, 1549–53.

COOMBS, D. S., ELLIS, A. J., FYFE, W. S. *and* A. M. TAYLOR. 1959. The Zeolite Facies, with Comments on the Interpretation of Hydrothermal Syntheses. *Geochim. cosmochim. Acta*, **17**, Nos. 1/2, 53–107.

CRADDOCK, C., BASTIEN, T. W. *and* R. H. RUTFORD. 1964. Geology of the Jones Mountains Area. (*In* ADIE, R. J., *ed. Antarctic Geology*. Amsterdam, North-Holland Publishing Company, 171–87.)

CROFT, W. N. 1947. Geological Reports for the Year Ending January 1947, Hope Bay (F.I.D.Sc. Bureau No. E89/47). Pt. 1–13, 182 pp. [Unpublished.]

DEER, W. A. *and* L. R. WAGER. 1939. Olivines from the Skaergaard Intrusion, Kangerdlugssuak, East Greenland. *Am. Miner.*, **24**, No. 1, 18–25.

———., HOWIE, R. A. *and* J. ZUSSMAN. 1963*a*. *Rock-forming Minerals. Vol. 2. Chain Silicates*. London, Longmans, Green and Co. Ltd.

———. 1963*b*. *Rock-forming Minerals. Vol.* 4. *Framework Silicates*. London, Longmans, Green and Co. Ltd.

DOLLAR, A. T. J. *and* J. E. GUEST. 1963. Iceland's New Island Volcano. *New Scient.*, **20**, No. 368, 591–93.

DUNHAM, K. C. 1933. Crystal Cavities in Lavas from the Hawaiian Islands. *Am. Miner*, **18**, No. 9, 369–85.

FERGUSON, D. 1921. Geological Observations in the South Shetlands, the Palmer Archipelago, and Graham Land, Antarctica. *Trans. R. Soc. Edinb.*, **53**, Pt. 1, No. 3, 29–55.

FERUGLIO, E. 1949. *Descripcion Geologica de la Patagonia*, **2**. Buenos Aires, Republica Argentina Ministerio de Industria y Comercio de la Nacion.

FISHER, R. V. 1961. Proposed Classification of Volcaniclastic Sediments and Rocks. *Bull. geol. Soc. Am.*, **72**, No. 9, 1409–14.

FITCH, F. J. 1965. Discussion. (*In* WALKER, G. P. L. *and* D. H. BLAKE. The Formation of a Palagonite Breccia Mass beneath a Valley Glacier. *Proc. geol. Soc.*, No. 1622, 73.)

FRANCO, R. R. *and* J. F. SCHAIRER. 1951. Liquidus Temperatures in Mixtures of the Feldspars of Soda, Potash, and Lime. *J. Geol.*, **59**, No. 3, 259–67.

FULLER, R. E. 1931. The Aqueous Chilling of Lava on the Columbia River Basalt. *Am. J. Sci.*, Ser. 5, **21**, No. 124, 281–300.

HAMILTON, J. 1957. Banded Olivines in Some Scottish Carboniferous Olivine-basalts. *Geol. Mag.*, **94**, No. 2, 135–39.

HAWKES, D. D. 1961. The Geology of the South Shetland Islands: II. The Geology and Petrology of Deception Island. *Falkland Islands Dependencies Survey Scientific Reports*, No. 27, 43 pp.

HOLTEDAHL, O. 1929. On the Geology and Physiography of Some Antarctic and Sub-Antarctic Islands. *Scient. Results Norw. Antarct. Exped.*, No. 3, 172 pp.

HOOPER, P. R. 1962. The Petrology of Anvers Island and Adjacent Islands. *Falkland Islands Dependencies Survey Scientific Reports*, No. 34, 69 pp.

KUNO, H. 1950. Petrology of Hakone Volcano and the Adjacent Areas, Japan. *Bull. geol. Soc. Am.*, **61**, No. 9, 957–1019.

———. 1960. High-alumina Basalt. *J. Petrology*, **1**, Pt. 2, 121–45.

LACROIX, A. 1936. *Le Volcan Actif de l'Ile de la Réunion et ses Produits*. Paris, Gauthier-Villars.

MACDONALD, G. A. 1960. Dissimilarity of Continental and Oceanic Rock Types. *J. Petrology*, **1**, Pt. 2, 172–77.

———. *and* T. KATSURA. 1964. Chemical Composition of Hawaiian Lavas. *J. Petrology*, **5**, Pt. 1, 82–133.

MATHEWS, W. H. 1947. "Tuyas", Flat-topped Volcanoes in Northern British Columbia. *Am. J. Sci.*, **245**, No. 9, 560–70.

MOREY, G. W. 1922. The Development of Pressure in Magmas as a Result of Crystallization. *J. Wash. Acad. Sci.*, **12**, No. 9, 219–30.

———. 1924. The Temperatures of Hot Springs and the Sources of Their Heat and Water Supply. II. Relation of Crystallization to the Water Content and Vapor Pressure of Water in a Cooling Magma. *J. Geol.*, **32**, No. 4, 291–95.

MUIR, I. D. *and* C. E. TILLEY. 1964. Basalts from the Northern Part of the Rift Zone of the Mid-Atlantic Ridge. *J. Petrology*, **5**, Pt. 3, 409–34.

MUNRO, M. 1963. Errors in the Measurement of 2V with the Universal Stage. *Am. Miner.*, **48**, Nos. 3 and 4, 308–23.

NAYUDU, Y. R. 1961. Origin of Seamount Terraces and Guyots as Suggested by the Petrographic Evidences from Cobb and Bowie Seamounts. *Abstracts of Symposium Papers, Tenth Pacif. Sci. Congr., Honolulu*, 382.

NICHOLS, R. L. 1960. Geomorphology of Marguerite Bay Area, Palmer Peninsula, Antarctica. *Bull. geol. Soc. Am.*, **71**, No. 10, 1421–50.

NOCKOLDS, S. R. *and* R. ALLEN. 1953. The Geochemistry of Some Igneous Rock Series. *Geochim. cosmochim. Acta*, **4**, No. 3, 105–42.

———. 1954. The Geochemistry of Some Igneous Rock Series: Part II. *Geochim. cosmochim. Acta*, **5**, No. 6, 245–85.

———. 1956. The Geochemistry of Some Igneous Rock Series—III. *Geochim. cosmochim. Acta*, **9**, Nos. 1/2, 34–77.

NORDENSKJÖLD, O. 1905. Petrographische Untersuchungen aus dem westantarktischen Gebiete. *Bull. geol. Instn Univ. Upsala*, **6**, Pt. 2, 234–46.

———. *and* J. G. ANDERSSON. 1905. *Antarctica*. London, Hurst and Blackett, Ltd.

O'HARA, M. J. 1965. Primary Magmas and the Origin of Basalts. *Scott. J. Geol.*, **1**, Pt. 1, 19–40.

PEACOCK, M. A. *and* R. E. FULLER. 1928. Chlorophaeite, Sideromelane and Palagonite from the Columbia River Plateau. *Am. Miner.*, **13**, No. 7, 360–82.

POWERS, M. C. 1953. A New Roundness Scale for Sedimentary Particles. *J. sedim. Petrol.*, **23**, No. 2, 117–19.

PRIOR, G. T. 1899. Petrographical Notes on the Rock-specimens Collected in Antarctic Regions during the Voyage of H.M.S. Erebus and Terror under Sir James Clark Ross, in 1839–43. *Mineralog. Mag.*, **12**, No. 55, 69–91.

ROSS, C. S. *and* R. L. SMITH. 1955. Water and Other Volatiles in Volcanic Glasses. *Am. Miner.*, **40**, Nos. 11 and 12, 1071–89.

————., FOSTER, M. D. *and* A. T. MYERS. 1954. Origin of Dunites and of Olivine-rich Inclusions in Basaltic Rocks. *Am. Miner.*, **39**, Nos. 9 and 10, 693–737.

SEN, S. K. 1959. Potassium Content of Natural Plagioclase and the Origin of Antiperthites. *J. Geol.*, **67**, No. 5, 479–95.

SHEPHERD, E. S. 1938. The Gases in Rocks and Some Related Problems. *Am. J. Sci.*, Ser. 5, **35A**, 311–51.

SMITH, W. W. 1959. Pseudomorphs after Olivine in Markle Basalt. *Mineralog. Mag.*, **32**, No. 247, 324–31.

SNYDER, G. L. *and* G. D. FRASER. 1963. Pillowed Lavas, I: Intrusive Layered Lava Pods and Pillowed Lavas, Unalaska Island, Alaska. *Prof. Pap. U.S. geol. Surv.*, No. 454-B, B1–23.

STANDRING, A. J. 1956. Geological Report for 1954–55, Hope Bay. [Unpublished.]

STEWART, D. B. *and* E. H. ROSEBOOM. 1962. Lower Temperature Terminations of the Three-phase Region Plagioclase—Alkali Feldspar—Liquid. *J. Petrology*, **3**, Pt. 2, 280–315.

TOMKEIEFF, S. I. 1939. Zoned Olivines and Their Petrogenetic Significance. *Mineralog. Mag.*, **25**, No. 164, 229–51.

TUTTLE, O. F. 1952. Optical Studies on Alkali Feldspars. *Am. J. Sci.*, **Bowen Volume**, Pt. 2, 553–67.

TYRRELL, G. W. *and* M. A. PEACOCK. 1926. The Petrology of Iceland. I: The Basic Tuffs. *Trans. R. Soc. Edinb.*, **55**, Pt. 1, No. 3, 51–76.

WAGER, L. R. *and* W. A. DEER. 1939. Geological Investigations in East Greenland. Pt. III. The Petrology of the Skaergaard Intrusion, Kangerdlugssuak, East Greenland. *Meddr Grønland*, **105**, No. 4, 1–352.

WALKER, F. 1953. The Pegmatitic Differentiates of Basic Sheets. *Am. J. Sci.*, **251**, No. 1, 41–60.

————. *and* L. O. NICOLAYSEN. 1953. The Petrology of Mauritius. *Colon. Geol. Miner. Resour.*, **4**, No. 1, 3–43.

————. *and* A. POLDERVAART. 1949. Karroo Dolerites of the Union of South Africa. *Bull. geol. Soc. Am.*, **60**, No. 4, 591–705.

WALKER, G. P. L. 1951. The Amygdale Minerals in the Tertiary Lavas of Ireland. I. The Distribution of Chabazite Habits and Zeolites in the Garron Plateau Area, County Antrim. *Mineralog. Mag.*, **29**, No. 215, 773–91.

————. 1960*a*. The Amygdale Minerals in the Tertiary Lavas of Ireland. III. Regional Distribution. *Mineralog. Mag.*, **32**, No. 250, 503–27.

————. 1960*b*. Zeolite Zones and Dike Distribution in Relation to the Structure of the Basalts of Eastern Iceland. *J. Geol.*, **68**, No. 5, 515–28.

————. 1964. Iceland's Volcanoes. *The Times Science Review*, No. 51, 3–5.

WATSON, K. DE P. *and* W. H. MATHEWS. 1944. The Tuya-Teslin Area, Northern British Columbia. *Bull. Dep. Mines Petrol. Resour. Br. Columb.*, No. 19, 52 pp.

WILKINSON, J. F. G. 1955. The Terms Teschenite and Crinanite. *Geol. Mag.*, **92**, No. 4, 282–90.

————. 1956. Clinopyroxenes of Alkali Olivine-basalt Magma. *Am. Miner.*, **41**, Nos. 9 and 10, 724–43.

————. 1958. The Petrology of a Differentiated Teschenite Sill near Gunnedah, New South Wales. *Am. J. Sci.*, **256**, No. 1, 1–39.

————. 1962. Mineralogical, Geochemical, and Petrogenetic Aspects of an Analcite-basalt from the New England District of New South Wales. *J. Petrology*, **3**, Pt. 2, 192–214.

YODER, H. S. 1954. Synthetic Basalt. *Yb. Carnegie Instn Wash.*, No. 53, 106–07.

————. 1958. Effect of Water on the Melting of Silicates. *Yb. Carnegie Instn Wash.*, No. 57, 189–91.

————. *and* C. E. TILLEY. 1962. Origin of Basalt Magmas: an Experimental Study of Natural and Synthetic Rock Systems. *J. Petrology*, **3**, Pt. 3, 342–532.

————., STEWART, D. B. *and* J. R. SMITH. 1957. Ternary Feldspars. *Yb. Carnegie Instn Wash.*, No. 56, 206–14.

LEGEND

DIP IN DEGREES AT POINT OF ARROW

DIP DIRECTIONS OF PALAGONITE-BRECCIAS (VALUE C. 35°)

BEDS WITH ASYMPTOTIC DIP AND DIRECTION

HORIZONTAL BEDDING

FAULTS, OBSERVED AND INFERRED

PROBABLE SITE OF LAVA/PALAGONITE-BRECCIA VOLCANO CENTRE OR OUTFLOW OF LARGE LAVA STREAMS FROM ABOVE SEA-LEVEL, AND NUMBER OF PHASE

PROBABLE SITE OF ASH-CONE CENTRE

ANALCITE-BEARING OLIVINE-DOLERITE PLUGS

ZEOLITE GRADES

ZEOLITES VERY RARE 1

MINOR CHABAZITE 2

CHABAZITE AND PHILLIPSITE 3

ANALCITE 4

SNOW FIELDS

MIDDLE TO UPPER MIOCENE JAMES ROSS ISLAND VOLCANIC GROUP

- PHASE V. OLIVINE-BASALT FLOW LAVAS — V1
- PHASE V. PALAGONITE-BRECCIAS — Vb
- PHASE IV OLIVINE-BASALT FLOW LAVAS — IV1
- PHASE IV PALAGONITE-BRECCIAS — IVb
- PHASE III OLIVINE-BASALT FLOW LAVAS — III1
- PHASE III PALAGONITE-BRECCIAS — IIIb
- PHASE II. OLIVINE-BASALT FLOW LAVAS — II1
- PHASE II PALAGONITE-BRECCIAS — IIb
- PHASE I OLIVINE-BASALT FLOW LAVAS — I1
- PHASE I PALAGONITE-BRECCIAS — Ib
- TUFFACEOUS CONGLOMERATE — Tc
- PALAGONITE-TUFFS (UNDIFFERENTIATED) — Ps
- OLIVINE-BASALT DYKES — D

UPPER CRETACEOUS — SNOW HILL ISLAND SERIES

- UPPER SANDSTONE GROUP
- *Rotularia collaza* CALC-SILTSTONE GROUP
- MIDDLE SANDSTONE GROUP
- *Rotularia doroshevia* CALC-SILTSTONE GROUP
- LOWER SANDSTONE GROUP
- HUMPS ISLAND GROUP
- *Rotularia* BEDS
- HIDDEN LAKE BEDS
- STONELEY POINT CONGLOMERATE BEDS
- UPPER KOTICK POINT BEDS
- LOWER KOTICK POINT BEDS
- LAGRELIUS POINT CONGLOMERATES

CONTOUR INTERVAL 1000 ft

SPOT HEIGHTS IN FEET *1430

MILES 0 5 10

km. 0 5 10 15

TRINITY PENINSULA

BROAD VALLEY

CAIN NUNATAK

ABEL NUNATAK

DUSE BAY

BROWN BLUFF

JONASSEN ISLAND

ANDERSSON ISLAND

TABARIN PENINSULA

SEVEN BUTTRESSES

FRIDTJOF SOUND

CONE NUNATAK

CAPE BURD

CAPE GREEN

BEAK ISLAND

EAGLE ISLAND

EGG ISLAND

TAIL ISLAND

CORRY ISLAND

VORTEX ISLAND

RED ISLAND

GUSTAV CHANNEL

ROSAMEL ISLAND

CAPE LACHMAN

KELTIE HEAD

CAPE WELL-MET

DEVIL ISLAND

BIBBY POINT

HERBERT SOUND

VEGA ISLAND

SANDWICH BLUFF

CAPE GORDON

BRANDY BAY

STONELEY POINT

RINK POINT

CARLSON ISLAND

PRINCE GUSTAV CHANNEL

LAGRELIUS POINT

ANDREASSEN POINT

CAPE LAMB

FALSE ISLAND POINT

CARRO PASS

MATKAH POINT

THE NAZE

TERRAPIN HILL

EREBUS AND TERROR GULF

KOTICK POINT

HIDDEN LAKE

PALISADE NUNATAK

INTRUSIVE LACCOLITH

BLANCMANGE HILL

HUMPS ISLAND

DREADNOUGHT POINT

DOBSON DOME

STARK POINT

CROFT BAY

SKEP POINT

ULA POINT

LONELY ROCK

CAPE OBELISK

FLATCAP POINT

COLEY GLACIER

CAPE GAGE

EKELÖF POINT

GOURDON GLACIER

ST. RITA POINT

HOBBS GLACIER

RABOT POINT

RÖHSS BAY

PERSSON ISLAND

JAMES ROSS ISLAND

MOUNT HADDINGTON 5340

COCKBURN ISLAND

PECTEN CONGLOMERATE

LOWER MIOCENE SEDIMENTS

SEYMOUR ISLAND

NYGREN POINT

TAIT GLACIER

SUNGOLD HILL

JEFFORD POINT

HAMILTON POINT

ADMIRALTY SOUND

WEDDELL SEA

CAPE FOSTER

LOCKYER ISLAND

SNOW HILL ISLAND

58°00′ 57°45′ 57°30′W. 57°15′ 57°00′ 56°45′ 56°30′

63°40′ 63°50′ 64°00′S. 64°10′ 64°20′

1 MILE 1000 ft

Map 1
Geological map of the James Ross Island group.

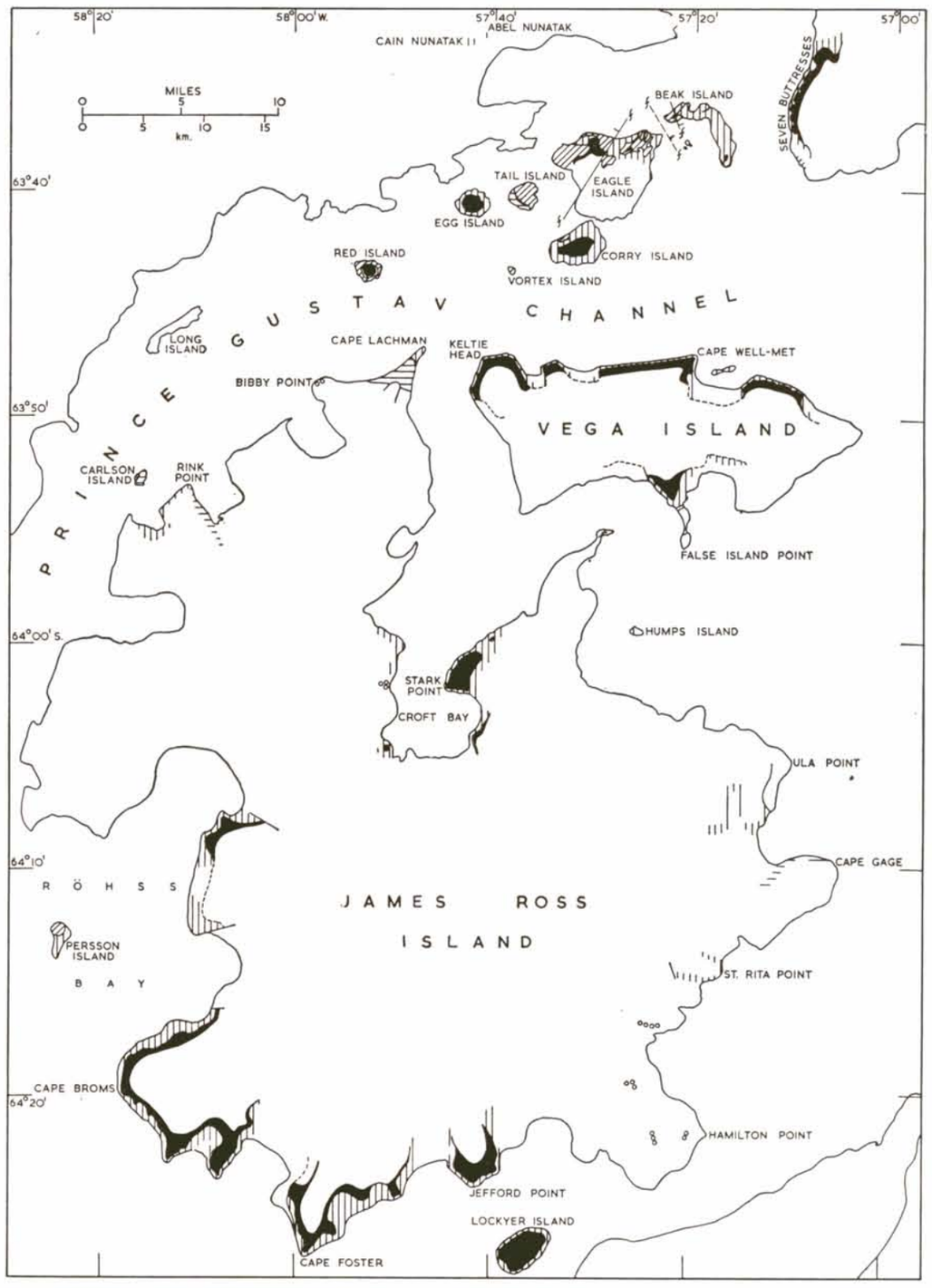

A

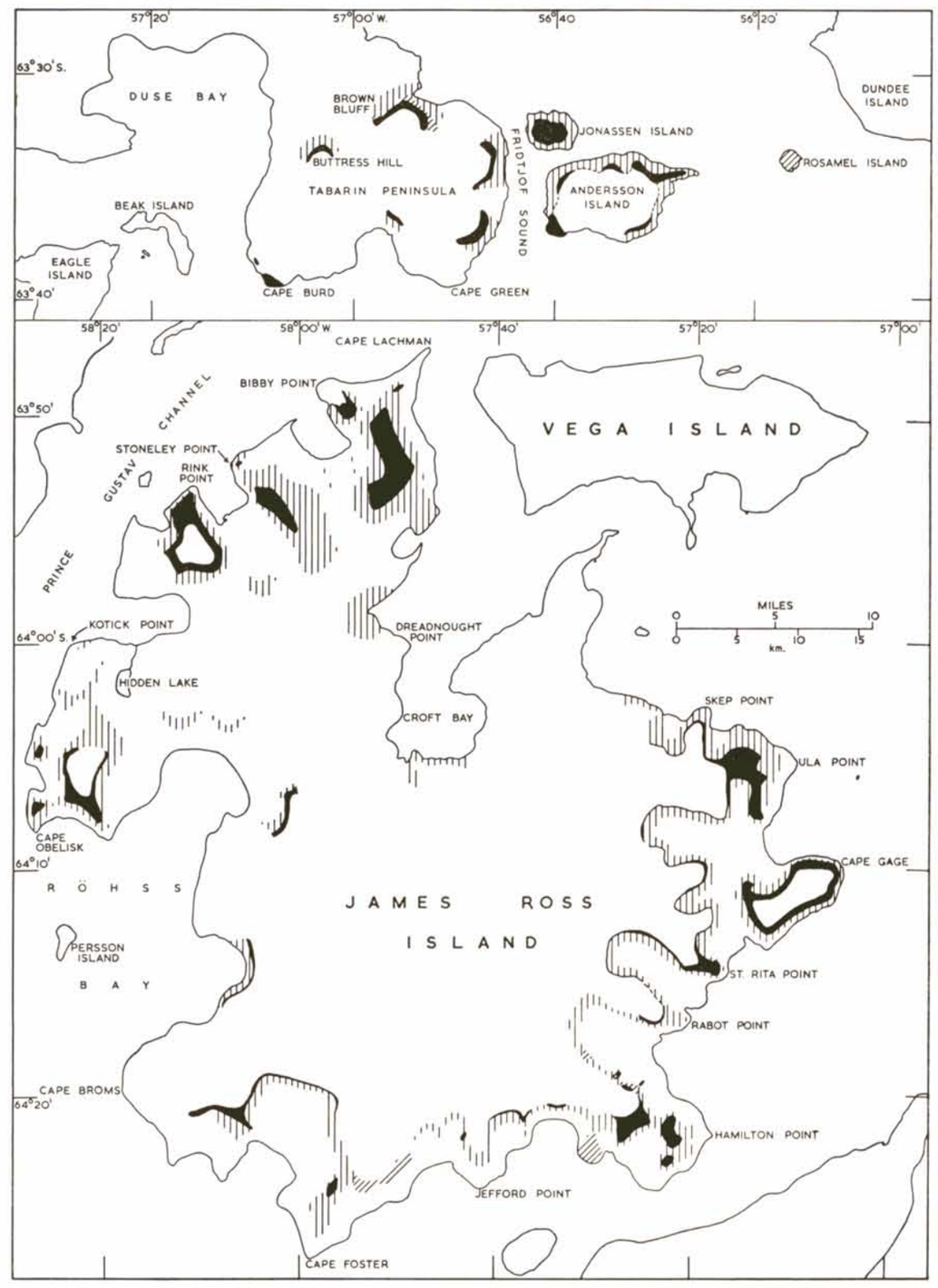

B

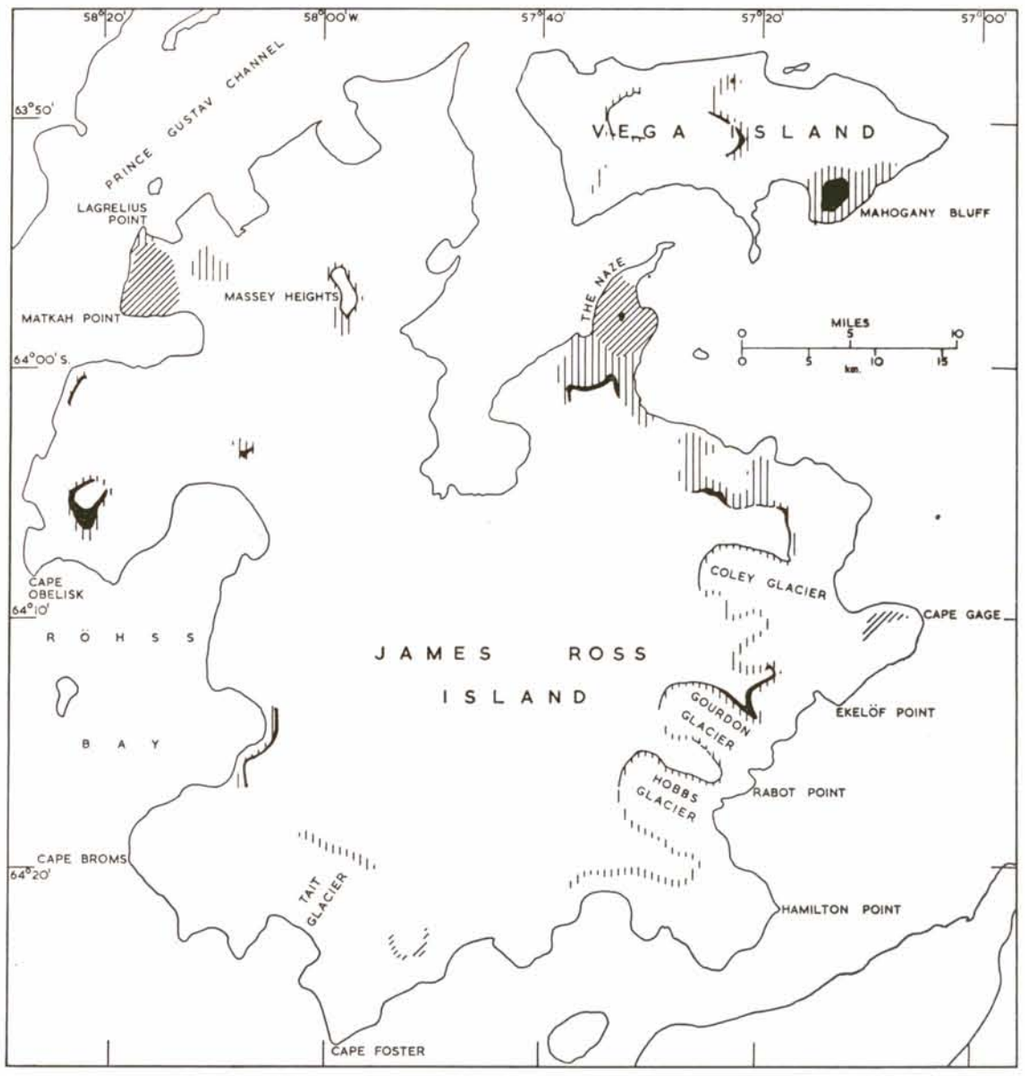

C

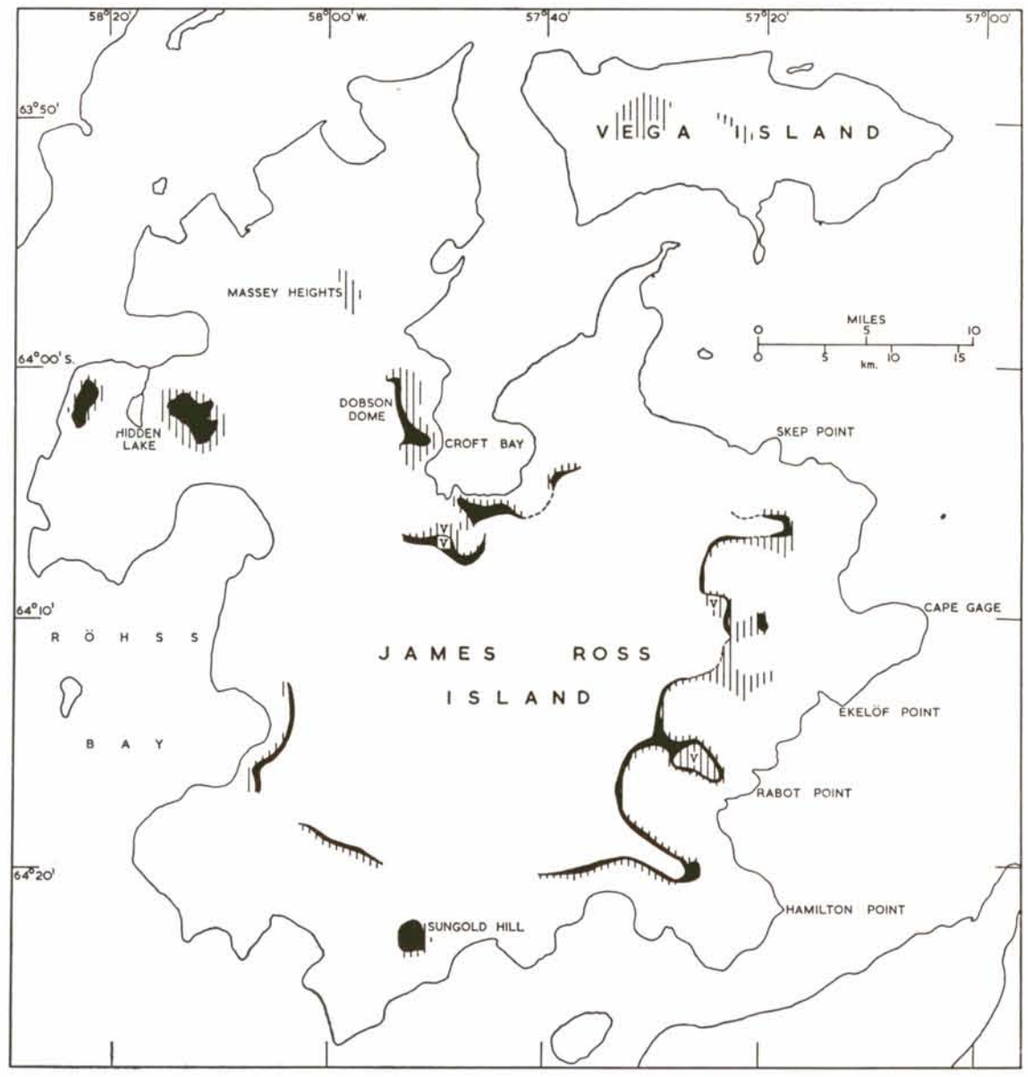

D

MAP 2

Geological maps of part of north-east Graham Land, showing the distribution of the different phases of the James Ross Island Volcanic Group.

A. Phase I. B. Phase II. C. Phase III. D. Phases IV and V.

Black	Olivine-basalt flow lavas.
Vertical hatching	Palagonite-breccias.
Horizontal hatching	Subaqueous palagonite-tuffs.
Diagonal hatching	Subaerial palagonite-tuffs.
Small circles	Tuffaceous conglomerates.
$\swarrow^{f}$	Faults (tick on the downthrow side).
V	Indicates phase V lavas and palagonite-breccias in D.

PLATE I

a. The Hobbs Glacier amphitheatre, James Ross Island, looking north-west towards the ice dome of Mount Haddington (centre skyline). The cliffs are up to 2,000 ft. (610 m.) high and are composed of lavas and palagonite-breccias of phases III and IV.

b. Small glacier rimmed by terminal and lateral moraines 3 miles (4·8 km.) west of Ekelöf Point, James Ross Island. The glacier is mainly fed by an ice fall from the ice cap of Mount Haddington.

c. The Watchtower, south-east James Ross Island, viewed from the west. It is a flat-topped mesa, reaching 1,300 ft. (396 m.) above sea-level, composed of phase II lavas and palagonite-breccias of the James Ross Island Volcanic Group overlying Upper Cretaceous sediments of the Snow Hill Island Series.

d. Red Island, which is 1,620 ft. (494 m.) high, viewed from the east, showing the tuff core and palagonite-breccias of a lava/palagonite-breccia volcano exposed in the eastern cliff. Sub-horizontal flow lavas occur on the ice-free flat top of the island.

a

b

c

d

PLATE I

PLATE II

a. A small cliff of tuffaceous conglomerates near the west coast of Croft Bay, 3 miles (4·8 km.) west of Stark Point, James Ross Island. The crude stratification dips at 20° to the south. The ice-axe (bottom right) is approximately 3 ft. (0·9 m.) long.

b. The base of an ash cone south of Hobbs Glacier (Plate VIIb), showing fine-grained, ripple-bedded palagonite-tuffs overlying a tuffaceous conglomerate. Pebbles, cobbles and boulders of intrusive rocks and quartz-veined greywackes typical of Trinity Peninsula occur in the conglomerate. The hammer shaft is 1 ft. (0·3 m.) long and the scale is in inches.

c. An olivine-basalt pillow in phase II palagonite-breccias, showing a contorted crustal flow pattern; Lachman Crags, James Ross Island. The hammer shaft is 1 ft. (0·3 m.) long and the scale is in inches.

d. An olivine-basalt pillow in phase II palagonite-breccias, showing concentric zoning and radial cracks; south of Leal Bluff, Vega Island. The hammer shaft is 1 ft. (0·3 m.) long and the scale is in inches.

a

b

c

d

PLATE II

PLATE III

a. Phase II flow lavas overlying fine-grained palagonite-tuff (grey) in the north-western cliff of Brown Bluff, Tabarin Peninsula. A wedge of palagonite-breccias between the lavas and the palagonite-tuff is exposed in the right-hand side of the cliff, which is approximately 500 ft. (152·5 m.) high.

b. Horizontally bedded palagonite-tuffs overlain by phase II palagonite-breccias and flow lavas in the coastal cliffs 1 mile (1·6 km.) west of Cape Gage, James Ross Island. The cliffs are approximately 900 ft. (274 m.) high.

c. Ripple-bedding and intraformational deformation in fine-grained palagonite-tuffs at north-east Tail Island. The hammer shaft is 1 ft. (0·3 m.) long and the scale is in inches.

d. Intraformational deformation in fine-grained palagonite-tuffs at north-east Tail Island, showing a continuation of the same bed as in Plate IIIc approximately 6 ft. (1·8 m.) to the right (north-east). The hammer shaft is 1 ft. (0·3 m.) long and the scale is in inches.

a

b

c

d

PLATE III

PLATE IV

a. Well-laminated subaqueous palagonite-tuffs at north-west Terrapin Hill, James Ross Island. The overall thickness of the finely laminated tuffs is approximately 10 ft. (3 m.).

b. Palagonite-tuff pillar, approximately 25 ft. (7·6 m.) high, on the northern slopes of Terrapin Hill, James Ross Island. This is one of several desert erosion residuals, the forms of which are controlled by joint planes.

c. The western cliff (approximately 125 ft. (37 m.) high) of Palisade Nunatak, James Ross Island, looking eastwards from the rim of the wind-scoop. The light grey sub-horizontal streaks near the top of the cliff are probably dolerite-pegmatite schlieren.

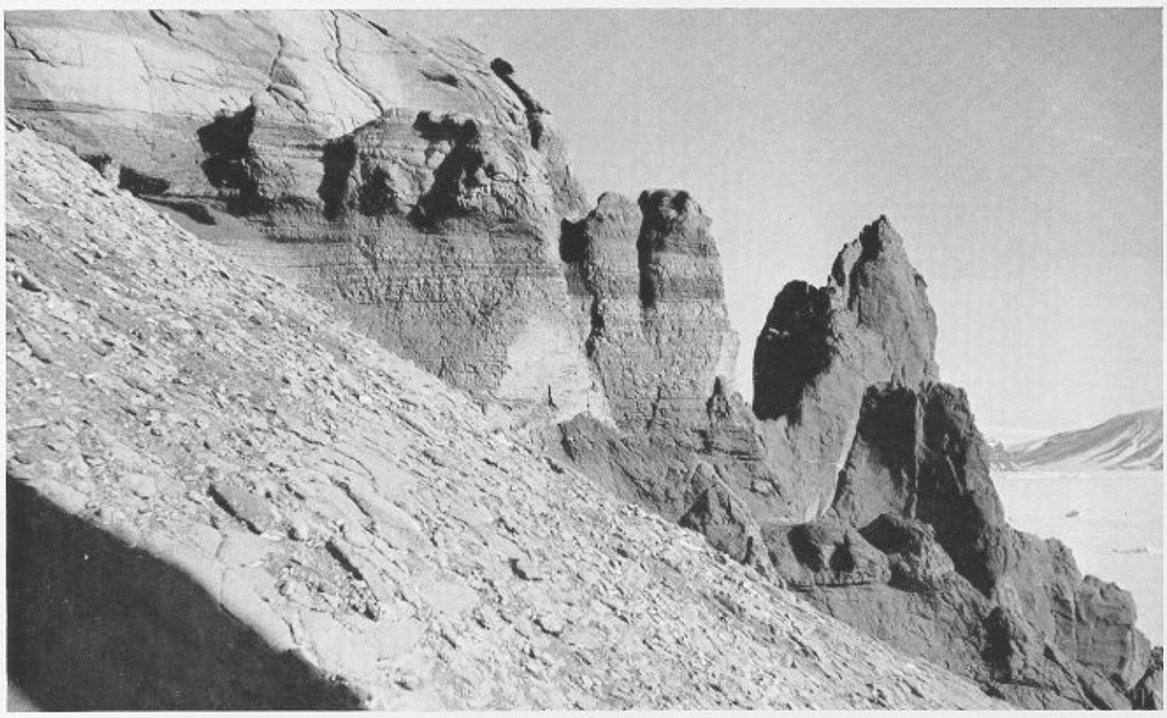

a

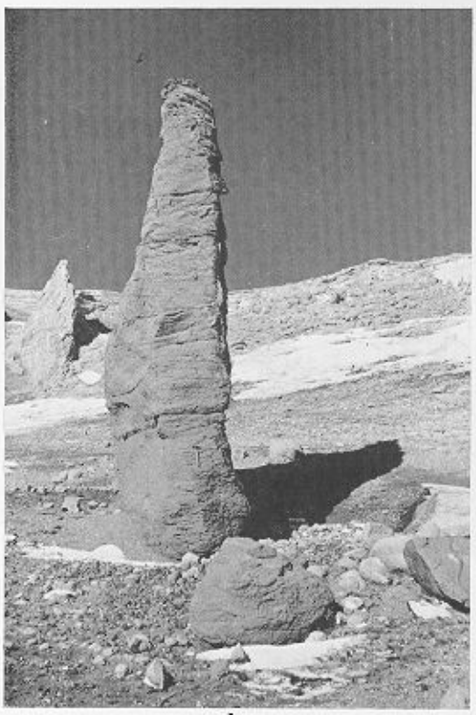

b

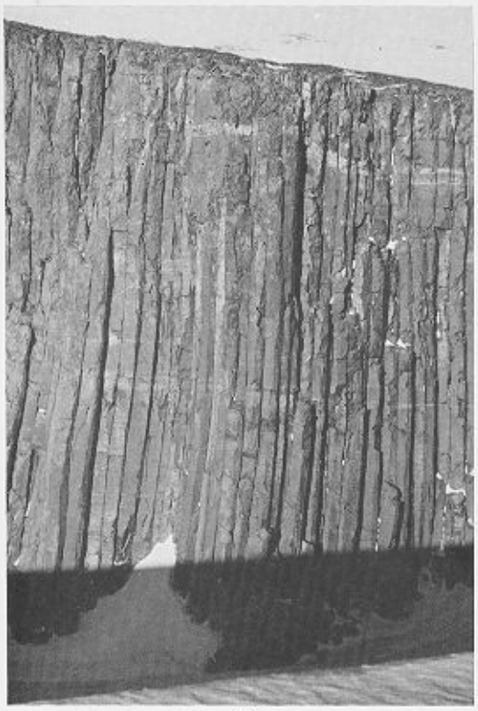

c

PLATE V

a. Pillow lavas in the palagonite-tuffs on the north coast of Carlson Island. The hammer shaft is nearly 2 ft. (0·6 m.) long and the scale is in inches. (Photograph by N. Aitkenhead.)

b. A xenolithic olivine-basalt flow lava 2 miles (3·2 km.) north-east of Hidden Lake, James Ross Island. The cracks and partial assimilation of the xenoliths suggest that the cooling of the host lava was protracted. The hammer shaft is 1 ft. (0·3 m.) long and the scale is in inches.

c. Cross-lamination in palagonite-tuffs south-east of Bibby Point, James Ross Island. A part of Lachman Crags, capped by sub-horizontal phase II lavas, is in the background. The hammer shaft is 1 ft. (0·3 m.) long and the scale in in inches.

d. A non-vesicular olivine-basalt dyke cutting Upper Cretaceous sandstones south of Hobbs Glacier, James Ross Island. An ash cone (Plate VIIb) crops out in the cliffs immediately to the left (east) of this photograph. The ice-axe is approximately 3 ft. (0·9 m.) long.

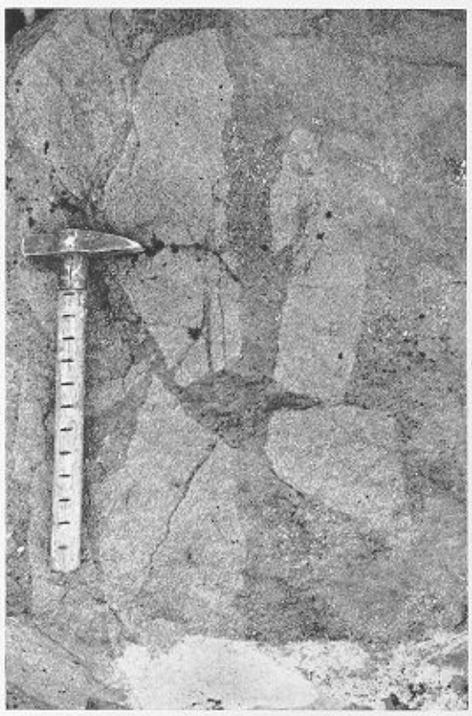

b

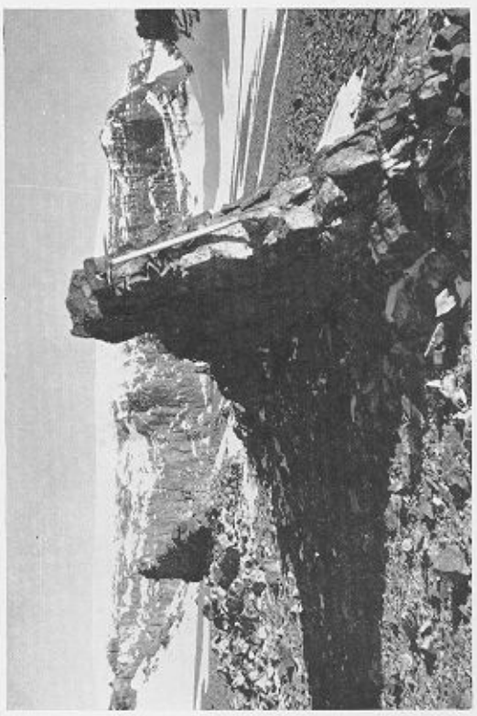

d

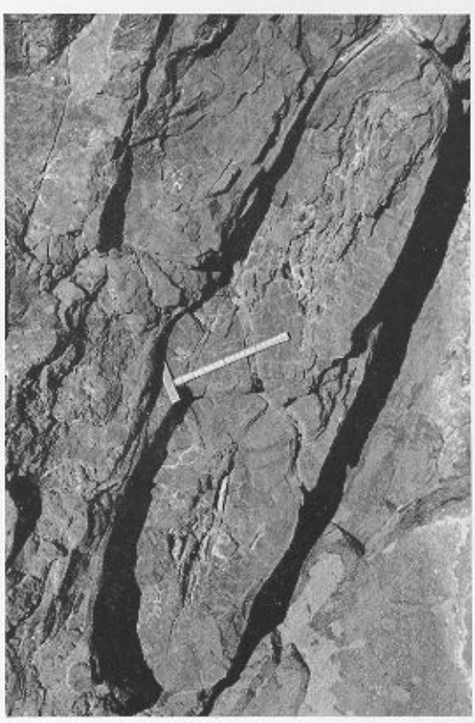

a

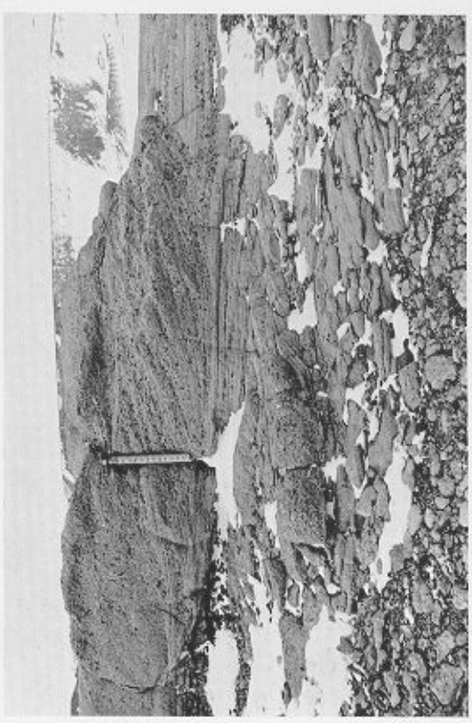

c

PLATE VI

a. The eastern side of Palisade Nunatak, James Ross Island, showing the large-scale columnar jointing of the intrusion and the bedding in the Upper Cretaceous sandstones which cap the nunatak. The maximum rock elevation visible in this photograph is approximately 800 ft. (244 m.).

b. The youngest of three phase III palagonite-breccia cones south of Terrapin Hill, James Ross Island, looking towards the south-east. The cliff in the foreground, in which the radial dip of the palagonite-breccias is apparent, reaches 1,000 ft. (305 m.) above sea-level.

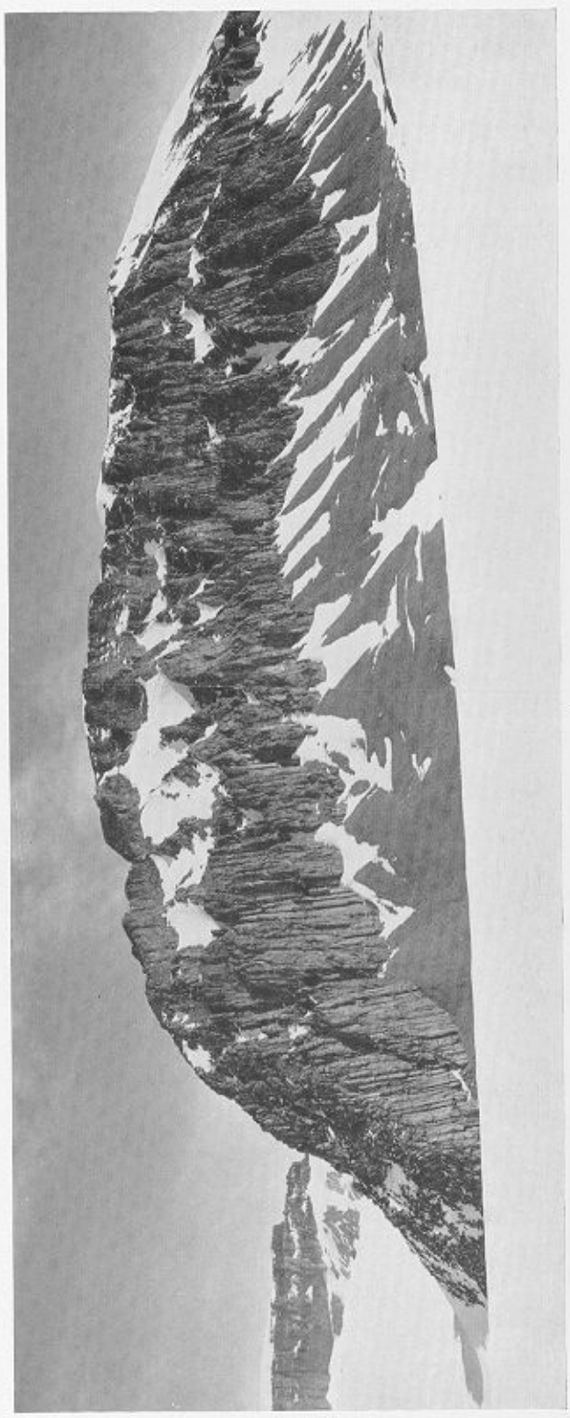

a

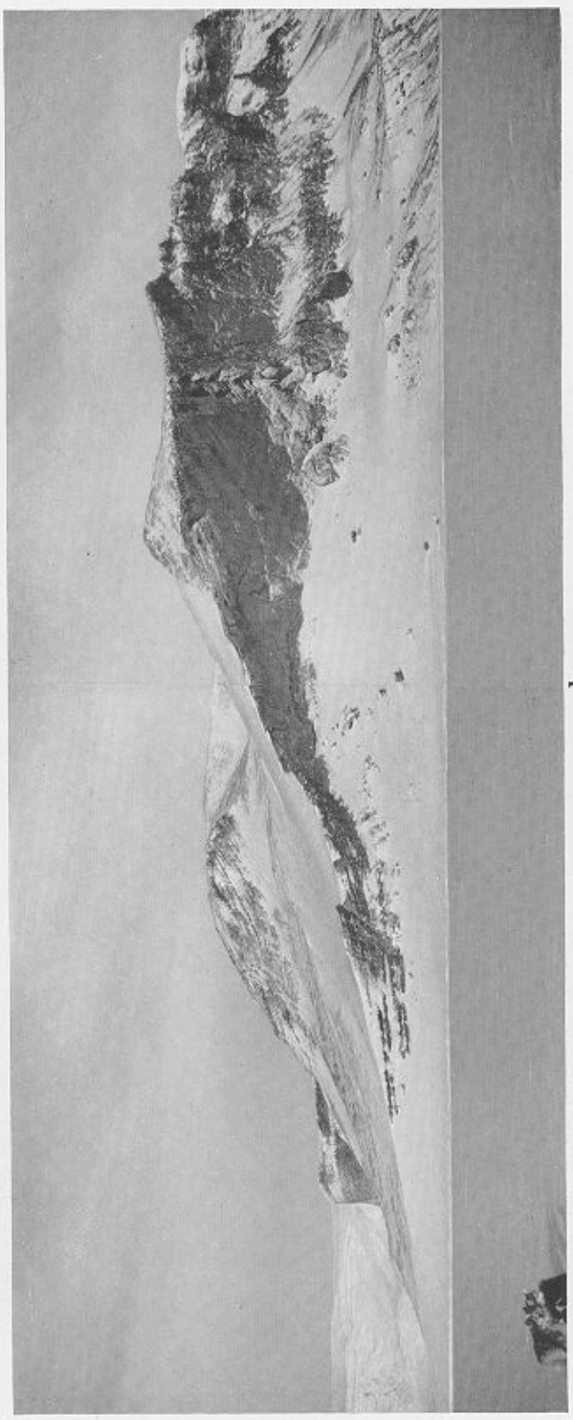

b

PLATE VII

a. A volcanic plug forming a knoll 1 mile (1·6 km.) north-east of Stoneley Point, James Ross Island. Two subsidiary conduits, approximately 30 ft. (9·1 m.) in diameter, are exposed in the flanks, while the main plug forms the summit of the hill.

b. An ash cone exposed in the cliffs south of the Hobbs Glacier snout, James Ross Island. The tuffaceous conglomerate shown in Plate IIb occurs at the end of the small ridge terminating at the cliff base in the bottom left of the photograph. The cliff, which is approximately 900 ft. (274 m.) high, reaches an altitude of 1,710 ft. (521 m.) above sea-level.

c. The coastal cliff at Cape Broms, James Ross Island, showing phase I lavas and palagonite-breccias. In the centre of the photograph there is a brecciated lava flow, which transgresses the lava/palagonite-breccia horizon from right to left (south to north; the same direction as the dip of the palagonite-breccias). The cliff is approximately 500 ft. (152 m.) high.

d. Small-scale faults, along which sinuous dykes have been injected, in the western cliffs of Mahogany Bluff, Vega Island. The cliff is approximately 1,000 ft. (305 m.) high.

a

b

c

d

PLATE VII

PLATE VIII

a. The transition from the olivine-hyalobasalt margin to the adjacent turbid zone of a palagonite-breccia pillow of phase II; Cape Obelisk, James Ross Island (D.4078.2; ordinary light; ×4·7).

b. Olivine-hyalobasalt from the glassy zone of a pillow of phase II, showing olivine phenocrysts and plagioclase microlites set in a matrix of brown basalt glass; Lachman Crags, James Ross Island (D.3749.1; ordinary light; ×37).

c. The turbid zone of an olivine-basalt pillow of phase II, showing the concentration of opaque dusty ore minerals around phenocrysts and microlites; Lachman Crags, James Ross Island (D.3749.1; ordinary light; ×37).

d. Palagonite-breccia of phase I composed of palagonite-rimmed fragments of olivine-hyalobasalt completely cemented with chabazite; near Cape Foster, James Ross Island (D.4068.2; ordinary light; ×10).

e. Palagonite-breccia of phase I, showing an isolated fresh olivine phenocryst in the zeolitized matrix; near Cape Foster, James Ross Island (D.4068.2; ordinary light; ×43).

f. Olivine-hyalobasalt fragment in a palagonite-breccia of phase I, showing contraction cracks around an olivine phenocryst; near Cape Foster, James Ross Island (D.4068.2; ordinary light; ×43).

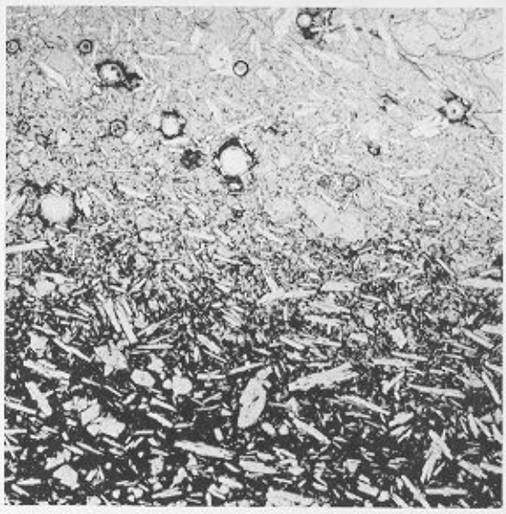

a

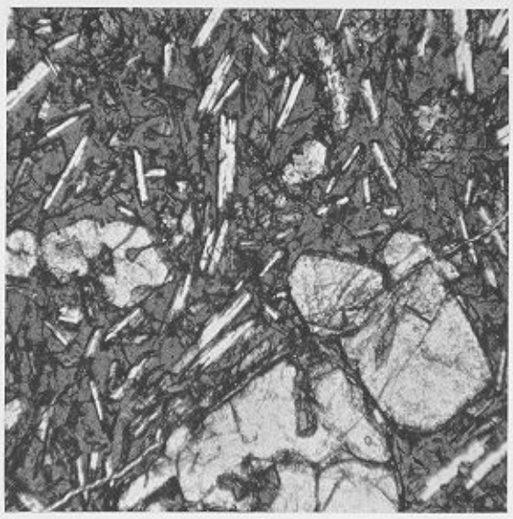

b

c

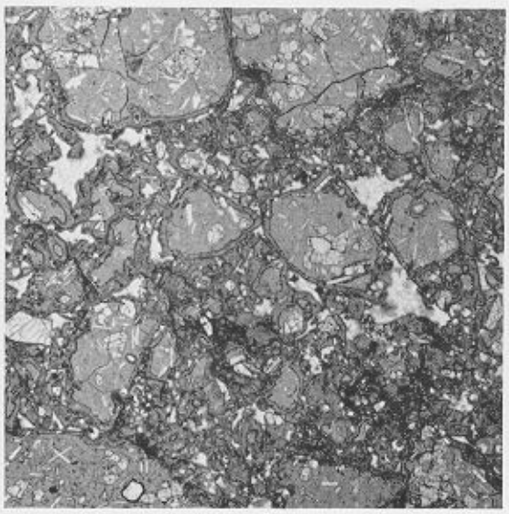

d

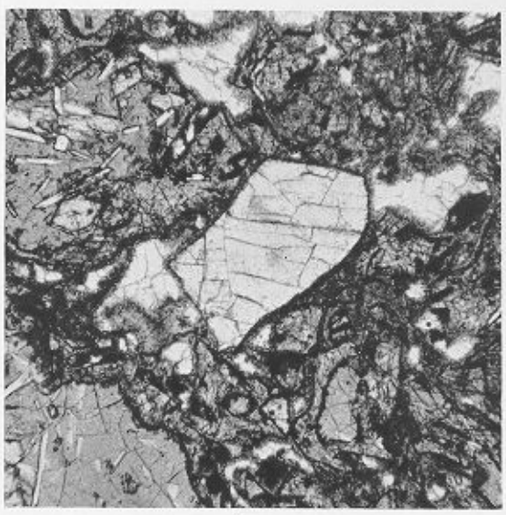

e

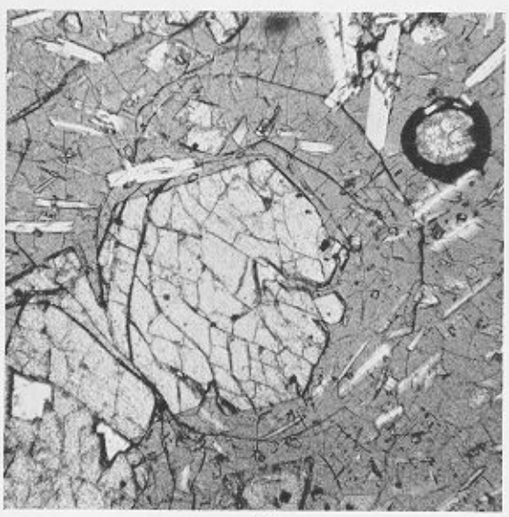

f

PLATE IX

a. Olivine-basalt of phase I with a trachytic texture composed of glomeroporphyritic aggregates of magnesian olivine and iron ore set in a groundmass of plagioclase, pyroxene and ore grains; western Beak Island (D.3711.3; X-nicols; ×60).

b. Olivine-basalt associated with phase I palagonite-tuffs, showing a glomeroporphyritic cluster of calcic plagioclase, olivine and small titanaugite crystals set in an aphanitic groundmass; southern Tail Island (D.3771.1; X-nicols; ×50).

c. A segregation vein of phase II, composed of large, anhedral, zoned titanaugite crystals, plagioclase, anorthoclase and apatite; Lachman Crags, James Ross Island (D.3748.3; ordinary light; ×8).

d. Olivine-basalt of phase III, showing a large calcic plagioclase phenocryst rich in spinel and opaque ore inclusions and with a core of olivine; Gourdon Glacier, James Ross Island (D.4053.1; X-nicols; ×27).

e. Olivine-basalt of phase III with a semi-glassy groundmass and large phenocrysts and aggregates of olivine and plagioclase. Minute hollow olivine crystals occur in the groundmass; Gourdon Glacier, James Ross Island (D.4053.8; X-nicols; ×37).

f. Oceanitic basalt of phase III, showing large subhedral olivine phenocrysts set in a fine-grained groundmass with a trachytic texture; Gourdon Glacier, James Ross Island (D.4053.12; ordinary light; ×8).

a

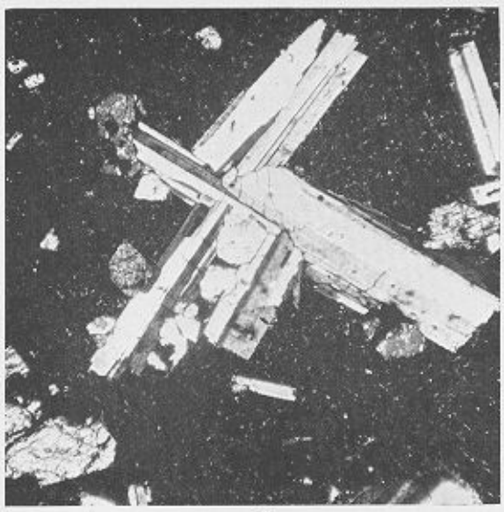

b

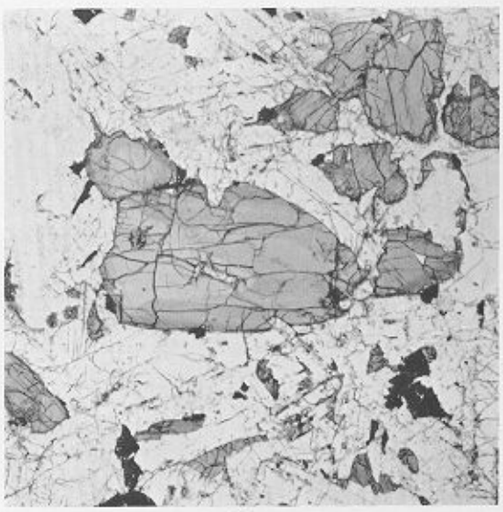

c

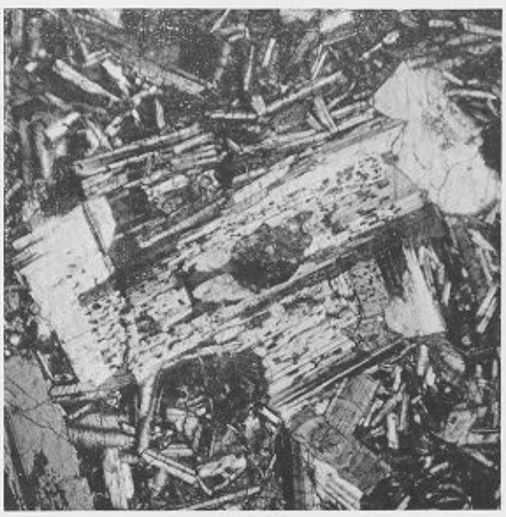

d

e

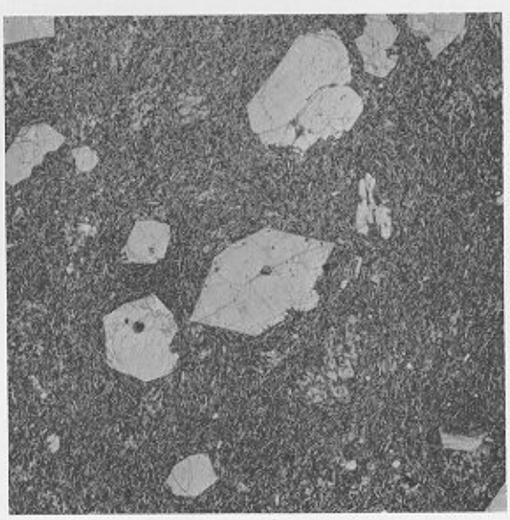

f

PLATE X

a. Part of a subophitic olivine-dolerite dyke (probably phase II) composed of zoned olivine phenocrysts and ophitically intergrown titanaugite and plagioclase; Blancmange Hill, James Ross Island (D.3740.1; ordinary light; ×37).

b. A peridotite nodule composed of olivine, enstatite, diopside and spinel, showing banding sub-parallel to (100) in a cracked anhedral olivine crystal; dyke 1 mile (1·6 km.) north-west of Ekelöf Point, James Ross Island (D.4049.3; X-nicols; ×33).

c. An analcite-bearing olivine-dolerite from a plug (probably phase II), showing interstitial analcite containing a minute apatite needle (centre of field); south-west of Lachman Crags, James Ross Island (D.3756.1; ordinary light; ×37).

d. A dolerite-pegmatite showing skeletal ilmenite and hyalosideritic olivine containing hexagonal, prismatic apatite inclusions; Palisade Nunatak, James Ross Island (D.4086.3; ordinary light; ×27).

e. A dolerite-pegmatite showing a complex graphic intergrowth of plagioclase and titanaugite crossed by skeletal ilmenite crystals; Palisade Nunatak, James Ross Island (D.4086.3; ordinary light; ×6).

f. A dolerite-pegmatite showing epitaxial overgrowth of anorthoclase on Carlsbad-albite twinned plagioclase. Acicular apatite crystals are present in the anorthoclase and analcitization has affected the plagioclase core; Palisade Nunatak, James Ross Island (D.4086.3; X-nicols; ×27).

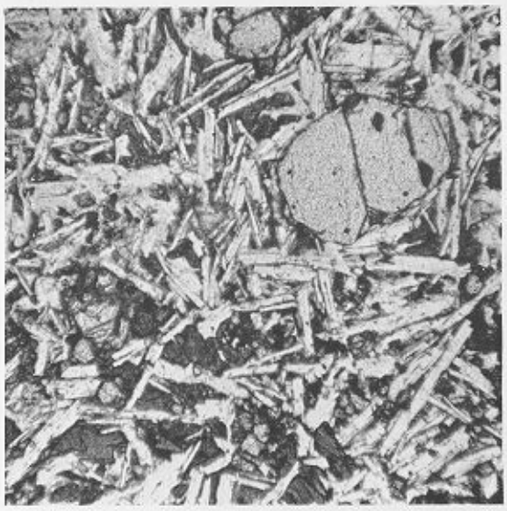

a

b

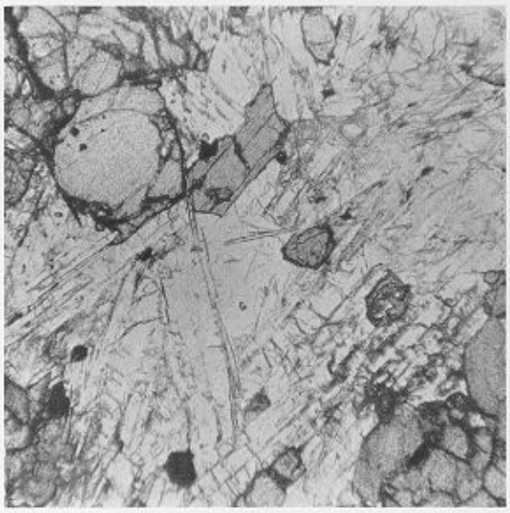

c

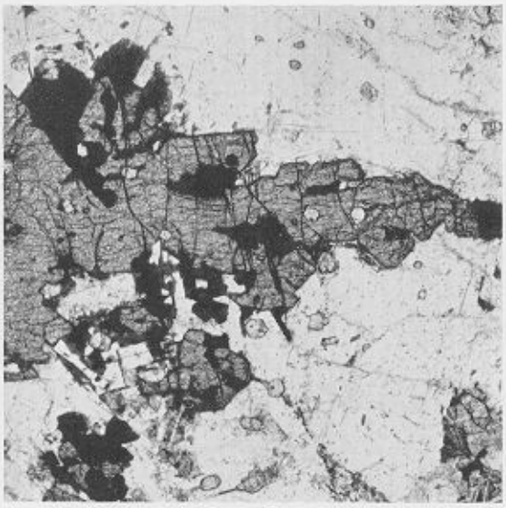

d

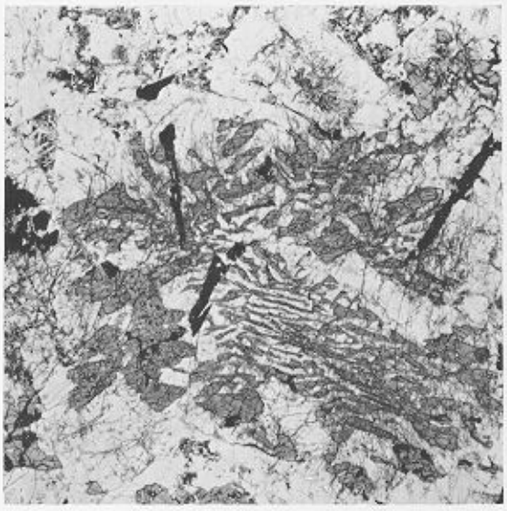

e

f

PLATE XI

a. Part of a late-stage felsitic vein, showing the sub-parallelism of potassium-rich sanidine crystals; Palisade Nunatak, James Ross Island (D.4088.4; X-nicols; ×27).

b. Part of a late-stage felsitic vein, showing an "amygdale" of analcite and spherulitic thomsonite surrounded by sanidine crystals; Palisade Nunatak, James Ross Island (D.4088.4; X-nicols; ×27).

c. An amygdale of granular chabazite in an olivine-basalt dyke; north-east Carlson Island (D.3766.1; X-nicols; ×50).

d. A palagonite-tuff with sub-spherulitic phillipsite cement displaying interpenetrant twinning on a micro-scale; south-west Croft Bay, James Ross Island (D.3738.6; X-nicols; ×60).

e. A palagonite-tuff cemented with fibrous spherulitic phillipsite; south-east Croft Bay, James Ross Island (D.3729.1; X-nicols; ×60).

f. Phillipsite amygdales in a foreign block of olivine-basalt flow lava in palagonite-breccias. The phillipsite displays both lamellar and interpenetrant twinning; Leal Bluff, Vega Island (D.3745.1a: X-nicols: ×40).

a

b

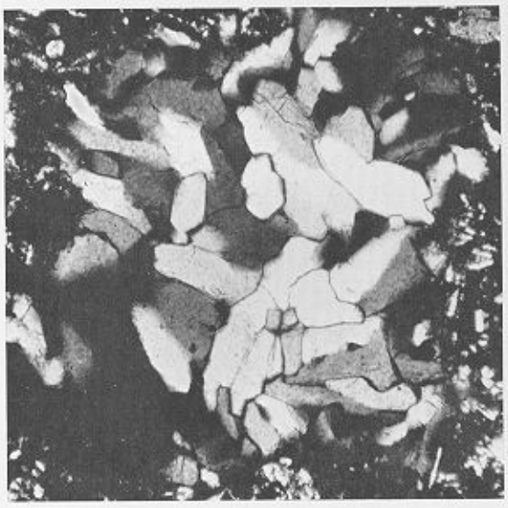

c

d

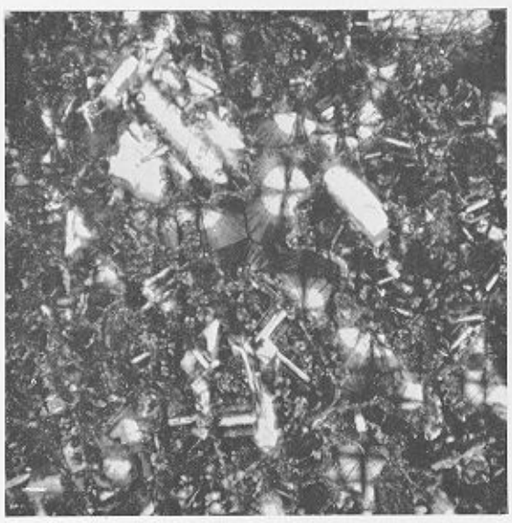

e

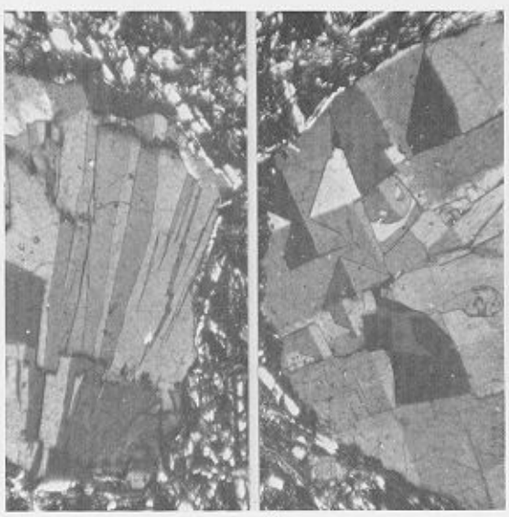

f